VOL. 5 NO. 4 APRIL 1963

Journal of

ELECTROANALYTICAL CHEMISTRY

International Journal Dealing with all Aspects of Electroanalytical Chemistry, Including Fundamental Electrochemistry

ELSEVIER

GENERAL INFORMATION

Types of contributions

(a) Original research work not previously published in other periodicals.
(b) Reviews on recent developments in various fields.
(c) Short communications.
(d) Bibliographical notes and book reviews.

Languages

Papers will be published in English, French or German.

Submission of papers

Papers should be sent to one of the following Editors:

Professor J. O'M. BOCKRIS, John Harrison Laboratory of Chemistry, University of Pennsylvania, Philadelphia 4, Pa., U.S.A.
Dr. R. PARSONS, Department of Chemistry, The University, Bristol 8, England.
Professor C. N. REILLEY, Department of Chemistry, University of North Carolina, Chapel Hill, N.C., U.S.A

Authors should preferably submit two copies in double-spaced typing on pages of uniform size. Legends for figures should be typed on a separate page. The figures should be in a form suitable for reproduction, drawn in Indian ink on drawing paper or tracing paper, with lettering etc. in thin pencil. The sheets of drawing or tracing paper should preferably be of the same dimensions as those on which the article is typed. Photographs should be submitted as clear black and white prints on glossy paper.
All references should be given at the end of the paper. They should be numbered and the numbers should appear in the text at the appropriate places.
A summary of 50 to 200 words should be included.

Reprints

Twenty-five reprints will be supplied free of charge. Additional reprints can be ordered at quoted prices. They must be ordered on order forms which are sent together with the proofs.

Publication

The *Journal of Electroanalytical Chemistry* appears monthly and has six issues per volume and two volumes per year, each of approx. 500 pages.

Subscription price (post free): £ 10.15.0 or $ 30.00 or Dfl. 108.00 per year; £ 5.7.6 or $ 15.00 or Dfl. 54.00 per volume.
Additional cost for copies by air mail available on request.
For advertising rates apply to the publishers.

Subscriptions

Subscriptions should be sent to:

ELSEVIER PUBLISHING COMPANY, P.O. Box 211, Spuistraat 110-112, Amsterdam-C., The Netherlands.

TOXIC AGENTS

a series of monographs

edited by Ethel Browning

volumes appeared

TOXICITY OF ARSENIC COMPOUNDS

by W. D. Buchanan

viii + 155 pages 4 tables 6 illustrations 1962 25s.

TOXICOLOGY AND BIOCHEMISTRY OF AROMATIC HYDROCARBONS

by H. W. Gerarde

xiv + 329 pages 63 tables 89 illustrations 1961 32s.

TOXIC ALIPHATIC FLUORINE COMPOUNDS

by F. L. M. Pattison

xii + 227 pages 31 tables 6 illustrations 1959 19s.

CARCINOGENIC AND CHRONIC TOXIC HAZARDS OF AROMATIC AMINES

by T. S. Scott

xiv + 208 pages 20 tables 50 illustrations 1962 30s.

TOXICITY OF BERYLLIUM COMPOUNDS

by L. B. Tepper, H. L. Hardy and R. I. Chamberlin

viii + 192 pages 12 tables 10 illustrations 1961 20s.

ELSEVIER PUBLISHING COMPANY
AMSTERDAM LONDON NEW YORK

119 E

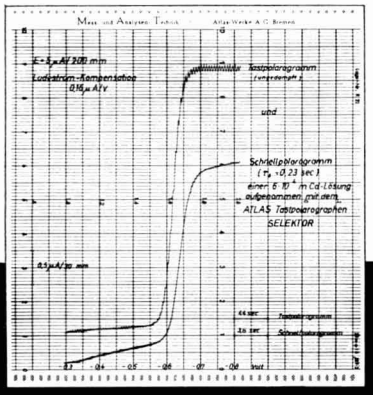

Selector

Tast-Polarograph

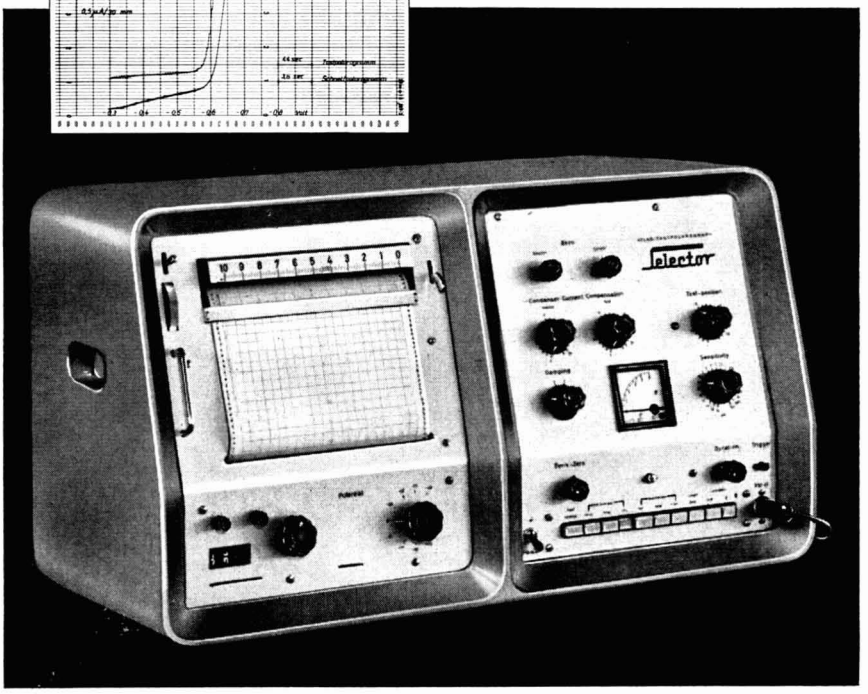

An instrument designed for high demands as to accuracy, sensitivity and safety in taking and recording

conventional polarograms
tast-polarograms
derivative tast polarograms
rapid polarograms

The construction of the SELECTOR combines the precision required for scientific tasks with easy operation necessary for routine analyses.

68 e

ATLAS MESS- UND ANALYSENTECHNIK GMBH
BREMEN

MAT

EFFECT OF CONCENTRATION OF THE REACTANTS ON THE MEASUREMENT OF TRANSFER COEFFICIENT AND RATE CONSTANT OF FERROUS-FERRIC REDOX PROCESS UNDER IDEAL CONDITIONS

H. P. AGARWAL

Department of Chemistry, Motilal Vigyan Mahavidyalaya, Bhopal (India)

(Received July 14th, 1962)

The rectification of alternating current by electrodes in an aqueous solution containing a reversible redox couple has been reported by DOSS AND AGARWAL[1]. This rectification is caused by an electrode reaction due to the asymmetry of its current–potential characteristic with respect to the equilibrium potential. It was originally named the *redoxokinetic effect*[1] but is now usually called the faradaic rectification[2,3]. The theoretical treatment given by DOSS AND AGARWAL[4,5] for equimolar concentration of the reactants, whose diffusion coefficients are equal, and the generalised treatment given by BARKER[3] and also by VDOVIN[6] have made possible the study of fast electrode processes. The theory has been worked out assuming a concentration of reactants of the order of a few mmoles/l[4,5]. In the present work, the effect of change in concentration of the reactants on the measurement of transfer coefficient has been studied. The transfer coefficient thus obtained for an ideal solution of the reactants was used for determining the standard rate constant at equilibrium.

EXPERIMENTAL

The small change in the mean potential when an electrode is polarised by an alternating current, was measured by the method described previously[7]. The frequency of the alternating current was checked during the course of the experiment on a Philips oscillograph Type GM 3156 which was also used for the measurement of the applied a.c. voltage (sensitivity 1 mV r.m.s./cm). All the data were obtained for platinum/aqueous solutions. Solutions of the desired strengths were prepared by dissolving the calculated amounts of ferric ammonium sulphate (A.R.) and ferrous ammonium sulphate (A.R.) in 1 *N* sulphuric acid (A.R.). To determine the effect of dilution on the transfer coefficient, equimolar concentrations of the cations Fe^{2+} and Fe^{3+} ranging from 0.01 *M* to 0.001 *M* were used. A few readings were also taken using 0.001 *M* ferric ion and 0.002 *M* ferrous ion, and *vice versa*. The results obtained at varying frequencies are shown in Tables I and II. For the sake of brevity the readings of ψ, the shift in mean potential, have only been given at 4 mV. a.c. in Tables I and II. At 8 mV a.c., the values of ψ are exactly 4 times greater than those measured at the corresponding frequency and at the particular dilution of the reactants used.

TABLE I

Dimensions of bright, polished, platinum foil electrodes used: 1. length 1.60 cm, breadth 0.90 cm; 2. length 1.60 cm, breadth 1.00 cm (earthed); reference electrode, length 1.60 cm, breadth 1.00 cm. Temperature of the thermostat 35° ± 0.05°

A.c. frequency (f') (c/sec)	*Values of ψ at the following concentrations of oxidant and reductant ions at 4 mV a.c. (μV)*				*Remarks*
	0.01 M	*0.004 M*	*0.002 M*	*0.001 M*	
50	− 4	− 7	−11	−11	At all frequencies, the magnitude of ψ increases with dilution of reactants up to 0.002 *M*. On further dilution, ψ becomes constant at the respective frequency. At all dilutions, $\psi \propto \sqrt{f'}$ approximately, but at dilutions of 0.002 *M* and above, the relationship holds good more rigorously.
100	− 6	−11	−15	−15	
200	− 8	−16	−21	−21	
500	−11	−24	−24	−24	
1000	−11	−24	−26	−26	
2000	−11	−24	−26	−26	
5000	−11	−24	−26	−26	

TABLE II

Dimensions of bright polished platinum foil electrodes used: 1. length 1.60 cm, breadth 0.90 cm; 2. length 1.60 cm, breadth 1.00 cm (earthed); reference electrode, length 1.60 cm, breadth 1.00 cm. Temperature of the thermostat 35° ± 0.05°

A.c. frequency (f') (c/sec)	*Values of ψ at the following oxidant : reductant ratios at 4 mV a.c. (μV)*		*Remarks*
	0.002 N : 0.001 N	*0.001 N : 0.002 N*	
50	−20	−20	The values of ψ are constant at a frequency of 500 c/sec or above, in both of the cases, but at lower frequencies *i.e.* below 500 c/sec, φ is not proportional to $\sqrt{f'}$ though it decreases with the lowering in frequency in both of the columns.
100	−24	−22	
200	−30	−26	
500	−36	−40	
1000	−36	−40	
2000	−36	−40	
5000	−36	−40	

TABLE III

Values of concentration gradient and of mean concentration for diffusion of 0.001 *M* ferric ammonium sulphate in 1 *N* sulphuric acid. Volume of 0.001 *M* ferric ammonium sulphate solution taken in compartment A of porous diaphragm cell, 60 ml. Volume of 1 *N* sulphuric acid taken in compartment B of porous diaphragm cell, 110 ml. Characteristic constant of the cell 3.46. Temperature of the thermostat 35° ± 0.05°

t_1 *(min)*	*Concn. of the diffused salt,* C_1 *(g equiv./l·10⁶)*	t_2 *(min)*	*Concn. of the diffused salt,* C_2 *(g equiv./l·10⁶)*	*Concn. gradient* $\left(\frac{dc'}{dt}\cdot 10^6\right)$	*Mean concentration, C (g equiv./l·10⁶)*
275	19.9	601	29.8	0.030	24.8
302	20.6	570	29.2	0.032	24.9
339	22.4	542	28.2	0.028	25.3
376	23.7	514	26.9	0.023	25.3
			Mean of first three	0.028	25.0

Similarly the values of concentration gradient and mean concentration for diffusion of ferric ions at higher concentrations in 1 *N* sulphuric acid were obtained. Their mean values at 35° are given overleaf.

Initial concentration of ferric ion prior to diffusion M	*Concentration gradient* $\left(\frac{dc'}{dt}\cdot 10^6\right)$	*Mean concentration* $(C'\cdot 10^6)$
0.002	0.051	63.0
0.005	0.12	56.8
0.02	0.33	116.0

To find the value of the rate constant under ideal conditions when the salt completely ionises, it was necessary to determine the diffusion coefficient of ferric ammonium sulphate or ferrous ammonium sulphate at zero concentration in 1 N sulphuric acid at the desired temperature. To do this, diffusion coefficients of the reactants at varying concentrations were determined by the porous diaphragm cell method, the details of which are given in a separate communication[14]. As the diffusion coefficients determined at a particular concentration of ferrous salt or ferric salt were equal, only the values of the concentration gradient and the mean concentration for the diffusion of ferric ammonium sulphate at concentrations varying from 0.02 M to 0.002 M in 1 N sulphuric acid are given in Table III.

RESULTS AND DISCUSSION

Redox couple having equimolar concentration

At all dilutions ψ is proportional to the square of the applied a.c. voltage. It can be seen from Table I that with increase in concentration of Fe^{2+} and Fe^{3+} ions (between 0.01 M and 0.004 M), ψ decreases in magnitude at the corresponding frequencies. The decrease in ψ with the increase in concentration of the reactants can be explained by considering the equivalent circuit of the cell which is of the form shown in Fig. 1, where R_C is the internal resistance of the cell, C_{dl} is the double

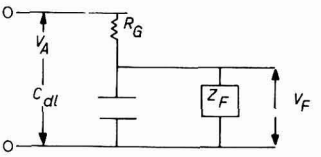

Fig. 1.

layer capacity of the electrode and Z_F is the faradaic impedance. The change in mean potential depends upon V_F which may be somewhat smaller than the applied voltage V_A. It seems probable that the decrease in ψ with increasing concentration of the redox couple (Table I), is mainly caused by a decrease in Z_F which, for concentrations of 10^{-2} M, is no longer much larger than R_C. At all dilutions, and below a frequency of 500 c/sec the shift in mean potential decreases with decreasing frequency and it varies with the square root of the a.c. frequency (especially when the concentration is of the order of 0.002 M to 0.001 M) in accordance with the theoretical analysis[5]. The decrease in ψ with decreasing frequency is presumably due to the fact that the faradaic impedance contains an appreciable reactive component at the lowest frequency. If this interpretation is correct, R_C must be approximately equal to 0.5 Z_F when the reactant concentrations are both 10^{-2} M. As there is an appreciable

decrease in ψ at 50 c/sec the value of R_C may be of the order of 0.2 Ω and the rate constant about $2.5 \cdot 10^{-2}$ cm/sec.

ANSON[8] has shown that both ferrous and ferric ions are strongly adsorbed at the metal electrode surface. Hence the decrease in the value of ψ with increasing concentration of the reactants may be due to adsorption of such ions on the platinum electrodes. From Table I it can be seen that ψ does not vary at any particular voltage or frequency used when the concentration of the reactants is between 0.002 M and 0.001 M, showing that in this range the effect is independent of variation in concentration. Therefore, in this concentration range, the values of α, the transfer coefficient, can be measured free from influence of changes in concentration of the reactants (activity coefficient approaches unity). Further, it is doubted whether the adsorption of the reactants would affect the validity of the simple expression for ψ when the frequency is sufficiently high for the reaction to be controlled by the kinetics of the electrode reaction. Under these conditions, the transfer coefficient of the ferrous–ferric redox system may be measured correctly, as the value of the frequency independent resistance, R_K, may be negligible[9].

When ψ does not change with the variation in concentration of the reactants (when the concentration of each of the reactants is of the order of 0.002 M or less) and with variation in frequency of the alternating current, the value of α, can be calculated from the following equation derived earlier[5].

$$\alpha = 0.5 - \frac{2\psi RT}{V^2 nF}$$

where R is the gas constant, T is the absolute temperature, n is the valency, F is the Faraday number and V is the applied a.c. voltage. On substituting, from Table I, the values of $\psi = -26\,\mu$V at 0.001 M equimolar concentration of the redox couple, $V = 0.004$ V and $T = 308$ in the above equation, the value of α obtained is 0.586. As this value is less than 0.6, the adsorption of the reducible ion at the electrode surface is very low[10]. Therefore, when the concentration of the reactants is of the order of 0.002 M or less, the values of α could be determined correctly. The transfer coefficient diminishes with the increase in concentration of the reactants, as does[11] ψ, beyond 0.002 M. The values of α have been given to 3 decimal places since α varies by approximately 0.001 when the temperature is varied by 5 degrees.

To determine the value of K_s, the value of the diffusion coefficient at zero concentration of the reactant is obtained from the data for the diffusion coefficients of the reactant at varying concentrations. The diffusion coefficient of ferric ion at a particular concentration in 1 N sulphuric acid (supporting electrolyte) is calculated from the data for the concentration gradient and mean concentration given in Table III, by adopting the method of HARTLEY AND RUNNICLES[12]. The calculation is illustrated below for of 0.001 M ferric ion in 1 N sulphuric acid.

The average value of concentration, $\bar{C}$, before and after the diffusion $= 0.001 - (110/60)0.000025 = 0.000954$

$$\Delta C = \bar{C} - \bar{C}' = 0.000954 - 0.000025 = 0.000929$$

$$\therefore K\bar{D} = \frac{dc'}{dt \cdot \Delta C} = \frac{0.028 \cdot 10^{-6}}{0.000929} = \frac{0.028}{929}$$

where K is the cell constant and $\bar{D}$ is the mean diffusion coefficient.

$$\bar{D} = \frac{0.028}{929 \cdot 3.46} = 8.7 \cdot 10^{-6} \text{cm}^2\text{sec}^{-1}$$

The values of the diffusion coefficients of ferric ion at concentrations of 0.001 M, 0.002 M, 0.005 M and 0.02 M were obtained similarly from data given in Table III, and are summarized in Table IV.

TABLE IV

VALUES OF DIFFUSION COEFFICIENTS DETERMINED FOR VARIOUS CONCENTRATIONS AT 35°

Concn. of ferric ions (g mol/l)	$\bar{D}_{c'}^{\bar{c}}$ *(cm² sec⁻¹·10⁶)*
0.001	8.7
0.002	8.1
0.005	7.1
0.02	4.8

From the above table it can be seen that the diffusion coefficient varies with the change in concentration of the diffusing ion, hence the ONSAGER AND FUOSS equation[13] as modified by HARTLEY AND RUNNICLES could be used more accurately for the determination of the correct diffusion coefficient values under ideal conditions. It has been shown by ONSAGER AND FUOSS that the ratio of the diffusion coefficient at a sufficiently low concentration c, to that at zero concentration, is given by

$$\frac{D_c}{D_0} = \frac{\text{d log } f}{\text{d log } c} \tag{1}$$

where f is the mean activity coefficient, provided that there is no influence of interionic forces on the mobilities. The use of osmotic coefficient g in Guggenheim's equation is very convenient for the calculation of $\bar{D}_0^c$ *i.e.* the mean diffusion coefficient at a particular concentration. For concentrations below 0.1 N the following equations were used by HARTLEY AND RUNNICLES.

$$\frac{\text{d log } (fc)}{\text{d log } c} = \frac{\text{d}(gc)}{\text{d}c} \tag{2}$$

whence, denoting the ONSAGER–FUOSS mobility by $\phi(c)$, we have

$$\int_0^c \frac{\bar{D}_0^c}{D_0}\,\text{d}c = \int_0^c [1 - \phi(c)]\,\text{d}(gc) \tag{3}$$

$$\frac{\bar{D}_0^c}{D_0} = g - \frac{1}{c}\int_0^c \phi(c)\,\text{d}(gc) \tag{4}$$

To verify the above equation the values of $\bar{D}_0^c$ and D_0 were calculated by HARTLEY AND RUNNICLES using the following equation:

$$\bar{D}_0^c = \bar{D}_{c'}^{\bar{c}} + \frac{\bar{c}'}{c}(\bar{D}_0^{\bar{c}'} - \bar{D}_{c'}^{\bar{c}})$$

The values of $D_{\bar{c}'}^{\bar{c}}$, given in the above table were plotted against $\sqrt{c}$. On extrapolating the plot to $c = 0$ the value of $\overline{D}_0^{\bar{c}}$ was found to be $9.7 \cdot 10^{-6}$ cm²/sec. The value so obtained is identical to D_0 as $\bar{c}$ is very low. The value of D_0 thus obtained was used for calculating the ratio of $\bar{D}_{\bar{c}'}^{\bar{c}}/D_0$ which can be considered equal to $\bar{D}_0^{\bar{c}}/D_0$ as $\bar{c}'$ is almost zero. The values of $D_0^{\bar{c}}/D_0$ were plotted against c as shown in Fig. 2, to verify eqn. (4). Figure 2 shows an asymptotic curve as predicted by eqn. (4).

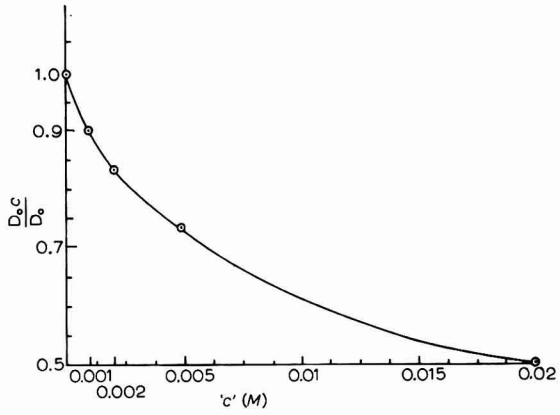

Fig. 2.

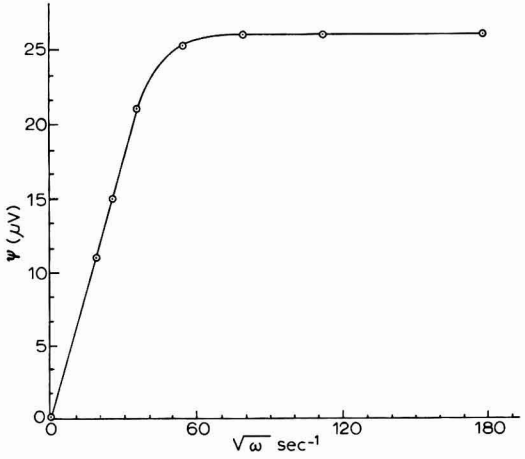

Fig. 3. Relationship between ψ, the shift in mean potential, and $\sqrt{\omega}$, where ω is the angular frequency at 4 mV a.c., at 35°.

On plotting ψ, (for 0.001 M concentration of the reactants see the last column of Table I) against $\sqrt{\omega}$ (where $\omega = 2\pi f'$, f' being the frequency of alternating current used), a curve as shown in Fig. 3 is obtained. It can be seen from Fig. 3 that ψ varies linearly with $\sqrt{\omega}$ when the a.c. frequency lies between 0 and 200 c/sec, whereas

at a frequency of 1000 c/sec or above, ψ is found to be independent of variation in frequency. The slope of the plot between 0 and 200 c/sec gives the value of $\psi/\sqrt{\omega}$. On substituting the value of $\sqrt{\omega}/\psi$ ($1.7 \cdot 10^6$ sec^{-1}/V), α (0.586) and D_0 ($9.7 \cdot 10^{-6}$) in the theoretical eqn. (5) of faradaic rectification applicable at low frequency *i.e.*

$$K_s = (0.5 - \alpha)\frac{V^2nF}{4RT\psi}\sqrt{\frac{\omega D_0}{2}} \tag{5}$$

where V is the applied a.c. voltage, n is the valency, F is the Faraday number, R is the gas constant, T is the absolute temperature and ω is the angular frequency, the value of the rate constant at equilibrium obtained is 0.048 cm sec^{-1} at 35°.

Effect of change of redox concentration ratio on transfer coefficient

From the generalised theoretical analysis given by BARKER *et al.*[3] (when $C_0 \neq C_r$, $D_0 \neq D_r$), it was found that ψ tends towards the limiting value $(0.5 - \alpha)\ V^2nF/2\ RT$ as the frequency increases. Hence the values of α were obtained by substituting the values of V, T and ψ, at a frequency of 1000 c/sec or more, from Table II. The values of α obtained for the platinum/aqueous solution containing 0.002 M oxidant and 0.001 M reductant (in 1 N sulphuric acid) and *vice versa* are 0.619 and 0.633, respectively. It is interesting to note that the value of α for either of the redox ratios is higher than those obtained at the same temperature using equimolar concentrations of the reactants in the same dilution range. This shows that the rectification becomes more pronounced when the concentration of either of the two components (oxidant and reductant) exceeds the other in the mixture. The rather large limiting values of ψ with increasing frequency (Table II) suggest some change in the state of the electrode surface which accounts for the higher values of the transfer coefficient. The rate constant for such systems can be determined at frequencies below 500 c/sec, if the diffusion coefficients for oxidants and reductants at concentrations of 0.002 M and 0.001 M are known.

ACKNOWLEDGEMENT

The author is indebted to Dr. G. C. BARKER (A.E.R.E., Harwell, England) for his valuable suggestions in explaining some of the results discussed.

SUMMARY

When the equimolar concentration of a redox couple is 0.002 M or less, the values of the transfer coefficient for Pt/Fe^{2+}, Fe^{3+}, 1 N H_2SO_4, can be determined by the faradaic rectification method, independent of the change in concentration of the reactants. With increasing concentration (above 0.002 M) of the redox couple (at equal concentrations), the transfer coefficient, α, decreases. The values of α and of K_s, the rate constant at equilibrium, were determined for a platinum/aqueous solution containing equimolar concentrations of ferrous and ferric ions at infinite dilution.

The values of α obtained with unequal concentrations of oxidant and reductant in the redox mixture are found to be higher than those obtained with equimolar concentrations.

REFERENCES

1 K. S. G. Doss and H. P. Agarwal, *J. Sci. Ind. Res. (India)*, 9B (1950) 280.
2 K. B. Oldham, *Trans. Faraday Soc.*, 53 (1957) 80.
3 G. C. Barker, *Anal. Chim. Acta*, 18 (1958) 118; G. C. Barker, R. Faircloth and A. Gardner, *Nature*, 181 (1958) 247.
4 K. S. G. Doss and H. P. Agarwal, *Proc. Indian Acad. Sci.*, 34 (1951) 263.
5 K. S. G. Doss and H. P. Agarwal, *Proc. Indian Acad. Sci.*, 35 (1952) 45.
6 A. Vdovin, *Dokl. Akad. Nauk SSSR*, 120 (1958) 554.
7 H. P. Agarwal, *J. Electronal. Chem.*, 5 (1962) in press.
8 F. C. Anson, *J. Am. Chem. Soc.*, 83 (1961) 2387.
9 M. Senda and P. Delahay, *J. Phys. Chem.*, 65 (1961) 1580.
10 G. C. Barker and Yeager, *Transactions of the Symposium on Electrode Processes*, John Wiley and Sons, Inc., New York, 1961, p. 325.
11 P. Delahay, M. Senda and C. H. Weis, *J. Am. Chem. Soc.*, 83 (1961) 312.
12 G. S. Hartley and D. F. Runnicles, *Proc. Roy. Soc. (London)*, 168 (1938) 401.
13 L. Onsager and R. M. Fuoss, *J. Phys. Chem.*, 36 (1932) 2689.
14 H. P. Agarwal, *Proc. Indian Acad. Sci.*, 56 (1962) 108.

FARADAIC ADMITTANCE, A DIFFUSION MODEL. III

S. K. RANGARAJAN

Central Electrochemical Research Institute, Karaikudi (India)

(Received June 28th, 1962)

The object of the present paper is to compare the expressions for the elements of the equivalent circuit derived earlier[1] for a *perturbed* diffusion model, with those obtained for other models which explicitly take into account the corrections due to the migration in the diffuse double layer or the adsorption of the reactants.

§ 1. DIFFUSE DOUBLE LAYER

MATSUDA AND DELAHAY[2] have solved the eqns.

$$D_i \frac{\partial}{\partial x}\left(\frac{\partial C_i}{\partial x} + \frac{Z_i F}{RT} \cdot C_i \frac{\mathrm{d}\phi}{\mathrm{d}x}\right) = \frac{\partial C_i}{\partial t} \quad (i = O,R) \tag{1}$$

with the initial and the boundary conditions

$$C_i(x,0) = C_i^{\circ} \exp(-Z_i F\phi/RT)$$

$$D_i\left(\frac{\partial C_i}{\partial x} + C_i \frac{Z_i F}{RT} \frac{\mathrm{d}\phi}{\mathrm{d}x}\right) = \frac{\pm i(t)}{nFA} \tag{2}$$

(positive sign for oxidant, negative sign for reductant)

$$\lim_{x\to\infty} C_i(x,t) = C_i^{\circ}$$

(Z_i is the valency of the species i, with sign; $\phi(x)$ is potential distribution in the Gouy Layer).

To solve this, the electrode-bulk region has been split up into two regions $x \leqslant \delta_i$ and $x \geqslant \delta_i$. In the former, migration-effects are taken into account whereas for the latter, they are omitted. The solutions are fitted at the boundary $x = \delta_i$ so as to ensure the continuity of mass transfer (*i.e.*, the concentrations and the fluxes are equated at $x = \delta_i$). The effects of this on faradaic impedance manifest themselves in the elements of the equivalent circuit which are proved to be

$$R_r' = R_r + \frac{RT}{n^2F^2}\left(\frac{a_O}{\varkappa C_O^{\circ} D_O} + \frac{a_R}{\varkappa C_R^{\circ} D_R}\right) \tag{3}$$

$$1/\omega C_r' = 1/\omega C_r$$

with

$$a_i = g_i(\pm|Z_i/Z|) - g_i(\mp|Z_i/Z|)$$

$$g_i(y) = \frac{\exp[(y-\tfrac{1}{2}) \mid Z \mid F \mid \phi_o \mid /RT] - 1}{(y-\tfrac{1}{2})} \qquad (i = O,R)$$

assuming a $Z:Z$ supporting electrolyte with upper signs for the case of repulsion, and lower, for attraction. (It may be mentioned that in the expression for R_r, I_o represents the *apparent exchange current density*; MATSUDA AND DELAHAY[2] use the notations R_s and $1/\omega C_s$ instead of R_r' and $1/\omega C_r'$ as given here).

A sufficient condition for this first approximation to hold good is

$$\left(\frac{\omega^{\frac{1}{2}}}{\varkappa D_i^{\frac{1}{2}}}\right) g_i(\pm \mid Z_i/Z \mid) < 0.1$$

An alternate solution has been obtained by RANGARAJAN[3] and the expressions for R_s and $1/\omega C_s$ are of the same form except that a_o in this case, has the corrected form

$$a_o = 2\varkappa \int_0^\infty \sinh\left(\pm \left|\frac{Z_i}{Z}\right| \frac{F \mid \phi \mid}{RT}\right) dx \qquad (4)$$

In either case, it may be seen that such *perturbations* cause a *parallel shift* in the straight line R_r *vs.* $1/\sqrt{\omega}$ *i.e.*, only the intercept gets changed. Also $1/\omega C_r$ remains unaffected, to this order of approximation. A comparison of the above model with the perturbed diffusion model shows that $a_i/\varkappa$ corresponds to $\nu_i[(D_{i_2}/D_{i_1}) - 1]$ so that, $a_i < 0$ (attraction in the diffuse layer) implies $D_{i_2} < D_{i_1}$ and $a_i > 0$ (repulsion of the oxidant) corresponds to the condition $D_{i_2} > D_{i_1}$. The parameters which may be taken as indexes to the *order of perturbations* in the two models are $(1/\varkappa)\sqrt{\omega/D_{i_2}} \cdot a_o$ and $\sqrt{\omega/D_{i_2}} \cdot \nu_o\sqrt{D_{i_2}/D_{i_1}}$.

In the case of *repulsion*, it may be easily seen that order of $a_o/\varkappa^2(\sqrt{\omega/D_{i_2}})^2$ corresponds to that of

$$\nu_o^2 \cdot \frac{\omega}{D_{o_1}}\left(1 - \frac{D_{o_1}}{D_{o_2}}\right) \Big/ g(- \mid Z_i/Z \mid)$$

This may be seen to be so if one writes $a_i/\varkappa$ as equal to

$$\frac{g(\mp \mid Z_i/Z \mid)}{\varkappa}\left[\frac{g(\pm \mid Z_i/Z\mid)}{g(\mp \mid Z_i/Z \mid)} - 1\right]$$

and relate $1/\varkappa\ g(\mp|Z_i/Z|)$ with ν_i and D_{i_2}/D_{i_1} with $g(\pm|Z_i/Z|)/g(\mp|Z_i/Z|)$. The orders of $g(-|Z_i/Z|)$ and $(1-D_{i_1}/D_{i_2})$ can be taken to be that of unity, (this corresponds to the case $D_{i_1} < D_{i_2}$). Hence a sufficient condition for the validity of the first order approximation in the diffuse layer model *viz.*, $a_i\omega/\varkappa^2 D_{i_2} \ll 1$, is equivalent to the condition $\nu_o^2\omega/D_{i_1}$ in this diffusion model.

Similarly in the case of *attraction* in the diffuse layer, a *sufficient* condition for writing (3) will be $a_i^2\omega/\varkappa^2 D_{i_2} \ll 1$ which is of the same order as $\nu_i^2\omega/D_{i_2}$ (since in this case $D_{i_1} > D_{i_2}$).

§ 2. ADSORPTION OF THE REACTANTS

To explain the anomalous value of the phase angle between the alternating components of the faradaic current and the potential, LAITINEN AND RANDLES[4] had proposed a model wherein it was assumed that "the loss or gain of an electron by

ions of the reactant (*which remain adsorbed* on the electrode surface) contribute to the additional current". The rate equation in its usual form is assumed and surface concentration is related to the current through

$$nFA \frac{\mathrm{d}}{\mathrm{d}t}[(1 - x)\Gamma] = i(t)$$

where Γ = total surface concentration and x = fraction of coverage of the oxidant.

It has been shown that a corresponding diffusion model would be that wherein $D_{i_1} \gg D_{i_2}$ so that $v_i\sqrt{\omega/D_{i_1}} \ll 1$. Such a model has been discussed in detail elsewhere[5] and one comes across some striking similarities, on comparison.

As an example, one may compare the boundary conditions

$$\begin{aligned} -i(t)/nAF &= -\frac{\mathrm{d}}{\mathrm{d}t}(1 - x)\Gamma \\ &= \frac{\mathrm{d}}{\mathrm{d}t} x\Gamma \end{aligned} \tag{5}$$

$$D_{O_1} \frac{\partial C_O}{\partial x}\Big)_{x = v_O} = 0$$

$$D_{O_1} \frac{\partial C_O}{\partial x}\Big)_{x = 0} = i(t)/nAF$$

$$D_{O_1} \frac{\partial^2 C_O}{\partial x^2} = \frac{\partial C_O}{\partial t}$$

For the diffusion model one can easily prove that

$$\frac{\mathrm{d}}{\mathrm{d}t}\left[\int_0^{v_O} C_O(x,t)\,\mathrm{d}x\right] = \int_0^{v_O} D_{O_1} \frac{\partial^2 C_O}{\partial x^2}\,\mathrm{d}x = \left(D_{O_1} \frac{\partial C_O}{\partial x}\right)_0^{v_O} = -i(t)/nAF \tag{6}$$

Thus the condition

$$\frac{\mathrm{d}}{\mathrm{d}t}\left[\int_0^{v_O} C_O(x,t)\mathrm{d}x\right] = -i(t)/nAF$$

corresponds to

$$\frac{\mathrm{d}}{\mathrm{d}t}(x\Gamma) = -i(t)/nAF$$

and similarly

$$\frac{\mathrm{d}}{\mathrm{d}t}\left[(1 - x)\Gamma\right] = +i(t)/nAF$$

corresponds to

$$\frac{\mathrm{d}}{\mathrm{d}t}\left[\int_0^{v_O} C_R(x,t)\,\mathrm{d}x\right] = +i(t)/nAF.$$

In an earlier communication[5] $x(t)\Gamma$, the instantaneous surface concentration of the oxidant, has been identified with $v_O C_O(0,t)$. Further comparisons based on this model were found to be consistent and self-explanatory. This was possible because of the inequality $v_O\sqrt{\omega/D_{O_1}} \ll 1$.

As $x(t)\Gamma$ refer to those ions that are *bound* to the surface, it may be interesting to relate them *not to* $v_O C_O(0,t)$ of the diffusion model, but to the *integrated instantaneous* number present in the volume bounded by the planes $x = 0$ and $x = v_O$ with unit area of cross section; *i.e.*, to relate the quantities $x(t)\Gamma$ and $\int_0^{v_O} C_O(x,t)\mathrm{d}x$ (moles/cm^2).

$\bar{C}_O(x,p)$ has been proved to be[5] equal to

$$C_O^\circ + A \exp(\sqrt{p/D_{O_1}}x) + B \exp(-\sqrt{p/D_{O_1}}x)$$

with

$$A - B = \bar{i}(p)/nFA\sqrt{D_{O_1}p} \tag{7}$$

and

$$A - B \exp(-2\sqrt{p/D_{O_1}} \cdot v_O) = 0 \tag{8}$$

$$\mathscr{L}\left[\int_0^{v_O} C_O(x,t)\mathrm{d}x\right] = C_O^\circ v_O - (A - B)\sqrt{D_{O1}/p} + \sqrt{D_{O1}/p}(A \exp\sqrt{p/D_{O_1}}v_O - B \exp -\sqrt{p/D_{O_1}}v_O) \tag{9}$$

which gives, in view of eqns. (7) and (8)

$$\mathscr{L}\left[\int_0^{v_O} C_O(x,t)\mathrm{d}x\right] = C_O^\circ v_O - \bar{i}(p)/nFAp \tag{10}$$

Hence, if $x(t)\Gamma$ is taken to correspond to $\int_0^{v_O} C_O(x,t)\ \mathrm{d}x$, $x_O\Gamma$ corresponds to $C_O^\circ v_O$ $(= \int_0^{v_O} C_O(x,0)\mathrm{d}x)$ and

$$\frac{\mathrm{d}}{\mathrm{d}t}\left[\Delta x(t)\Gamma\right] \rightarrow -\frac{i(t)}{nFA}$$

Also

$$\int_0^{v_O}\left[C_O(x,t) + C_R(x,t)\right]\ \mathrm{d}x = \text{constant} = C_O^\circ v_O + C_R^\circ v_R \tag{11}$$

Cf. (ref.[4]) the equation: $x(t)\Gamma + [1-x(t)]\Gamma = \text{constant} = \Gamma$.

§ 3. ADSORPTION OF THE REACTANTS WITH DIFFUSION AS THE SOLE MODE OF MASS TRANSFER

LLOPIS *et al.*[6] have made a detailed study of the effects of the adsorption process in the expression of the faradaic impedance of an electrode, in the presence of a redox system and it will be of interest to note how the results of some other models are deduced from these. It is also shown that under certain conditions, the results of the *perturbed* diffusion model correspond with those derived when the adsorption rates have not been assumed to be infinite.

The surface coverage θ_i, net anodic current j and the net desorption rate v_i are related as

$$\varkappa\frac{\mathrm{d}\theta_i}{\mathrm{d}t} = \pm\frac{j}{nF} - v_i \tag{12}$$

where

$$v_i = k_i^a\theta_i - k_i^c(1 - \bar{\theta})^r C_i = -D_i\left(\frac{\partial C_i}{\partial x}\right)_{x\,=\,0}$$

(positive sign for $i = O$, negative for $i = R$)

For the particular case, $D_O = D_R = D$, and $K_O^s = K_R^s = K^s$ and $K_O^d = K_R^d = K^d$, LLOPIS *et al.*[6] have proved that the amplitudes of the periodic variations $\delta\theta_i$ in the surface coverage of the oxidant and the reductant and the phase angle of $\delta\theta_i$ with the current are given by $\delta\theta_i = \Delta\theta_i \exp(i\omega t)$

with

$$\Delta\theta_O = -\Delta\theta_r = \frac{\Delta j}{nF} \cdot \frac{1 + \beta K^s(1 - i)}{k^d + \varkappa\omega i + \varkappa\omega\beta k^s(1 + i)} \tag{13}$$

where the current (net anodic) is taken as $\Delta j \exp(i\omega t)$ and β stands for $(1-\bar{\theta})/\sqrt{2\omega D}$ ($i = \sqrt{-1}$).

Diffusion is the sole mode of mass transfer and the presence of diffusion is *felt* in the quantitative expressions through the *dimensionless* parameter $\beta k^s = (1 - \bar{\theta})\, k^s/\sqrt{2\omega D}$. A small value of this parameter, compared to unity, means (by writing the parameter $\beta\, k^s$ in the form

$$\frac{k^s(1 - \bar{\theta})}{\omega}\sqrt{2D/\omega}$$

and noting that $\sqrt{D/\omega} \approx$ diffusion layer thickness, the significance of this parameter can be realised at once) that diffusion *has no say in the matter*. Similarly, a high value for βk^s (at least comparable to unity) is to be expected when a diffusion phenomenon is to have significance.

Yet another dimensionless parameter of interest is $\varkappa\omega/k^d$ where $\varkappa$ has the dimensions of moles/cm^2. A zero value of this *equates* the net current with the flux $\pm [D_i(\delta/C_i)/(\delta/x)]_{x=0}$ as has been assumed for the linear diffusion models with no specific adsorption of the reactants. Thus, it is seen that a small $\varkappa\omega/k^d$ is another index of deviation from the classical diffusion model[7]; (we are considering, of course, only small deviations).

Some limiting cases which illustrate the significance of the parameters βk^s and $\varkappa\omega/k^d$ are:

(i) $\beta k^s \gg 1$, $\varkappa\omega/k^d \ll 1$ and $\beta k^s \varkappa\omega/k^d \ll 1$.

(ii) $\beta k^s \ll 1$, $\varkappa\omega/k^d \gg 1$ and $\beta k^s \varkappa\omega/k^d \ll 1$.

(iii) $\varkappa\omega/k^d \gg 1$ and $\beta k^s \varkappa\omega/k^d \gg 1$.

(iv) $\beta k^s \gg 1$, $\varkappa\omega/k^d \ll 1$ and $\beta k^s \varkappa\omega/k^d \gg 1$.

(v) $\beta k^s \gg 1$, $\varkappa\omega/k^d \ll 1$ and $\beta k^s \varkappa\omega/k^d$: o (1).

Case (i)

$$\Delta\theta_O \to \frac{\Delta j}{nF} \cdot \frac{\beta k^s(1 - i)}{k^d}$$

so that

$$\frac{\Delta\theta_O}{{}^\circ\theta_O} \to \frac{\Delta j}{nF} \frac{k^s(1 - \bar{\theta})}{k^d\, {}^\circ\theta_O} \frac{1}{\sqrt{i\omega D}}$$

$$= \frac{\Delta j}{nF} \frac{1}{C_O{}^\circ\sqrt{i\omega D}} \left[\text{since } \frac{{}^\circ\theta_i}{(1 - {}^\circ\theta_i)} = \frac{k^s}{k^d} C_i{}^\circ\right] = \frac{\partial C_O}{C_O}$$

a result already derived for the classical case[7].

Case (ii)

$$\Delta\theta_O = \frac{\Delta j}{nFk^d} \cdot \frac{1 + \beta k^s(1 - i)}{(1 + \varkappa\omega i/k^d + \varkappa\omega\beta k^s(1 + i)/k^d)} \rightarrow \frac{\Delta j}{nF\varkappa i\omega} \tag{14}$$

a result derived already by LAITINEN AND RANDLES[4]. The relationship of this limiting case with the diffusion model has already been discussed[5]. (Also refer § 2 of this paper.)

In view of the form taken by $\Delta\theta_O$ in the limit, it can be seen that the parameter $\varkappa$ can be identified with Γ (of ref.[4]), the total surface coverage (*cf.* the result derived by LAITINEN AND RANDLES which reads $\mathrm{d}(x)/\mathrm{d}t = -i(t)/nFA/$; the discrepancy in the sign is due to the different conventions chosen for the net current in the two formulations[6]).

Case (iii)

By writing

$$\Delta\theta_O = \frac{\Delta j}{nFk^d} \cdot \frac{1 + \beta k^s(1 - i)}{\left\{1 + \frac{\varkappa\omega_i}{k^d}[1 + \beta k^s(1 - i)]\right\}}$$

it is observed that

$$\Delta\theta_O \rightarrow \frac{\Delta j}{nF\varkappa\omega i} \text{ if } \frac{\beta k^s\varkappa\omega}{k^d} \gg 1 \text{ and } \frac{\varkappa\omega}{k^d} \gg 1;$$

Note that this result was also obtained for case (ii).

Case (iv)

Since $\beta\ k^s \gg 1$ and $\varkappa\omega/k^d \ll 1$ with $\beta k^s\varkappa\omega/k^d \gg 1$, $\Delta\theta_O \rightarrow \Delta j/nF\varkappa i\omega$ — a limiting result identical with those for cases (ii) and (iii).

Case (v)

For the particular case, $\beta k^s \gg 1$, $\varkappa\omega/k^d \ll 1$, with $\varkappa\omega\beta k^s/k^d$ comparable to unity.

$$\Delta\theta_O \rightarrow \frac{\Delta j}{nFk^d} \cdot \frac{\beta k^s(1 - i)}{1 + \varkappa\omega\frac{\beta k^s}{k^d}(1 + i)} = \frac{\Delta j}{nF\varkappa i\omega} \cdot \frac{\beta k^s\varkappa\omega(1 + i)/k^d}{1 + \beta k^s\varkappa\omega(1 + i)/k^d} \tag{15}$$

To compare this with the result one would obtain with the diffusion model[1], we identify the ratio $\Delta\theta_O/\theta$ $(t = 0)$ with

$$\frac{\int_0^{\nu_O}[C_O(x,t) - C_O(x,0)]\mathrm{d}x}{\int_0^{\nu_O} C_O(x,0)\mathrm{d}x}$$

(*cf.* § 2, for its significance). It can easily be seen that,

$$\mathscr{L}\left[\frac{\int_0^{\nu_o}[C_o(x,t) - C_o(x,0)]\mathrm{d}x}{C_o^\circ \nu_o}\right]$$

$$= -\frac{1}{C_o^\circ \nu_o}\left[\frac{\bar{\imath}(p)}{nFAp} - \left(A \exp\sqrt{p/D_{o_1}}\nu_o - B \exp\left(-\sqrt{p/D_{o_1}}\nu_o\right)\right)\sqrt{D_{o_1}}/p\right]$$

(refer eqn. (9))

$$= -\frac{\bar{\imath}(p)}{nFApC_o^\circ \nu_o} + \frac{i(p)}{nFApC_o^\circ \nu_o} \cdot \frac{\exp\left(-\sqrt{p/D_{o_1}}\nu_o\right)(1 + D'_o)}{1 + D'_o \exp\left(-2\sqrt{p/D_{o_1}}\nu_o\right)}$$

$$= -\frac{\bar{\imath}(p)}{nFApC_o^\circ \nu_o} \cdot 1 - \frac{(1 - \sqrt{p/D_{o_1}}\nu_o)}{1 - 2D'_o/(1 + D'_o)\sqrt{p/D_{o_1}}\nu_o}$$

approximately.

$$D'_o = \frac{\sqrt{D_{o_2}} - \sqrt{D_{o_1}}}{\sqrt{D_{o_2}} + \sqrt{D_{o_1}}}.$$

(for Details, refer Appendix I, reference 1).

$$= -\frac{\bar{\imath}(p)}{nFApC_o^\circ \nu_o}\left[\frac{\sqrt{p/D_{o_1}}\nu_o(1 - D'_o)/(1 + D'_o)}{1 - 2D'_o/(1 + D'_o)\sqrt{p/D_{o_1}}\nu_o}\right] \tag{16}$$

Since

$$1 - D'_o = 2\sqrt{D_{o_1}}/(\sqrt{D_{o_1}} + \sqrt{D_{o_2}})$$

and

$$1 + D'_o = 2\sqrt{D_{o_2}}/(\sqrt{D_{o_1}} + \sqrt{D_{o_2}})$$

eqn. (16) becomes

$$= \frac{-i(p)}{nFApC_o^\circ \nu_o} \frac{\sqrt{p/D_{o_2}}\nu_o}{1 + (1 - \sqrt{D_2/D_1})\sqrt{p/D_{o_2}}\nu_o} \tag{17}$$

Hence, one can prove that, for the steady state,

$$\int_0^{\nu_o}[C_o(x,t) - C_o(x,0)]\mathrm{d}x / \int_0^{\nu_o} C_o(x,0)\mathrm{d}x$$

$$\to \frac{I}{nFAC_o^\circ \nu_o i\omega} \cdot \frac{\sqrt{\omega/2D_2} \cdot \nu_o(1 + i)}{1 + \sqrt{\omega/2D_2}(1 + i)\nu_o(1 - \sqrt{D_2/D_1})} \tag{18}$$

Correspondingly, for the steady state, as obtained from the model used by LLOPIS *et al.* and under the conditions $\beta k^s \gg 1$ and $\varkappa\omega/k^d \ll 1$, we have

$$\frac{\Delta\theta_o}{{}^{\circ}\theta_o} = + \frac{\Delta j}{nF\varkappa i\omega\,{}^{\circ}\theta_o} \cdot \frac{\beta k^s \varkappa\omega(1+i)/k^d}{1 + \varkappa\omega\beta k^s(1+i)/k^d}$$

$$= + \frac{\Delta j}{nF(i\omega)C_o{}^{\circ}\,\dfrac{\varkappa k^s}{k^d}} \cdot \frac{\sqrt{\omega/2D_2}(1+i)\varkappa k^s/k^d}{1 + \sqrt{\omega/2D_2}(1+i)\dfrac{\varkappa k^s}{k^d}(1-\bar{\theta})} \qquad (19)$$

Since I represents the total *cathodic* current, $-I/A$ corresponds to j, the net *anodic* current density. Hence we conclude, on comparison of the expressions in eqns. (18) and (19), that the parameter v_o (cm) corresponds to $\varkappa k^s/k^d$ and $\sqrt{D_{o_2}/D_{o_1}}$ to $(1-\bar{\theta})$. Since, for this limiting case a small $\bar{\theta}$ is to be expected, we find that, generally, the value for D_{i_1}/D_{i_2} will have to be greater than unity, if comparisons are to be made with adsorption models.

CONCLUSIONS

The results obtained in the diffusion model are compared with those derived from models wherein the effects due to the migration in the diffuse double layer or due to the specific adsorption of the reactants are accounted for. No conclusions have been attempted with regard to the interpretation of these parameters. The limiting expressions that one obtains from the adsorption model of LLOPIS *et al.* are also discussed in detail.

ACKNOWLEDGEMENT

The author wishes to thank Professor K. S. G. Doss, Director, Central Electrochemical Research Institute, Karaikudi for his kind encouragement and valuable discussions during this work.

SUMMARY

The results obtained for the *perturbed* diffusion model[1] are compared with those obtained for other models, taking into consideration the effects due to migration in the diffuse double layer or the specific adsorption of the reactants. The limiting expressions obtained from the adsorption model of LLOPIS *et al.* are also discussed.

REFERENCES

1 S. K. RANGARAJAN AND K. S. G. DOSS, *J. Electroanal. Chem.*, 5 (1963) 114.
2 H. MATSUDA AND P. DELAHAY, *J. Phys. Chem.*, 64 (1960) 332; H. MATSUDA, *ibid.*, 64 (1960) 339.
3 S. K. RANGARAJAN, (unpublished results).
4 H. A. LAITINEN AND J. E. B. RANDLES, *Trans. Faraday Soc.*, 51 (1955) 54.
5 S. K. RANGARAJAN AND K. S. G. DOSS, *J. Electroanal. Chem.*, 4 (1962) 237.
6 J. LLOPIS, *Electrochim. Acta*, 1 (1959) 130.
7 J. E. B. RANDLES, *Discussions Faraday Soc.*, 1 (1947) 11.

POLAROGRAPHIC STUDIES IN MOLTEN MAGNESIUM CHLORIDE–SODIUM CHLORIDE–POTASSIUM CHLORIDE EUTECTIC

H. C. GAUR AND W. K. BEHL*

Department of Chemistry, University of Delhi, Delhi (India)

(Received August 10th, 1962)

INTRODUCTION

In recent years polarographic methods have been increasingly used for studying several aspects of molten salt systems, *e.g.* oxidation states of metals, analysis of solutions and the mechanism of electron transfer processes at the microelectrode. Applications in several fused binary and ternary metal nitrates and chlorides have been adequately covered in recent reviews[1-4]. This communication describes the polarographic behaviour of several metal ions in the fused ternary eutectic $MgCl_2$–NaCl–KCl (50 : 30 : 20 mole percent) which were studied as a part of extended electrochemical investigations[5,6] in this solvent.

Assuming that the electrode is subjected only to concentration polarization, that the electrode process is reversible, and that metal is deposited at the electrode surface at unit activity, the current–voltage functions of the polarographic wave on a solid microelectrode would be expressed by the equation[7]:

$$E_{\text{m.e.}} = E_m^0 - \frac{2.303RT}{nF} \log \frac{k_s}{f_s} + \frac{2.303RT}{nF} \log (i_d - i) \qquad (1)$$

where the symbols have their usual thermodynamic significance; in this case the half-wave potential ($E_{\frac{1}{2}}$) would shift with metal ion concentration (C) according to:

$$E_{1/2} = \frac{2.303RT}{nF} \log \frac{C}{2} \qquad (2)$$

However, in the use of solid microelectrodes several other variable factors, such as the nature of the electrode and the surface conditions, the reactivity of the deposited metal, and the overvoltages in the deposition of ions on that electrode, have also to be considered. DELIMARSKII AND GORODISKII[8] in applying the theory of absolute reaction rates found, on the other hand, that polarographic waves with *solid* microelectrodes should be represented by the equation:

$$E_{\text{m.e.}} = E_{1/2} - \frac{2.303RT}{\alpha nF} \log \left(\frac{i}{i_d - i} \right) \qquad (3)$$

which is similar to the Heyrovský–Ilkovič equation[9] for a dropping mercury

* Present address: *Department of Chemistry, New York University, New York 3, N.Y. (U.S.A.).*

electrode; the activity of the metal deposited on the microelectrode would be a function of the current strength, and $E_{\frac{1}{2}}$ would be independent of the depolarizer concentration.

In polarographic studies in molten salts using solid microelectrodes, the applicability of both eqns. (1)[10-12] and (3)[8,13-15] has been claimed. This aspect is considered in detail in this paper.

EXPERIMENTAL TECHNIQUES

Experiments were carried out in a pyrex cylindrical cell which was about 350 mm long, 58 mm. o.d., closed at the bottom and having a side tube near the top. In use, the mouth of the vessel was closed with a rubber stopper having a number of holes which supported, *inter alia*, the different electrodes, thermocouple sheath and gas delivery tube. The cell was vertically mounted in an electrical furnace up to a depth of about 200 mm (melt level in the vessel being 40–60 mm) and could either be connected to a vacuum manifold or a stream of hydrogen chloride or nitrogen.

The electrical furnace, rated at 750 watts and having a rectangular cavity 80 × 80 × 200 mm deep, was fabricated in the laboratory. A set of four heaters on the sides provided the bulk of the heat which was just less than that needed for a particular temperature setting; an additional heater at the bottom was switched on or off, as needed, by a temperature controller, the temperature sensing element being a chromel–alumel thermocouple. The working temperature was 475°. A temperature control of $\pm$ 2° of the melt in the cell was obtained.

The solvent was prepared by a method essentially similar to that employed by LAITINEN *et al.*[17] for the eutectic LiCl–KCl. A stream of oxygen-free nitrogen was passed over the melt surface throughout the experiment. The solvent in the cylindrical vessel was divided by using tubes with pyrex fritted-glass bottoms (medium porosity). The electrolytic resistance between two platinum foil electrodes dipping into two such compartments was of the order of 20 ohms and diffusion of the solute from one such compartment to another over a period of 3–4 h was not detected so long as the melt level in the compartments was the same.

The solvent had a decomposition potential span of over 2.5 V, limited by the electrolysis of the solvent itself, *i.e.*, anodic oxidation of Cl^- and cathodic reduction of Mg(II). A polarogram of the solvent with a platinum microelectrode (area 0.126 mm^2) and Pt/Pt(II) in the melt as reference, (Fig. 1), showed a residual current of the order of 2–3 μA up to an applied potential of -1.8 V.

The system Pt/Pt(II) in the melt was used as reference, having been shown earlier to be reversible and depolarized[6]; the Pt(II) solution was about 0.01 molal.

At the close of the experiment the compartment containing the solution was removed, and cooled in a desiccator. The contents were analysed for total chloride, from which the weight of the solvent was calculated.

Microelectrodes for polarographic work were fabricated by sealing suitable lengths of 0.3–0.4 mm platinum wires into 6–8 mm soda–lead glass tubing (Corning 0120) with the end ground flush with the seal to expose the cross-section. These were polished with 0/3 emery paper and the projected surface areas were determined by optical micrometry.

A manual polarographic arrangement was used. In all the experiments steady values of the current were recorded.

RESULTS

Polarography of lead, cadmium and tin

Representative polarograms for the reduction of Pb(II) and Sn(II) at a platinum microelectrode are presented in Figs. 1 and 2. Similar waves were obtained for reduction of Cd(II)[5], deposition potentials being *ca.* −1.15 V *vs.* a 0.01 molal platinum reference. In all these cases, in the concentration range 3–71 mmolal the current showed a plateau; the limiting current, after applying the residual current correction,

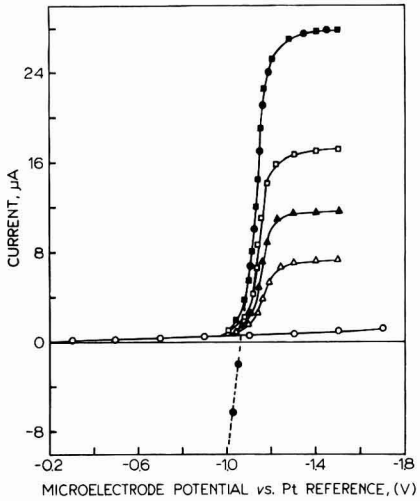

Fig. 1. Polarograms of lead(II) chloride. ○, residual polarogram of the melt; △, ▲, □ and ■, polarograms obtained on adding 21.6, 37.8, 60.2 and 82.6 mg of lead chloride to 7.16 g of the solvent; ●, reverse polarogram of curve ■.

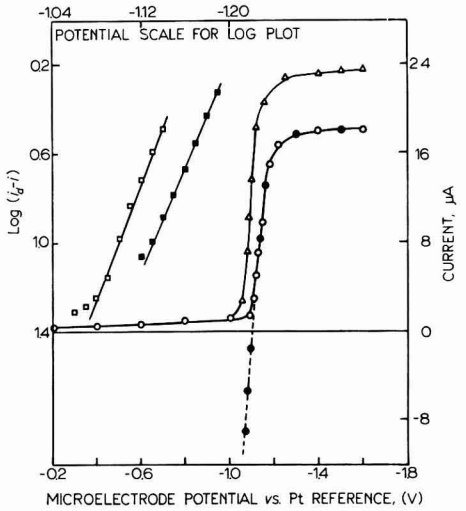

Fig. 2. Polarograms of tin(II) chloride. ○ and △, polarograms obtained on adding 29.6 and 35.4 mg of tin chloride to 5.47 g of the solvent; ●, reverse polarogram of curve ○; □ and ■, logarithmic plots for curves △ and ○, respectively.

was proportional to the metal ion concentration (Table I). The data recorded in different experiments, in separate batches of the melt and in one case using microelectrodes with different areas, give an estimate of the precision with which *in situ* metal ion concentration may be determined in these cases.

On reversing the direction of polarization, the curves were retraced up to the deposition potential, passed through zero current axis and then changed sign due to

TABLE I

RELATIONSHIP BETWEEN LIMITING CURRENTS AND CONCENTRATION

Reducible species	*Concentration (C) (mmolal)*	*Limiting current (i_d) (μA)*	*Limiting current constant. (μA mmolal^{-1} per sq. mm of the projected area)*
Cd(II)[a]	3.227	2.30	10.08
	7.866	5.55	9.95
	13.52	8.50	8.89
	17.10	12.50	10.34
Cd(II)[a]	12.60	9.00	10.10
	21.58	15.20	9.96
	37.27	35.60	13.51*
			Average 9.9
			Average deviation 0.3
Sn(II)[a]	3.278	2.10	9.06
	13.50	14.6	15.30*
	28.54	17.6	8.72
	34.14	22.1	9.15
Sn(II)[a]	51.50	32.8	9.00
	68.76	42.5	8.74
			Average 8.93
			Average deviation 0.16
Pb(II)[b]	10.85	6.4	4.69
	18.98	10.8	4.53
	30.25	16.7	4.39
	41.51	26.9	5.16
Pb(II)[a]	11.48	3.7	4.56
	22.34	7.0	4.43
	40.74	15.4	5.35*
Pb(II)[a]	10.45	2.35	3.18*
	20.90	6.35	4.30
	29.41	8.20	3.95
Pb(II)[b]	28.64	15.20	4.22
	41.60	26.00	4.97
	54.91	41.00	5.76*
Pb(II)[a]	23.19	6.25	3.81
	40.03	13.80	4.88
	52.76	16.25	4.36
	71.85	22.05	4.34
			Average 4.53
			Average deviation 0.03

* Not used for calculation of average.
[a] Electrode area 0.071 mm^2.
[b] Electrode area 0.126 mm^2.

anodic dissolution of the metal deposited at the microelectrode. At potentials anodic to the deposition potential, the current gradually decreased to the residual value at that potential. Once the deposited metal was stripped off, the residual polarogram could be further retraced up to the dissolution potential of platinum. In this way it was possible to take several polarograms of the same or different solutions with the same microelectrode; for a given polarogram the current values were reproducible within $\pm$ 2%. The anodic process Sn(II) $\rightarrow$ Sn(IV) did not take place within the above potential range[18].

Polarographic reduction of Co(II), Ag(I), Ni(II) and Pt(II)

Some of the typical polarograms using platinum microelectrodes with an area 0.071 mm^2 are shown in Fig. 3. In these cases the electrolysis current did not show a clearly defined limiting current plateau. At the end of the S-shaped curve, the current

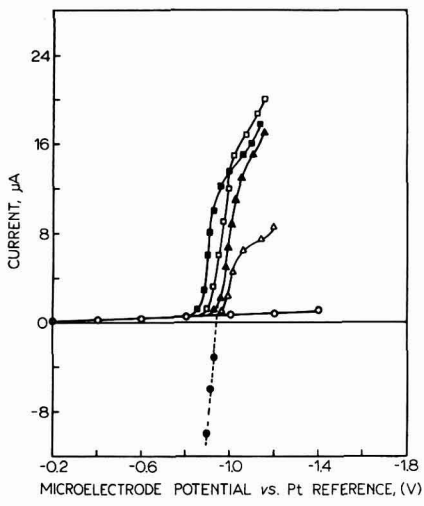

Fig. 3. Polarograms of chlorides of cobalt, nickel and silver. ○, residual polarogram of the melt; △ and ▲, polarograms obtained on adding 19.0 and 27.6 mg of $CoCl_2$ to 4.64 g of the melt; ●, reverse polarogram of curve ▲; □, polarogram of AgCl; ■, polarogram of $NiCl_2$.

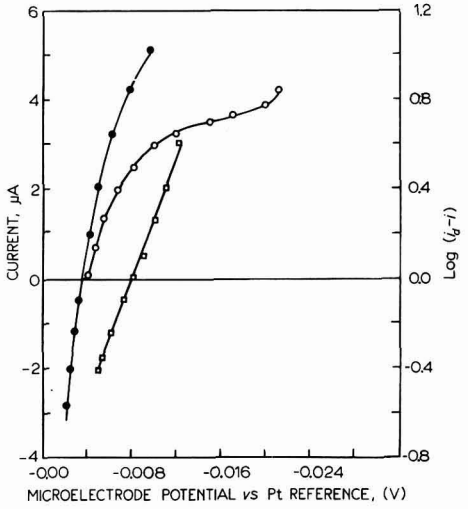

Fig. 4. Polarogram of platinum(II) chloride. ○, initial polarogram of $PtCl_2$; ●, reverse and successive polarogram of curve ○; □, logarithmic plot for the initial polarogram.

increased on increasing the cathodic polarization and also with time. At higher metal ion concentrations the plateau was even less well defined, and the increment in the current was not proportional to the increase in metal ion concentration. On reversing polarization the cathodic portion of the current was not reproducible, although in each case the current became zero at the deposition potential. The deposited metal could be completely stripped off, slopes of the curves showing that the process was uncomplicated by any passivation etc.[19]. With a stripped microelectrode surface, current values in the polarograms for the reduction of Ag(I), Ni(II) and Co(II) were reproducible to within 5%. In the reduction of Pt(II) on a platinum microelectrode,

the initial and successive polarograms on the same microelectrode (with or without stripping) are presented in Fig. 4. After the initial polarogram the current readings for successive polarograms in this case were reproducible to within 4–5%.

Polarography of Cu(I), Fe(II) and Cr(II)

Polarograms for the cathodic reduction of these ions (Fig. 5) using platinum microelectrodes (area 0.071 mm²) were similar to those obtained for the deposition of Pt(II), Ag(I), Ni(II) and Co(II). Well defined limiting current plateaux were not obtained and the rising portions of the curve were not retraced on reversed polariza-

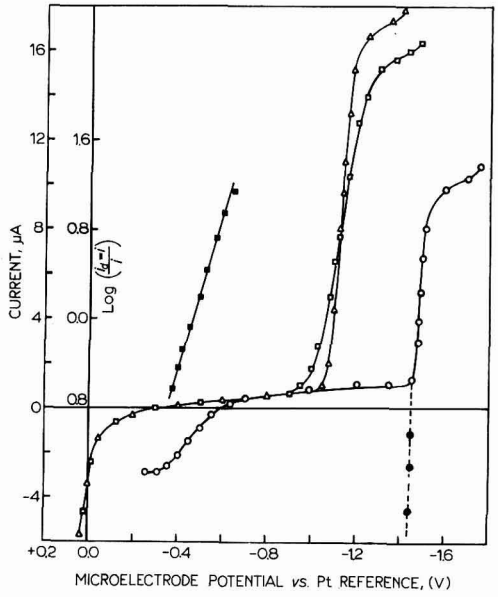

Fig. 5. Polarograms of chlorides of metals with two stable oxidation states in the melt. ○, polarogram of chromium(II) chloride; ●, reverse polarogram of curve ○; △, polarogram of iron(II) chloride; □, polarogram of copper(I) chloride; ■, logarithmic plot for the anodic wave of chromium(II) chloride, curve ○.

tion; at potentials anodic to the deposition potential the metal could be completely stripped off, the electrolysis current decreasing to the residual value at that potential. The anodic processes Cr(II) → Cr(III), Fe(II) → Fe(III) and Cu(I) → Cu(II) commenced at about −0.65, −0.11 and −0.10 V respectively *vs.* a 0.01 molal platinum reference. A limiting current plateau was obtained only for the oxidation process Cr(II) → Cr(III); the redox potential for Fe(II)-Fe(III) and Cu(I)–Cu(II) couples[6] are quite close to the platinum dissolution potential and hence these polarograms overlapped with the anodic platinum wave.

DISCUSSION

Polarograms

It has been observed that limiting current plateaux were obtained only in the reduction of Sn(II), Pb(II) and Cd(II) at the platinum microelectrode. In these cases

the working temperature (475°) is higher than the melting point of the metals, which therefore deposit as *liquid* on the microelectrode. Once the microelectrode surface is covered with the liquid film, there is no appreciable change in its area on further deposition. Thus a limiting wave can be visualized in such cases.

In other cases the metal is deposited as a *solid* on the platinum microelectrode. The deposit may have a dendritic growth and/or may increase the surface roughness. In such cases the area of the microelectrode and hence the electrolysis current would increase with increased polarization and also with time. This explains why the electrolysis current does not attain a limiting plateau in these cases. This "increasing current" tendency first observed by LAITINEN, LIU AND FERGUSON[11] for deposition of a solid metal on a microelectrode is not serious if electrodes with larger areas[12] are employed; however in the latter case rather dilute solutions have to be employed in order that the reference system does not become polarized, and even then the precision of the data (5–8%) is of a lower order than that obtained with microelectrodes of smaller areas (2–3%) as used in the present study. Since the area of microelectrode, with a metal deposited as solid on it, will not be well-defined, it also follows that the proportionality of limiting current with concentration is less reproducible in these cases.

A rather large increase in the electrolysis current in the deposition of Pt(II) after the initial polarogram is probably due to an increase in surface area of the microelectrode due to enhanced roughness from the deposition of the metal or anodic stripping.

Analysis of the polarographic waves

In the absence of a clearly defined limiting current plateau and the tendency of the electrolysis current to increase with time, a critical analysis of the polarograms involving the deposition of metals as solid on the platinum microelectrode was not possible in all the cases. The $E_{\text{m.e.}}$ *vs.* log $(i_d - i)$ plot for the initial polarogram for the reduction of Pt(II) on the platinum microelectrode (Fig. 4) had a slope of 0.072 compared with 0.0742 for a two-electron process at 475°. In other cases, also, the polarographic wave approximately obeyed eqn. (1). This leads to the conclusion that in all these cases deposition of solid metal occurred reversibly and without any alloy formation.

Polarograms in the reduction of Sn(II) were also satisfactorily expressed by eqn. (1). In four typical cases plots of $E_{\text{m.e.}}$ *vs.* log $(i_d - i)$ had slopes of 0.072, 0.084, 0.084 and 0.073 V compared with the calculated value of 0.0742 for a two-electron process at 475°. Changes in $E_{\frac{1}{2}}$ with increase in concentration were of the same order as the calculated values.

However, current–voltage functions of the polarographic waves for Pb(II) and Cd(II) reductions on platinum microelectrode could not be satisfactorily expressed by eqn. (1). $E_{\text{m.e.}}$ *vs.* log $(i_d - i)$ plots were always curved (Fig. 6). On the other hand, $E_{\text{m.e.}}$ *vs.* log $[i/(i_d - i)]$ plots were rectilinear, the slopes of the plots being of the order of the calculated pre-logarithimic terms and $E_{\frac{1}{2}}$ was, within limits of experimental error, independent of the metal ion concentration.

Liquid metals are known to be quite corrosive even at relatively low temperatures[20]. Platinum has appreciable solubility in liquid cadmium and also forms an alloy[21] of the the type Cd_2Pt. Similarly platinum has been reported to have poor resistance to attack by molten lead or tin[20]. Deposition of these metals as liquid on platinum

microelectrode could lead to the formation of "surface alloys" resulting in the current-dependent activity of the deposited metal. In such cases current–voltage functions of waves should be represented by a Heyrovský–Ilkovič type equation[9]. This is supported by the data for the reduction of Pb(II) and Cd(II) in this paper. Different behaviour in the reduction of Sn(II) could arise if the alloy formation was relatively slower, so that for the duration of the observation the equilibrium metal activity at the platinum microelectrode surface remained constant; further work would be needed to substantiate this point.

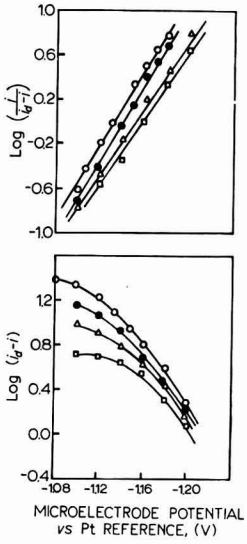

Fig. 6. Logarithmic plot for lead(II) chloride polarograms corresponding to different curves in Fig. 1.

ACKNOWLEDGEMENTS

The authors are grateful to the Council of Scientific and Industrial Research (India) for a financial grant, for the Junior Research Fellowship held by one of them (W.K.B.) and to Prof. R. P. MITRA and Dr. B. D. KHOSLA for their helpful suggestions.

SUMMARY

Polarographic studies of several metal ions in the molten ternary eutectic $MgCl_2$–NaCl–KCl at 475° were carried out using flush platinum microelectrodes as the cathode and Pt/Pt(II) in the melt as a reference. Limiting waves were obtained only in the reduction of those ions (Cd^{2+}, Pb^{2+} and Sn^{2+}) where the metal was deposited as a *liquid* on the microelectrode at the working temperature (475°); in these cases, the wave height was proportional to the metal ion concentration in the solution. In other cases, where the metal was deposited as a *solid* on the microelectrode, the electrolysis current at the end of the S-shaped curve increased with increasing cathodic polarization and also with time; this severely limited the analytical utility of these polarograms. It was found that the current–voltage functions of the polarographic wave in the former case (metal deposited as liquid) were expressed by the Heyrovský-

Ilkovič equation due to "surface-alloy" formation on the platinum microelectrode; in other cases the usual equation involving the deposition of a metal without alloy formation with the electrode was obeyed.

REFERENCES

1 Yu. K. Delimarskii, *Usp. Khim.*, 23 (1954) 766.
2 G. J. Hills and J. E. Oxley, *Z. Anal. Chem.*, 173 (1960) 5.
3 H. C. Gaur and B. B. Bhatia, *J. Sci. Ind. Res. (India)*, 21A (1962) 16.
4 G. J. Hills and K. E. Johonson, *Advances in Polarography (Proceedings of the 2nd International Congress on Polarography, Cambridge, 1959)*, Vol. 3, Pergamon Press, London, 1960, p. 974.
5 W. K. Behl and H. C. Gaur, *J. Sci. Ind. Res. (India)*, 20B (1961) 183; *Bull. Nat. Inst. Sci. (India)*, in press.
6 W. K. Behl, *Polarographic Studies and Standard Electrode Potential Measurements in Molten Magnesium Chloride–Sodium Chloride–Potassium Chloride Eutectic as Solvent*, University of Delhi, 1962, *Ph.D. Thesis*.
7 I. M. Kolthoff and J. J. Lingane, *Polarography*, 2nd ed., Vol. I, Interscience Publishers, Inc., New York, 1952, p. 203.
8 Yu. K. Delimarskii and O. V. Gorodiskii, *Dopovidi. Akad. Nauk. Ukr. RSR.*, (1955) 540.
9 J. Heyrovský and D. Ilkovič, *Collection Czech. Chem. Commun.*, 7 (1955) 198.
10 E. D. Black and T. de Vries, *Anal. Chem.*, 27 (1955) 906.
11 H. A. Laitinen, C. H. Liu and W. S. Ferguson, *Anal. Chem.*, 30 (1958) 1266.
12 D. L. Maricle and D. N. Hume *Anal. Chem.*, 33 (1961) 1188.
13 N. G. Chovnyk, *Dokl. Akad. Nauk SSSR.*, 100 (1955) 495; *Zh. Fiz. Khim.*, 30 (1956) 277.
14 Yu. K. Delimarskii and I. D. Panchenko, *Dokl. Akad. Nauk SSSR.*, 91 (1953) 115.
15 I. D. Panchenko, *Ukr. Khim. Zh.*, 21 (1955) 468; 22 (1956) 153.
16 E. M. Skobets, *Zh. Fiz. Khim.*, 33 (1959) 2807.
17 H. A. Laitinen, W. S. Ferguson and R. A. Osteryoung, *J. Electrochem. Soc.*, 104 (1957) 516.
18 N. G. Chovnyk, *Dokl. Akad. Nauk SSSR.*, 87 (1952) 1033.
19 H. A. Laitinen and H. C. Gaur, *J. Electrochem. Soc.*, 104 (1957) 730.
20 E. C. Miller, *Liquid Metals Handbook*, editor R. N. Lyon, U.S. Atomic Energy Commission and Navy Department, Washington D.C., 1952, p. 144.
21 H. A. Laitinen, R. P. Tischer and D. K. Roe, *J. Electrochem. Soc.*, 107 (1960) 546.

EXPERIMENTAL EVALUATION OF RATE CONSTANTS FOR DIMERIZATION OF INTERMEDIATES FORMED IN CONTROLLED-POTENTIAL ELECTROLYSES

LOUIS MEITES

Department of Chemistry, Polytechnic Institute of Brooklyn, Brooklyn, N.Y. (U.S.A.)

(Received September 20th, 1962)

INTRODUCTION

Earlier work on this subject[1,2] has already indicated that the literature contains numerous examples of controlled-potential electrolyses that lead to the formation of two products in varying proportions: one a dimer of an intermediate formed at the electrode surface by the reduction (or oxidation) of the starting material, the other the product of further reduction (or oxidation) of that intermediate; *e.g.*, the reduction of picric acid[3–5], the reduction of aromatic ketones[6,7], the oxidation of hydrazine[8], and various others. Coulometric measurements in all such cases give apparent n-values that vary with the initial concentration of the starting material; the higher this concentration, *ceteris paribus*, the higher the concentration of the intermediate at any instant, the greater the rate of its dimerization compared to that of its further reduction, and the smaller the apparent n-value.

Until now it has been impossible to evaluate the rate constant of the dimerization step in such a process, for lack of quantitative information on the relation between this rate constant and the experimentally observable parameters. This information has now been obtained by numerical calculations based on a simple model of the reaction mechanism. This paper describes in detail the results of these calculations, an empirical equation which reproduces these results with an accuracy better than can be expected from the experimental data, and the manner in which the significant parameters in this equation are obtained experimentally.

THEORETICAL

It is assumed that the overall reaction consists of three steps: the n_1-electron reduction of the starting material O to yield an intermediate I

$$O + n_1 e \rightarrow I, \tag{1a}$$

the pseudo-second-order reaction in which I dimerizes to yield an electrolytically inactive dimer D

$$2I \rightarrow D, \tag{1b}$$

and the n_2-electron reduction of the intermediate to the final reduced form R

$$I + n_2 e \rightarrow R. \tag{1c}$$

It is further assumed that the I produced at the electrode surface is at once homogeneously dispersed throughout the solution. In fact, the concentration of I will always be somewhat higher in the diffusion layer than has been taken into account in the following calculations, so that the results of the calculations must be lower than the actual extents of dimerization. Intuitively, however, it appears that the error will not be serious unless the rate of dimerization is very high. In principle it is possible to vary the extent of dimerization of the intermediate over a wide range (most simply by varying the initial concentration of the starting material). Moreover, it will be seen that experimental measurements made under such conditions that the rate of dimerization is very high are not well suited to the evaluation of the rate constant of the dimerization step. Thus one would normally prefer to select those conditions where the extent of dimerization is not too large. In this range of conditions this assumption is unlikely to lead to gross error.

On the basis of this assumption the rates of reactions (1) are given by

$$\frac{dC_O}{dt} = -\beta_O C_O = -\beta_O C_O^\circ e^{-\beta t} \tag{2a}$$

$$\frac{dC_I}{dt} = \tfrac{1}{2} k C_I^2 \tag{2b}$$

$$\frac{dC_R}{dt} = \beta_I C_I \tag{2c}$$

The values of β appearing in equations (2a) and (2c) are given, according to the Nernst diffusion-layer theory, by

$$\beta_i = \left(\frac{D}{\delta}\right)_i \frac{A}{V} \tag{3}$$

where D is the diffusion coefficient of the reducible species and δ the thickness of its diffusion layer, A is the electrode area, and V is the volume of the solution. Since the current obtained for the reduction of the i'th species is given by

$$i_i = n_i F D_i A C_i / \delta_i \tag{4}$$

it follows that

$$\beta_i = \frac{i_i / C_i}{n_i F V} \tag{5}$$

or, if i is expressed in mF per sec (a more convenient unit in coulometric work than amperes), C in mmoles per liter, and V in liters,

$$\beta_i = \frac{i_i / C_i}{n_i V} \tag{6}$$

It has been assumed here that $\beta_O = \beta_I$. Data on pairs of closely related substances that would bear on the validity of this assumption (which is reasonable in view of the general similarity of molecular sizes and structures to be expected between O and I), are nearly impossible to find. For vanadium (II) and (III) in bisulfate solutions under otherwise completely identical conditions, β_{II}/β_{III} is approximately 1.25[9]. But vanadium(II) and (III) form sulfate complexes of widely different stabilities, so that

the differences between their ions must be much larger than those between typical organic molecules and the free radicals formed on reducing them.

Applying the conservation rule, then, combining equations (1) gives

$$\frac{dC_I}{dt} = \beta C_O^\circ e^{-\beta t} - \beta C_I - kC_I^2 \qquad (7)$$

where β is the common value of β_O and β_I. It is the solution of this equation that has constituted the basis of the work reported here.

TECHNIQUE OF SOLUTION AND INTEGRATION

The form of eqn. (7) and the values that must be assigned to the variables proved ill suited to solution and integration with the desired accuracy by available analog computation equipment. The following procedure has therefore been followed.

The values chosen for β and C_O° define the value of dC_I/dt at zero time. This leads immediately to a value of C_I at a subsequent instant, where typically $\beta t = 0.01$. This in turn permits each of the terms on the right hand side of eqn. (7) to be computed at that instant, and from the new value of dC_I/dt one can then compute C_I at the instant where $\beta t = 0.02$, and so on. In general, calculations have been performed at intervals in βt of 0.01 up to 0.1, of 0.02 thence to 0.3, of 0.05 thence to 1, of 0.1 thence to 3, and of 0.2 thence to 10. Special care is necessary at points where the interval width changes; using the calculated value of dC_I/dt gives an erroneous value of C_I at the end of the first wider interval, and the nature of the eqn. is such that this soon leads to oscillating values of C_I that would cause difficulties in integration. In such cases the preceding values of dC_I/dt were extrapolated to obtain a value more properly representative of the wider interval.

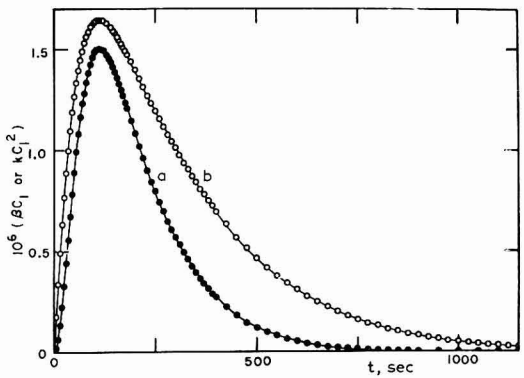

Fig. 1. Plots of ○ $10^6\beta C_I$ and ● $10^6 kC_I^2$ *vs.* t, as calculated for $\beta = 0.006$ sec^{-1}, $k = 20$ l mole^{-1} sec^{-1}, and $C_O^\circ = 0.001$ mole-l^{-1} with interval width Δ.

From such a computation there results a series of values of βC_I and of kC_I^2 which, when plotted against time, give curves resembling those in Fig. 1. These were carefully drawn on sheets of graph paper of appropriate size, and integrated by means of a Keuffel and Esser No. 4242 polar planimeter set for nearly the highest sensitivity.

To avoid errors resulting from variations of paper size with humidity, the paper was allowed to stand in a room of essentially constant humidity for several weeks before measurement, and each area was computed by comparing the planimeter reading with that obtained for a reference area nearly coincident with the curve. Variations of the order of 0.3% were found in the calibration figures obtained with sheets taken from the same lot of paper at different times of the year.

Four integrations of each curve were performed. The planimeter could always be read to better than $\pm 0.1\%$. The standard deviation of a single result was always of the order of $\pm 0.15\%$. The standard deviation of a set of 15 measurements of reference areas (delineated by straight printed lines on a single sheet of graph paper) was $\pm 0.09\%$.

The results of these integrations are, of course, incorrect; forcibly fitting the curve by a series of straight lines yields calculated values that are in error at every point. Calculations and integrations employing different interval widths give results such as those shown in Fig. 2, where the calculated percentage of I that dimerizes is plotted

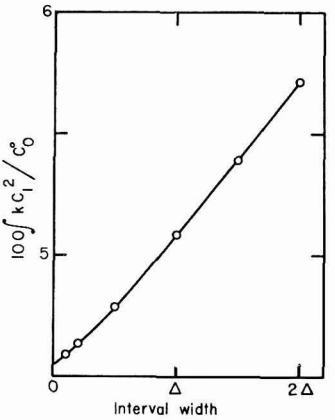

Fig. 2. Effect of interval width on the directly calculated value of

$$100 \int_0^\infty kC_I^2 \mathrm{d}t/C_o^\circ$$

(*i.e.*, the percentage of I that undergoes dimerization by reaction (1b). For a definition of the interval-width parameter Δ see the accompanying text.)

against the interval width. An interval width of Δ corresponds to the set of values given above (intervals of 0.01 in βt up to 0.1, etc.); for the calculations denoted by an interval width of 0.5Δ, each of the individual interval widths was halved (intervals of 0.005 in βt up to 0.1, of 0.01 up to 0.3, etc.).

Because the points in Fig. 2 do not lie on a straight line, extrapolation to zero interval width in this fashion is extremely tedious. An alternative procedure was therefore devised which yielded exactly the same result within the error of the graphical construction. It is obvious that the sum of

$$\int_0^\infty \beta C_I \mathrm{d}t \quad \text{and} \quad \int_0^\infty kC_I^2 \mathrm{d}t$$

obtained from any one calculation must be equal to C_0°. However, because of the systematic errors caused by the use of finite interval widths, this was never the case. It was therefore assumed that the relative error in $\int_0^\infty kC_I^2 dt$ was twice that in $\int_0^\infty \beta C_I dt$ — *i.e.*, that

$$(1 - 2\varepsilon) \int_0^\infty kC_I^2 dt + (1 - \varepsilon) \int_0^\infty \beta C_I dt = C_0^\circ \tag{8}$$

From this eqn. the relative error ε could be calculated, and this in turn permitted the calculation of a *corrected* integral, $(1 - 2\varepsilon) \int_0^\infty kC_I^2 dt$. All these steps were then repeated for a different interval width, almost always 2Δ. The value of ε was generally about 0.02 for an interval width of Δ and about 0.04 for an interval width of 2Δ. The behavior of the resulting *corrected* integral at different interval widths is shown in Fig. 3. This is linear and has a much smaller slope than the curve shown in Fig.2,

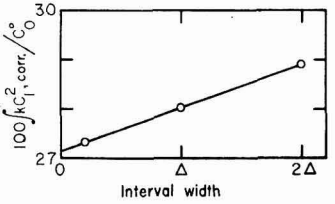

Fig. 3. Effect of interval width on the value of

$$100 \int_0^\infty kC_I^2 dt / C_0^\circ$$

after correction as described by eqn. (8) and the accompanying text.

and equally well-behaved curves were obtained with other values of the fundamental parameters. Hence the final values of $\int_0^\infty kC_I^2 dt$ were obtained by a linear numerical extrapolation of the above *corrected* integral from interval widths of 2Δ and Δ to an interval width of zero.

Various tests for internal consistency of the results, some of which are obvious from the Figs. that follow, indicate that none of the final values for percentage dimerization can be in error by as much as 0.3% absolute.

RESULTS AND DISCUSSION

It is convenient to express the results of these calculations in terms of a parameter π, which is the fraction of the intermediate I that undergoes dimerization, and which is given by

$$\pi = \frac{1}{C_0^\circ} \int_0^\infty kC_I^2 dt \tag{9}$$

where the integral is understood to be corrected to zero interval width as described above. Very little insight into the form of eqn. (7) is needed to produce the conviction that there are in fact only two fundamental variables, β and the product kC_0°. Calculations have been performed for values of β ranging from 0.001–0.05 sec^{-1} and for values of kC_0° ranging from 0.0002–5 sec^{-1}. For $\beta = 0.001$ sec^{-1} a simple mass-transfer-controlled single-step electrolysis would reach 90% completion after 2303

TABLE I

EXTENT OF DIMERIZATION UNDER VARIOUS CONDITIONS

The values in the body of the table are for the parameter π defined by eqn. (9).

$10^3 kC_0^\circ$ (sec^{-1})	$10^3\beta$ (sec^{-1})										
	1	1.5	2	3	4	5	7	10	15	20	50
0.5	0.1092	0.0744	0.0563	0.0378	0.0285	0.0230	0.0169	—	—	—	—
1	0.1850	0.1329	0.1039	0.0726	0.0559	0.0455	0.0333	0.0245	0.0170	—	—
2	0.2838	0.2159	0.1755	0.1288	0.1026	0.0855	0.0647	0.0478	0.0337	0.0268	—
5	0.437	0.358	0.306	0.2414	0.2001	0.1725	0.1367	0.1058	0.0783	0.0629	0.0308
10	0.559	0.482	0.427	0.354	0.306	0.2709	0.2234	0.1799	0.1387	0.1146	0.0605
20	0.669	0.602	0.552	0.480	0.430	0.391	0.336	0.2819	0.2274	0.1935	0.1111
50	0.779	0.731	0.693	0.634	0.590	0.554	0.500	0.443	0.379	0.336	0.2187
100	0.836	0.800	0.771	0.724	0.688	0.659	0.612	0.560	0.499	0.455	0.325
200	0.879	0.852	0.830	0.796	0.768	0.745	0.707	0.664	0.611	0.571	0.443
500	0.916	0.898	0.884	0.860	0.841	0.825	0.799	0.767	0.728	0.697	0.589
1000	0.935	0.922	0.911	0.894	0.880	0.868	0.848	0.824	0.794	0.770	0.682
2000	0.950	0.940	0.932	0.919	0.909	0.900	0.885	0.867	0.844	0.826	0.757
5000	0.960	0.953	0.947	0.937	0.929	0.923	0.911	0.898	0.881	0.867	0.815

sec; for $\beta = 0.05$ the corresponding time would be 46 sec. The calculations thus cover the entire conveniently accessible range of mass-transfer rates.

The values of π are given in Table I. A few values at high β and low kC_O° have not been computed, for under these conditions the extent of dimerization is too small for convenient coulometric measurement. Should values under these conditions be wanted for some other purpose, they can be very closely approximated by assuming π to be proportional to kC_O°. This reflects the fact that the value of C_I at any instant is insensitive to variations in the slight extent of dimerization under these conditions.

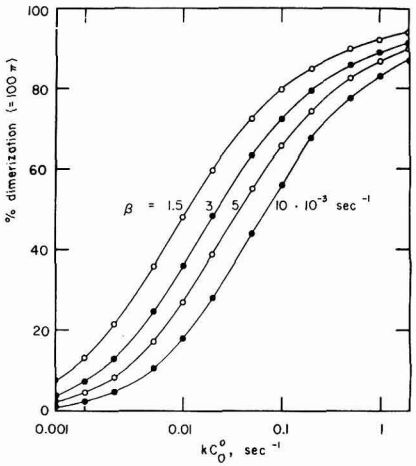

Fig. 4. Plots of 100π (*i.e.*, the percentage of I that dimerizes, after correction to zero interval width) *vs.* log kC_O° for various values of β.

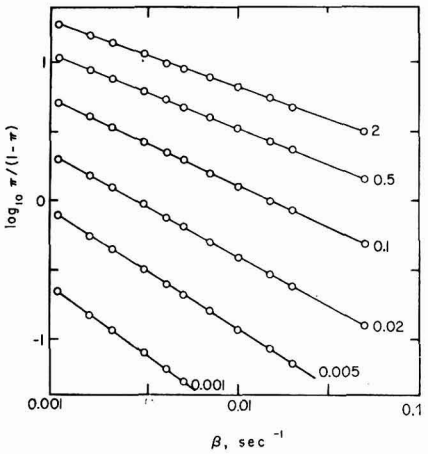

Fig. 5. Typical plots of $\log \pi/(1 - \pi)$ *vs.* log β. The number beside each line gives the coresponding value of kC_O° in sec^{-1}.

Some of these values are shown in Fig. 4. The familiar sigmoid shape of the curves suggests attempting to linearize them by plotting $\log \pi/(1 - \pi)$ *vs.* $\log \beta$. Such plots are accurately linear over the range $0.05 \leq \pi \leq 0.96$, as is shown by Fig. 5. However, it follows from the preceding paragraph that the variation of π with $\log kC_O^\circ$ is asymmetrical, so that linear plots are not obtained if $\log kC_O^\circ$ is taken as the independent variable instead of $\log \beta$. Hence it is convenient to write an equation of the form

$$\log \pi/(1 - \pi) = s_1 - s_2 \log \beta \qquad (10)$$

where s_1 and s_2 are functions of $\log kC_O^\circ$ and have the values given in Table II. These values serve to reproduce the calculated values of $\log \pi/(1 - \pi)$ with an average error smaller than ± 0.002. In turn they can be reproduced by eqns. of the form

$$s_i = t_i + t_i' \log kC_O^\circ + t_i'' (\log kC_O^\circ)^2 \qquad (11)$$

with an average error of about ± 0.004. There finally results an equation that may be written as

$$\log \pi/(1 - \pi) = -(0.295 + 0.485 \log \beta) + (0.646 + 0.088 \log \beta)(\log kC_O^\circ) - (0.145 + 0.024 \log \beta)(\log kC_O^\circ)^2 \qquad (12)$$

which is suitable for the direct calculation of kC_O° from experimental data on β and

TABLE II

PARAMETERS FOR THE CALCULATION OF LOG $\pi/(1-\pi)$

The body of the table gives values of the parameters s_1 and s_2 in eqn. (10). They were found by least-squares calculations from the original values of π at each of the values of kC_o° given in the first column.

kC_o° (sec^{-1})	s_1	s_2
0.0005	(−0.91)	(1.0)
0.001	−0.644	0.969
0.002	−0.402	0.897
0.005	−0.110	0.817
0.01	+0.102	0.761
0.02	0.305	0.711
0.05	0.548	0.648
0.1	0.708	0.604
0.2	0.860	0.565
0.5	1.036	0.518
1	1.158	0.487
2	1.274	0.459
5	1.378	0.432

π. When eqn. (12) was used to calculate kC_o° from values of β and π appearing in Table I, it reproduced the values of kC_o°, from which π had originally been calculated, with a mean error of $\pm 1.1\%$.

It may be remarked that if $n_1 = n_2 = 1$ and $\pi = 0.5$, so that the apparent n-value is 1.5 (*cf.* eqn. (13) below), a relative error of only $\pm 0.1\%$ in the experimental evaluation of the current integral is propagated into one of $\pm 0.3\%$ in the value of π (moreover, the ratio of the latter error to the former increases with increasing n_1/n_2), and this in turn leads to a relative error of $\pm 1.1\%$ in kC_o° as calculated from eqn. (12). This second propagation of errors becomes increasingly unfavorable as π deviates from 0.5 in either direction, as is clear from Fig. 4. In practice, therefore, one would prefer to adjust C_o° and β so as to obtain a value of π that is not too far from 0.5. From these considerations it follows that the error of just over $\pm 1\%$ inherent in the use of eqn. (12) is trivial by comparison with the probable experimental errors.

Thus the evaluation of k rests upon a prior knowledge of three quantities: C_o°, π, and β. The first is trivial. The value of π follows directly from the apparent n-value by virtue of the fact that

$$n_{app.} = n_1 + (1 - \pi)n_2 \tag{13}$$

or

$$\pi = (n_1 + n_2 - n_{app.})/n_2 \tag{14}$$

It goes without saying that enough must be known about the mechanism to permit decisions to be made about the values of n_1 and n_2. Comparing the values of π calculated from those of $n_{app.}$, under various assumptions regarding n_1 and n_2, with the behavior predicted by eqn. (12) may be of much help in making such decisions; except where a very large overall number of electrons is involved, it should suffice to find a pair of values of n_1 and n_2 that yields an approximately linear plot of log $\pi/(1-\pi)$ *vs.* log C_o° at constant β. For example, it has been suggested[3] that $n_1 = 17$

and $n_2 = 1$ for the reduction of picric acid in hydrochloric acid solutions, but these numbers, when applied to the experimental data[5], yield values of π that vary far too rapidly, and it is therefore clear that n_1 must be much smaller than 17 in this process.

The evaluation of β is not so straightforward. It has been customary in dealing with simple processes to evaluate β from the slope of a linear plot of log i *vs.* time. LINGANE[10] first showed that the current–time curve for such a process obeys the equation

$$i = i^{\circ}\, e^{-\beta t} \tag{15}$$

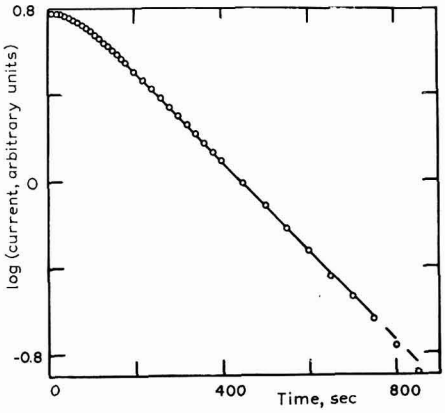

Fig. 6. Calculated current–time curve for $\beta = 0.006$ sec^{-1}, $kC_O^{\circ} = 0.02$ sec^{-1}, and $n_1 = n_2$. The quantity identified as *current, arbitrary units* is actually $10^6(\beta C_O^{\circ} e^{-\beta t} + \beta C_I)$, which is proportional to the current.

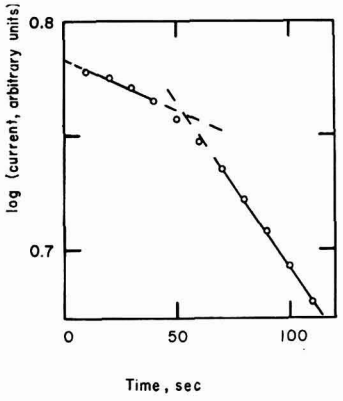

Fig. 7. Initial portion of Fig. 6.

(provided, of course, that other factors, such as resistance-limiting of the initial current, do not interfere). The danger of applying this procedure to the present case is illustrated by Fig. 6, which shows a typical calculated current–time curve. (Currents plotted here and in Fig. 7 have been obtained by extrapolation to zero interval width.) Initially, when C_I is low, nearly all of the I formed in reaction (1a) undergoes further

reduction according to (1c). So the concentration of material undergoing reduction remains virtually constant, and consequently the current too remains virtually constant if $n_1 = n_2$, as will often be the case. This behavior is apt to call forth the treatment of experimental data illustrated by Fig. 7, which strikingly resembles a current–time curve previously published[11] for the oxidation of hydrazine. Quite clearly the slope of the initial portion of such a curve is totally devoid of any relation to the value of β.

Two procedures are available. One is to plot either the current or its logarithm against time, extrapolate to zero time, and combine the resulting value of i° with eqn. (5) or (6) to calculate β. As Fig. 7 shows, the slope of either curve will tend to be small in this region, and therefore the error in β is unlikely to be significant in the light of what is said below regarding the manner of its propagation. The other is to plot $\log_{10} i$ *vs.* time in the usual fashion, measure the slope S of its long final linear portion (*cf.* Fig. 6), and compare this value with Fig. 8 to obtain the value of β.

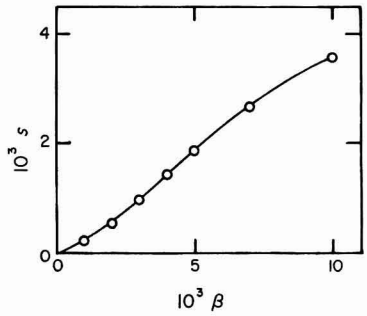

Fig. 8. Variation of S, the slope of the ultimate linear portion of a plot of $\log_{10} i$ *vs.* t, with β

The values plotted in this Fig. were obtained by summing $\beta C_O^\circ e^{-\beta t}$ and βC_I at each of a number of times, extrapolating the sum (which is proportional to the current) to zero interval width, plotting the logarithm of the extrapolated sum against time as in Fig. 6, and comparing the slope of the straight-line portion with the value of β taken for the original calculations. (It may be stressed that it is *not* permissible to compute β by the obvious equation $\beta = 2.303\, S$, for this is never true, and values of β thus obtained are always too high by 20% or more). Unexpectedly, it appeared from these calculations that for any value of β the ratio S/β is virtually independent (to better than $\pm 5\%$) of the value of kC_O°. Variations in the quantity of electricity accumulated during the electrolysis are almost entirely due, therefore, to variations in the duration of the initial portion of the curve, where the ultimate exponential decay of current with time has not yet begun, and, of course, in i°.

Of these two procedures, the second is more complex, more tedious, and less accurate; the first is unqualifiedly to be preferred.

For values of π around 0.5, an error of $\pm 5\%$ in β leads to an almost equal relative error in k. From the experimental data it should therefore be possible to evaluate β to such a degree of accuracy that its error will be responsible for an error in k that is much smaller than the error attributable to the measurement of the current integral.

SUMMARY

The equations and graphs presented here make possible the direct algebraic evaluation of the rate constant for the dimerization of an intermediate formed in a controlled-potential electrolysis whose mechanism is described by eqns. (1). The best results should be those obtained from data at such initial concentrations that about half of the intermediate dimerizes, provided that the stirring is sufficiently efficient to justify the assumption that the concentration of the intermediate is the same throughout the solution. Wide variations in the extent of dimerization can be effected by variations in initial concentration, electrode area, and solution volume. If this assumption is not justified — only experience with the technique and with the results obtained by it can permit this to be decided — there will be a progressively increasing deviation of $\log \pi/(1 - \pi)$ from the values predicted by eqn. (12), in the direction of an anomalously rapid increase of π with increasing C_O°. In this event there would remain the possibility of extrapolating the calculated values of k to $C_O^\circ = 0$.

Experimental tests of this and other methods of calculating the rate constant for the dimerization of an intermediate in an electrolytic reduction or oxidation will be described elsewhere.

REFERENCES

1 L. MEITES, *Controlled-Potential Electrolysis*, Chap. XLIX in *Physical Methods of Organic Chemistry* (*Techniques of Organic Chemistry*, Vol. 1, ed. A. WEISSBERGER), Interscience Publishers, Inc., New York, 1960.
2 L. MEITES, *Record Chem. Progr.*, 22 (1961) 80.
3 J. J. LINGANE, *J. Am. Chem. Soc.*, 67 (1945) 1916.
4 I. BERGMAN AND J. C. JAMES, *Trans. Faraday Soc.*, 50 (1954) 60.
5 L. MEITES AND T. MEITES, *Anal. Chem.*, 28 (1956) 103.
6 P. J. ELVING AND J. T. LEONE, *J. Am. Chem. Soc.*, 80 (1958) 1021.
7 M. J. ALLEN, *Proc. Intern. Comm. Electrochem. Thermodyn. Kinet.*, 6th Meeting, (1955) 481.
8 S. KARP AND L. MEITES, *J. Am. Chem. Soc.*, 84 (1962) 906.
9 Y. ISRAEL AND L. MEITES, unpublished results.
10 J. J. LINGANE, *J. Am. Chem. Soc.*, 67 (1945) 1916; *cf.* also J. J. LINGANE, *Electroanalytical Chemistry*, 2nd ed., Interscience Publishers Inc., New York, 1958, pp. 225–228.
11 S. KARP AND L. MEITES, *J. Am. Chem. Soc.*, 84 (1962) 906, Fig. 2.

DROP-GROWTH, AND MAXIMA, IN A DROPPING-MERCURY ELECTRODE

G. KNOWLES AND M. G. KEEN

Water Pollution Research Laboratory, Stevenage (England)

(Received September 3rd, 1962)

Considerable interest has been expressed in the motion of the mercury and the sample during polarography with the dropping-mercury electrode, especially when the abnormal polarographic currents, called maxima, are present. The wide-bore dropping-mercury electrode[1,2,3] was used in the present work, but the conventional electrode probably behaves in much the same way, since the two are very similar in polarographic behaviour. Physically they differ in that the wide-bore electrode points upwards at 45° and has a much larger internal diameter (0.8 mm as against 0.05 mm); this greater size makes it comparatively easy to study.

METHOD

The motion of the mercury was recorded by a cine-camera exposing a frame every 0.008 sec, and the polarographic current was displayed, throughout the life of each drop, on a d.c. oscilloscope. Motion of the aqueous sample, a hard tap-water with no added electrolyte, was shown by the deflection of coloured *traces* produced by the fall of small crystals of acid-fuchsin through the water; these were photographed with electronic-flash illumination. The polarographic current was due to about 8 p.p.m. by weight of dissolved oxygen, the potential of the dropping-mercury electrode being that corresponding to the maximum at the positive end of the first oxygen plateau, *i.e.*, about −0.5 V with respect to the saturated calomel electrode. A directly-immersed silver rod, coated with silver chloride, was used as the *reference* electrode. The resistance of the circuit, external to sample and electrodes, was about 400 ohms.

Figure 1 is an example of the type of cine-film records obtained; the electrodes were working in separate but chemically identical solutions. A maximum was present in the left-hand but not in the right-hand series, in which the potential of the dropping-mercury electrode was 0.05 V more negative.

BEHAVIOUR OF MERCURY

By examining the whole length of the film, which covered the lives of several drops, it was found that the growth and detachment of the drops were identical for the two electrodes, and exhibited the following interesting features:

(1) immediately before the fall of the mercury drop the aqueous sample entered the capillary for a length of about 1 mm between the mercury and the glass (Fig. 2, diagram B). After the drop had broken away, the mercury meniscus, already in the bore of the capillary, retreated still further down until about 2 mm from the exit

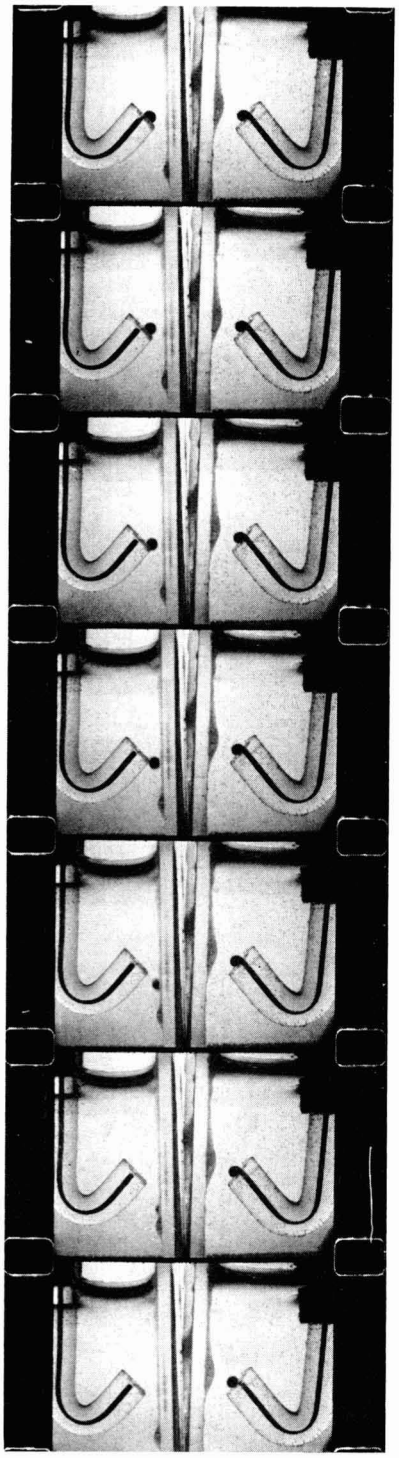

Fig. 1. Seven successive frames from 16-mm cine-films showing two dropping-mercury electrodes in separate vessels. A maximum was present in the left-hand solution but absent in the right-hand solution. Interval between frames about 0.008 sec, internal diameter of capillary 0.8 mm.

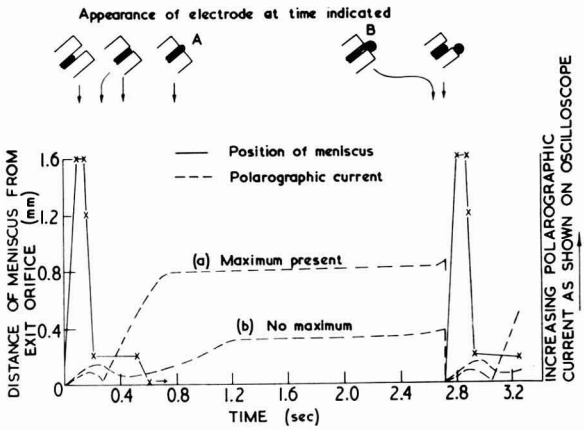

Fig. 2. Position of mercury meniscus and polarographic current during life of one drop of mercury before (A) and after (B) addition of a maximum suppressor. All data are for maximum at positive end of first plateau in polarogram for dissolved oxygen. Abscissa does not necessarily correspond to zero polarographic current.

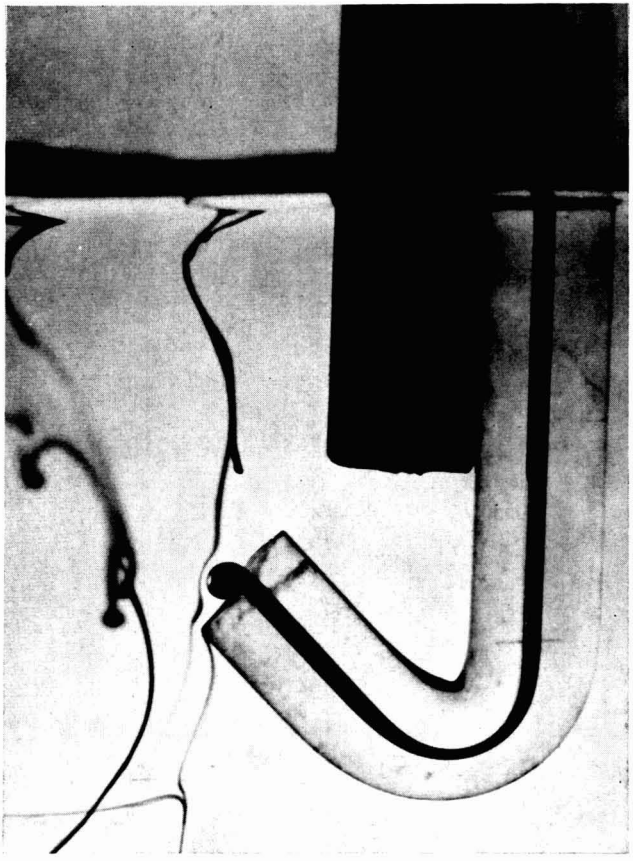

Fig. 3. Acid-fuchsin traces near dropping-mercury electrode in absence of maximum.

orifice. Similar behaviour has been suggested[4,5] but never proved, for the conventional dropping-mercury electrode, and would certainly explain why the 0.05 mm diameter bore is so easily blocked;

(2) as it moved up the capillary, the mercury meniscus stopped for about 0.3 sec just as it reached the exit orifice; this surprising pause no doubt accounts for the temporary decrease in polarographic current observed at that time (Fig. 2). On a number of occasions during the past few years the shape of the current–time curve for wide-bore electrodes has been examined and found to be as in Fig. 2; that given by LINGANE[5] for the conventional dropping-mercury electrode is similar, but does not show a temporary decrease in current early in the life of the drop.

MOVEMENT OF SOLUTION

Use of the acid-fuchsin technique showed that when there was no maximum the *traces* could be made almost to touch the drop as they fell, following the contour of the drop at a distance of about 0.3 mm from its surface (Fig. 3). With a maximum

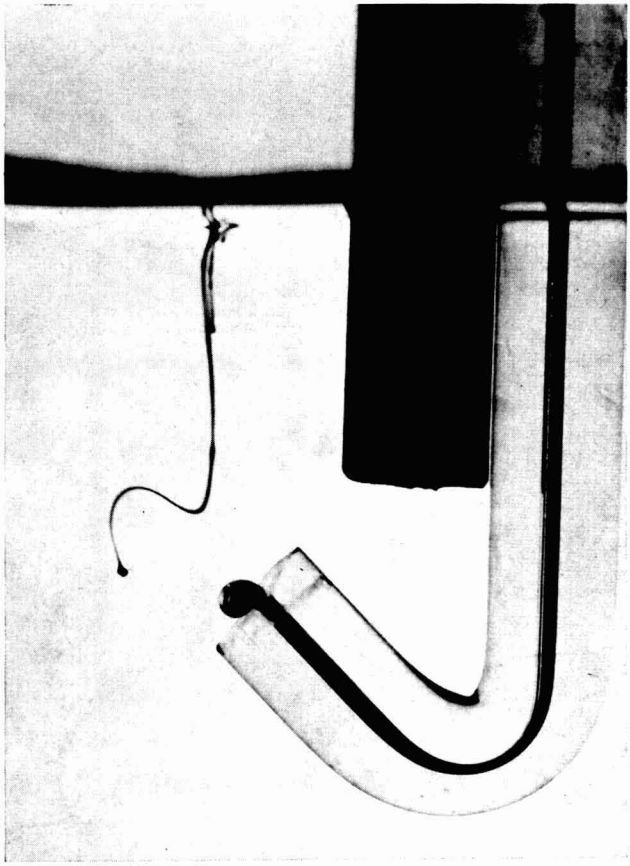

Fig. 4. Acid-fuchsin trace showing movement of solution near dropping-mercury electrode in the presence of a maximum.

present, however, and the drop of mercury partly formed (as in Fig. 2, diagram A, or larger) there was a rapid motion of liquid in the form of a narrow jet directed away from the electrode (Fig. 4); the jet was evidently of small cross-sectional area, since the *trace* of acid-fuchsin was not deflected unless it was close to the vertical plane through the capillary. This is much in agreement with the motion reported[6,7,8] for the case of *positive* maxima with the conventional electrode. (*Positive* here signifies maxima occurring, as in our work, with the mercury at a voltage more positive than that corresponding to the electro-capillary zero.)

The position of the reference electrode relative to the dropping-mercury electrode had no detectable effect on the position or direction of the rapid motion of solution occurring when a maximum was present.

On changing the applied voltage from one at which a maximum was not present to one at which it existed, the rapid motion of the solution began at once, provided that the mercury had emerged from the capillary at least as far as shown in Fig. 2, diagram A.

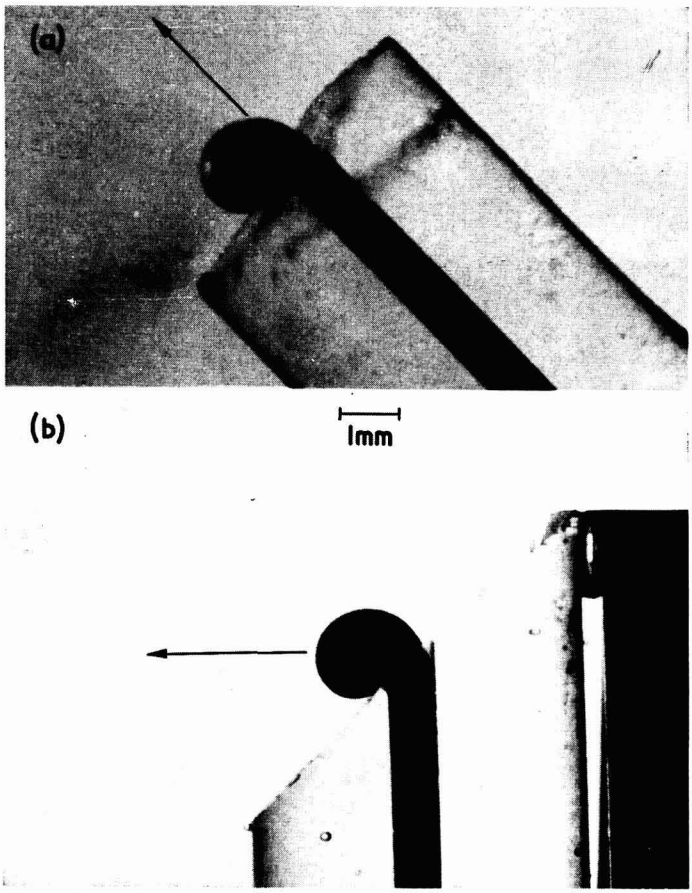

Fig. 5. Directions of rapid motion of aqueous solution in the presence of a maximum with two shapes of dropping-mercury electrode.

The direction of the rapid motion associated with a maximum depended on the shape of the electrode; *e.g.*, as indicated in Fig. 5, the direction was upwards and in line with the capillary for the usual wide-bore electrode (Fig. 5a), but was horizontal and at right-angles to the capillary for an electrode in which the capillary was vertical but the end of the tube was cut at an angle of 45° (Fig. 5b).

ACKNOWLEDGEMENT

This paper is published by permission of the Department of Scientific and Industria) Research.

REFERENCES

1 R. BRIGGS, G. V. DYKE AND G. KNOWLES, *Analyst*, 83 (1958) 304.
2 R. BRIGGS AND G. KNOWLES, *Analyst*, 86 (1961) 603.
3 R. BRIGGS AND W. H. MASON, *Lab. Pract.*, 11 (1962) 36.
4 O. H. MULLER, *The Polarographic Method of Analysis*, 2nd edn., Chemical Education Publ. Co., Easton, Pa., 1951.
5 J. J. LINGANE, *J. Am. Chem. Soc.*, 75 (1953) 788.
6 W. M. MACNEVIN AND S. R. STEELE, *Anal. Chim. Acta*, 24 (1961) 381.
7 I. M. KOLTHOFF AND J. J. LINGANE, *Polarography*, 2nd edn., Vol. 1, Interscience Publishers Inc., New York, 1952, p. 177.
8 H. J. ANTWEILER, *Z. Elektrochem.*, 43 (1937) 596; 44 (1938) 719, 831, 888. (Figures from these papers are reproduced in Reference[7]).

ELECTROMETRIC TITRATIONS OF TRIVALENT CERIUM WITH ALKALI MOLYBDATE

RAM SAHAI SAXENA AND MOHAN LAL MITTAL

Department of Chemistry, Government College, Kota (India)

(Received October 12th, 1962)

EXPERIMENTAL

Merck's extra pure cerous nitrate and sodium molybdate were used. Air-free conductivity water was used for the preparation of standard solutions and subsequent dilutions. Trivalent cerium was estimated volumetrically[2] and molybdenum in Na_2MoO_4 was determined as its quinoline complex[3].

Amperometric titrations

Using a manual polarograph, amperometric titrations were carried out between the reactants at several concentrations, both by the direct and inverse methods, in aqueous and aqueous–alcoholic media. A scalamp galvanometer with the sensitivity

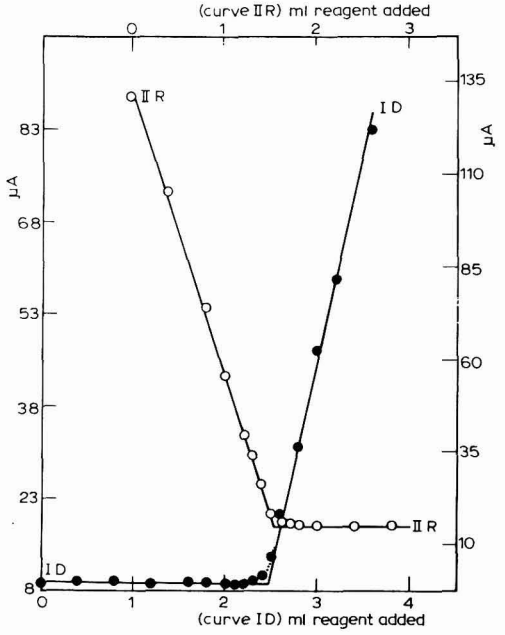

Fig. 1. Amperometric titrations. Curve I D (direct), volume of $M/15$ $Ce(NO_3)_3$ added to 20 ml $M/80$ Na_2MoO_4; curve IIR (reverse), volume of $M/5$ Na_2MoO_4 added to 20 ml $M/100$ $Ce(NO_3)_3$.

suitably adjusted was used as current recorder. A dropping mercury electrode in conjunction with S.C.E. was connected to the cell by a low resistance salt bridge. Polarograms of 0.01 *M* $Ce(NO_3)_3$ solution without any supporting electrolyte were drawn and from them the half-wave potential was calculated and found to be −1.95 V (*vs.* S.C.E.). This E.M.F. was applied in all titrations and 0.02% gelatin was used as maximum suppressor. 20 ml of the reagent was taken in the cell and the dissolved oxygen removed by bubbling nitrogen through the solution for 10–15 min. After each addition of the reagent, the deflection on the galvanometer was read and the corresponding current calculated and corrected for the dilution effect. This was then plotted against the volume of titrant added (Fig. 1).

pH and potentiometric titrations

The pH and E.M.F. of the solutions were measured on a Cambridge null-deflection type pH meter by means of a glass electrode and a bright platinum foil indicator electrode, respectively, in conjunction with a saturated calomel electrode. 0.05% of $Ce(NO_3)_4$ was added to $Ce(NO_3)_3$ to make a Ce^{4+}/Ce^{3+} electrode for use in potentiometric titrations with Na_2MoO_4. After each addition of cerous salt to the sodium molybdate in the electrode vessel the pH and E.M.F. were measured and plotted against the volume of the titrant added. The end-point was obtained from the sharp deflection in the titration curves. This was further checked by drawing differential graphs from which maxima in d(pH)/dV and d*E*/dV gave the equivalence point more accurately. The effect on the end-point of adding different concentrations of ethanol to the titre was also studied. 20 ml of the molybdate solution was used in the cell each time. The same concentrations of solutions were used in both types of titrations (Fig. 2).

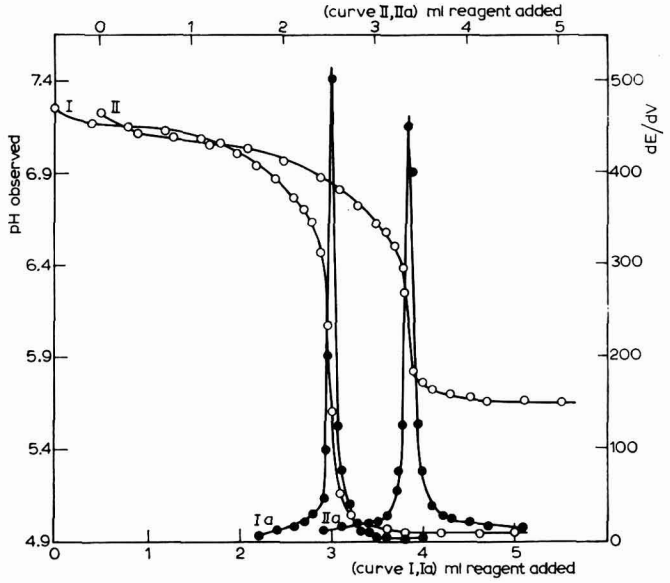

Fig. 2. pH and E.M.F. titrations. Curves I and Ia, volume of *M*/4.5 $Ce(NO_3)_3$ added to 20 ml *M*/20 Na_2MoO_4; curves II and IIa, volume of *M*/20 $Ce(NO_3)_3$ added to 20 ml *M*/80 Na_2MoO_4.

Conductometric titrations

A series of conductometric titrations was performed, using different concentrations of reactants, both by the direct and the reverse methods and also in the presence of various concentrations of ethanol. Conductance was measured by a Kohlrausch Universal bridge using an audio frequency generator as a source of a.c. An additional, sensitive amplifier applied to the signal leaving the bridge network increased the

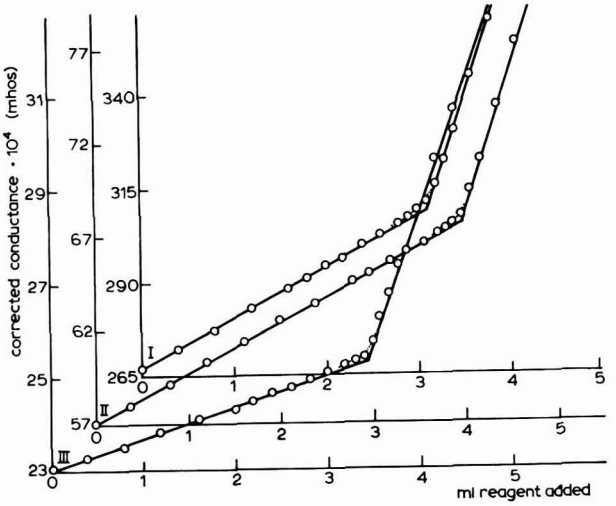

Fig. 3. Direct titrations. Curve I, volume of $M/4.5$ $Ce(NO_3)_3$ added to 20 ml $M/20$ Na_2MoO_4; curve II, volume of $M/30$ $Ce(NO_3)_3$ added to 20 ml $M/100$ Na_2MoO_4; curve III, volume of $M/80$ $Ce(NO_3)_3$ added to 20 ml of $M/300$ Na_2MoO_4.

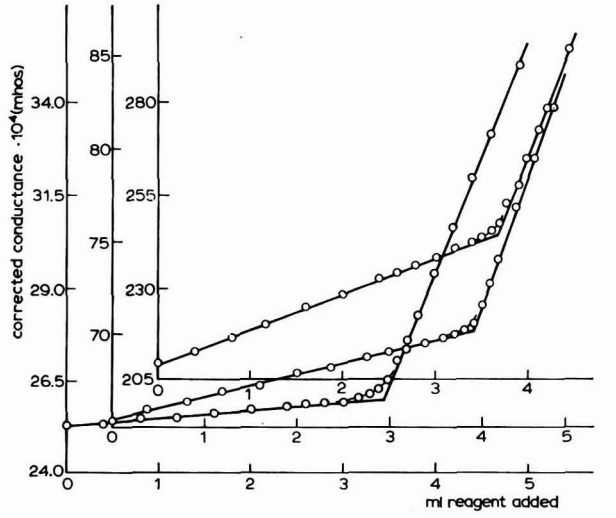

Fig. 4. Reverse titrations. Curve I, volume of $M/5$ Na_2MoO_4 added to 20 ml $M/40$ $Ce(NO_3)_3$; curve II, volume of $M/20$ Na_2MoO_4 added to 20 ml $M/150$ $Ce(NO_3)_3$; curve III, volume of $M/50$ Na_2MoO_4 added to 20 ml $M/420$ $Ce(NO_3)_3$.

sensitivity of the bridge setting and made possible rapid and accurate measurements of conductance. The observed conductance after each addition of the titrant was corrected for the dilution effect and plotted against the volume of the added reagent. The end-points were obtained from the distinct breaks in the titration curves (Fig. 3 and 4).

DISCUSSION

The pHs of the $Ce(NO_3)_3$ and Na_2MoO_4 solutions were measured by means of a glass electrode and found to be 4.75 and 7.40 respectively. The glass electrode titration curves (Fig. 2, curves I and II) represent the changes occurring in H^+ ion concentration when cerous salt solution from the micro-burette was added to molybdate solution in the electrode cell. At the beginning of the reaction a gradual decrease in pH was observed, until, at the stoichiometric end-point where the molecular ratio of Ce^{3+}; MoO_4^{2-} is 2 : 3, a sharp fall in pH was obtained corresponding to the formation of a yellow amorphous precipitate of normal cerous molybdate, having the molecular composition $Ce_2O_3 \cdot 3\ MoO_3$ at pH range 5.8–6.2.

An examination of the results of the potentiometric titrations (Fig. 2, curves Ia, IIa) reveals that the reaction between cerous nitrate and sodium molybdate can be suitably followed using a Ce^{4+}/Ce^{3+} electrode. As the titration proceeds, the E.M.F. remains almost constant until, in the vicinity of the end-point, a marked rise in potential is obtained and afterwards the E.M.F. remains practically unchanged. The same concentrations of reagents were used in glass electrode and E.M.F. titrations and differential graphs have been drawn in the latter case in order to show the equivalence point more clearly.

In potentiometric titrations the behaviour of the bright platinum indicator electrode in contact with Ce^{3+} and Ce^{4+} ions could be interpreted as that of a Ce^{4+}/Ce^{3+} electrode whose potential depends to a great extent upon the concentration of Ce^{3+} ions. On adding cerous salt to molybdate solution in the cell, molybdate ions are being continuously removed by precipitation as cerous molybdate and the E.M.F. remains constant. As soon as all the molybdate ions in the titration cell have been removed, the first excess of cerous nitrate added brings about a sharp rise in potential due to the function of Ce^{4+}/Ce^{3+} electrode, and further addition shows practically no change in observed E.M.F.

The glass electrode and potentiometric titration curves are regular in form; a pronounced maximum in d(pH)/dV and dE/dV is obtained at the stoichiometric end-point and the results are accurate and reproducible. After each addition of the reagent, it takes a little time for the pH and E.M.F. values to become steady. Each titration takes about half an hour for completion. The addition of alcohol in varying concentrations (20 and 30%) improves the end-point slightly as its presence decreases the solubility of the precipitated molybdate and also reduces the adsorption of MoO_4^{2-} and hence a closer approach to the theoretical values is envisaged in the experimental results in aqueous–alcoholic media.

Conductometric titration curves (Figs. 3 and 4) are similar and show strongly defined breaks at the end-point. The results are accurate to 1% at the concentrations studied, the break falling exactly at the position corresponding to the formation of $Ce_2O_3 \cdot 3\ MoO_3$.

Amperometric titrations between $Ce(NO_3)_3$ and Na_2MoO_4 solutions were carried out

at an applied E.M.F. of −1.95 V (*vs.* S.C.E.). In direct titrations, when molybdate is used as the titre (Fig. 1, curve ID) it is noted that the molybdate ion does not yield any measurable diffusion current and no change in the value of the current is observed on the addition of the titrant until the equivalence point is reached. After this the diffusion current due to Ce^{3+} ions increases with the addition of the latter. In the reverse titrations, (Fig. 1, curve IIR), on the addition of sodium molybdate, the diffusion currents due to cerous ions gradually decrease and reach a minimum at the end-point, beyond which the current remained almost constant. Amperometric titration curves have an L-shape and the reproducibility and accuracy of these titrations has been found to be excellent even at low dilutions of cerous salt (10^{-3} *M*).

A comparative study of the electrometric experiments clearly suggests that conductometric, potentiometric and glass electrode titrations yield accurate results only with concentrated solutions of reactants; at greater dilutions, the breaks and inflections are not strongly defined. Amperometric titrations, however, give very accurate end-points over a wider range of concentration of reactants. The titrations are simple, rapid and accurate and offer a quantitative method for the standardisation of Ce^{3+} ions as cerous molybdate (up to a strength of 10^{-3} *M* of $Ce(NO_3)_3$). The formation of normal cerous molybdate $Ce_2O_3 \cdot 3\,MoO_3$ in the pH range 5.8–6.2 as a yellow amorphous precipitate is confirmed.

SUMMARY

The reaction between Ce^{3+} and MoO_4^{2-} was investigated by electrometric techniques involving amperometric, potentiometric, pH, and conductometric titrations between $Ce(NO_3)_3$ and Na_2MoO_4 solutions at several concentrations in aqueous and aqueous–alcoholic media. The end-points obtained from the sharp breaks and inflexions in titration curves occur at a stage where the molecular ratio of Ce^{3+} and MoO_4^{2-} is 2 : 3 and correspond to the formation and precipitation of normal cerous molybdate $Ce_2O_3 \cdot 3\,MoO_3$ in the pH range 5.8–6.2. Amperometric titrations yield very accurate results up to 10^{-3} *M* concentration of $Ce(NO_3)_3$ and offer a simple and rapid method for the determination of trivalent cerium as molybdate.

No reference for the study of this reaction by electrometric methods has been found in the literature, although the reaction has provided conclusive results on the composition of other metal molybdates (SAXENA *et al.*)[1].

REFERENCES

[1] R. S. SAXENA AND C. M. GUPTA, *J. Inorg. & Nucl. Chem.*, 14 (1960) 297.
R. S. SAXENA AND C. M. GUPTA, *Z. Naturforsch.*, 138 (1958) 557.
R. S. SAXENA AND C. M. GUPTA, *Z. Physik. Chem.*, 19 (1959) 94.
R. S. SAXENA AND C. M. GUPTA, *Naturwissenschaften*, 47 (1960) 297.
R. S. SAXENA AND C. M. GUPTA, *J. Sci. Ind. Res. (India)*, 19B (1962) 30.
R. S. SAXENA AND M. L. MITTAL, ibid., 21B (1962) 92.
[2] A. I. VOGEL, *A Text Book of Quantitative Analysis*, Longmans, Green and Co., London, 1951, p. 310.
[3] R. NIERICKER AND W. D. TREADWELL, *Helv. Chim. Acta*, 29 (1946) 470.

CARBON MONOXIDE ADSORPTION ON PLATINUM ELECTRODES. CONSTANT CURRENT TRANSITION TIME STUDY

RONALD A. MUNSON

General Electric Research Laboratory, Schenectady, New York (U.S.A.)

(Received October 25th, 1962)

The application of a constant current to an electrode on which an electrochemically active species has adsorbed from solution, leads to the removal of that active species from the electrode surface. When the electroactive species has been completely removed from the surface (at the transition time), the electrode potential changes rapidly so that another electrochemical process may supply the constant current. If the rate of adsorption is not slow, the transition time will be increased by diffusion of the active species out of the solution adjacent to the electrode. If the adsorption is rapid, reversible, and sufficiently linear, the relationship between the current density i and the transition time τ is[1-3]

$$Y^0_{ad.} = iK^2/nFD\{2(D\tau)^{1/2}/\pi^{1/2}K + \exp(D\tau/K^2)\operatorname{erfc}[(D\tau)^{1/2}/K)] - 1\}, \quad (1)$$

where $Y^0_{ad.}$ is the initial surface concentration of the adsorbed species; F, the Faraday constant; D, the diffusion constant; n, the number of electrons exchanged with the electrode in the electrochemical reaction of one molecule of $Y_{ad.}$; K, the linear adsorption coefficient (expressed in cm) for the adsorbed species; and

$$\operatorname{erfc} x = 2/\pi^{1/2} \int_x^\infty e^{-z^2} dz.$$

For large values of the argument, eqn. (1) simplifies to

$$Y^0_{ad.} = iK/nFD[2(D\tau/\pi)^{1/2} - K]. \quad (2)$$

EXPERIMENTAL

The constant current was supplied to the cell electrodes by a regulated power supply through carbon resistors whose resistances were measured to within 1%. The current pulse was turned on and off by a 275 C mercury relay, activated by timing circuits which allowed pulse durations of 10 msec–25 sec. Oscillograms of the working electrode potential were registered photographically. The working electrode was a horizontal planar disk of platinum with rounded edges of 5.75 ± 0.10 cm² geometric area. A Luggin capillary was used in conjunction with the Ag–AgCl reference electrode. The cell was maintained at 25.0° by a mineral oil bath and a teflon stopcock allowed carbon monoxide to be bubbled through or over the solution. Solutions were prepared by diluting reagent grade 70% perchloric acid and 50% sodium hydroxide with triple distilled water. Carbon monoxide (C.P.) was further purified by scrubbing

with concentrated sulfuric acid, chromous sulfate (Zn excluded), 15% sodium hydroxide, and triple distilled water.

The working electrode was activated by the use of 250 msec anodic pulses at an apparent current density of 14 mA/cm^2. Following reattainment of + 0.4 V (*vs.* hydrogen electrode in the same solution), carbon monoxide was bubbled vigorously through the solution for thirty sec. The electrode and solution then remained quiescent for thirty sec prior to the experimental pulse. Deactivation of the electrode was found to proceed slowly.

RESULTS AND DISCUSSION

In spite of the irreversibility of the electro-oxidation, the transition times, which varied from 7 msec–23 sec, were, in general, well defined. The electro-oxidation was found to occur in a relatively narrow potential range. Potentiostatic sweep data indicate that the carbon monoxide removal at low current density is completed over a potential of less than 50 mV[4]. For the longer transition times the data were found to fit eqn. (2). Figure 1 presents the data obtained in 0.0947 *N* perchloric acid at 761.0 mm atmos. pressure. The solubility of carbon monoxide in water at 25° is $9.27 \cdot 10^{-4}$ moles/l[5]. The electrolyte tends to salt out the carbon monoxide from solution, but the reduction of the solubility in tenth normal acid may be estimated to be less than 1%[6]. With this information and the intercept of Fig. 1, the diffusion constant of carbon monoxide in water at 25° is found to be $2.50 \pm 0.10 \cdot 10^{-5}$ cm^2 sec^{-1}. At high current densities there appears to be partial simultaneous surface

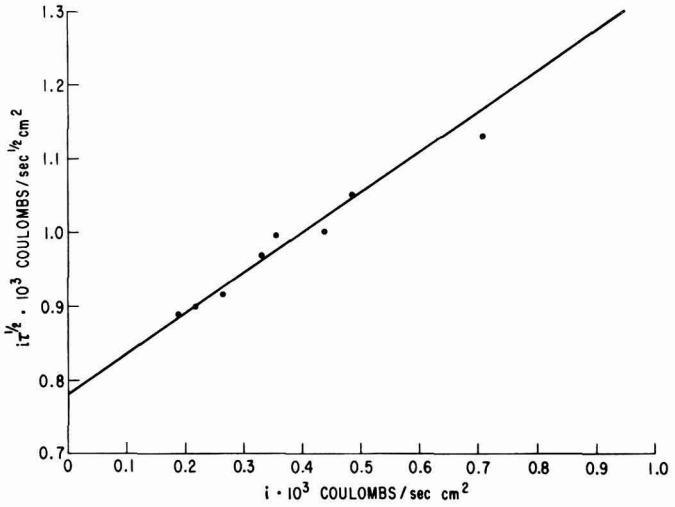

Fig. 1. Experimental data for long transition times according to eqn. 2.

oxidation of the platinum which leads to some ambiguity in the transition times. However, the data are not consistent with a rate limitation in the adsorption step. The case of rate limitation in the adsorption step has been discussed[3], and from this it is estimated that the first order rate constant for the adsorption of carbon monoxide onto platinum must be greater than 0.08 cm/sec. The current density independent

surface concentration obtained from the slope of Fig. 1 is $2.8 \cdot 10^{-9}$ moles carbon monoxide/cm^2. This surface concentration is roughly 30% greater than that found for hydrogen[3], which indicates that the dissociation of hydrogen into atoms tends to take up more of the available surface than the partial formation of the bridged carbon monoxide surface structure[7].

Investigations were also made in alkaline solutions up to 1.02 M in sodium hydroxide and no indication of rate limitation due to a pre-electrochemical step was obtained. Formate formation is to be expected in very alkaline solutions[8], but no trace of it was found analytically in these experiments. Constant current investigations of formate electro-oxidation in alkali, indicate the presence of a very slow pre-electrochemical step[9]. Formate formation, if it occurred, was smaller than 10^{-4} M. The intercepts of $i\tau^{1/2}$ *vs.* i plots, provide an accurate means of determining carbon monoxide concentration in alkaline as well as acidic solutions.

ACKNOWLEDGEMENT

This work was made possible by the support of the Advanced Research Projects Agency (Order No. 247–61) through the United States Army Engineer Research and Development Laboratories under Contract Number DA-44-009-ENG-4853.

SUMMARY

The rate of the electrochemical oxidation of carbon monoxide on platinum is not limited by any pre-electrochemical step other than the diffusion of the carbon monoxide to the surface. The diffusion constant of carbon monoxide in water at 25° is found to be $2.50 \pm 0.10 \cdot 10^{-5}$ cm^2/sec. The first order rate constant for the adsorption of carbon monoxide onto platinum is estimated to be larger than 0.08 cm/sec. The surface concentration of carbon monoxide is approximately 30% greater than that of hydrogen on the same surface at 1 atmos total pressure. Transition time measurements provide an accurate means of determining carbon monoxide concentration in aqueous solutions.

REFERENCES

1 W. LORENZ, *Z. Elektrochem.*, 59 (1955) 730.
2 W. H. REINMUTH, *Anal. Chem.*, 33 (1961) 322.
3 R. A. MUNSON, *J. Phys. Chem.*, 66 (1962) 727.
4 S. GILMAN, *J. Phys. Chem.*, in press.
5 *Handbook of Chemistry and Physics*, 34th edn., Chemical Rubber Publ. Co., Cleveland, Ohio, p. 1532.
6 G. TAMMANN, *Z. Anorg. Allgem. Chem.*, 158 (1926) 25; T. J. MORRISON AND F. BILLETT, *J. Chem. Soc.*, (1952) 3819.
7 R. P. EISCHENS AND W. A. PLISKIN, *Advances in Catalysis*, Vol. X, Academic Press Inc., New York and London, (1958).
8 G. R. FONDA, see J. W. MELLOR, *Treatise on Inorganic and Theoretical Chemistry*, Vol. V, Longmans, Green & Co., London, 1924, p. 924.
9 R. A. MUNSON, to be published.

HALF-WAVE POTENTIALS FOR REVERSIBLE PROCESSES WITH PRIOR KINETIC COMPLEXITY

RICHARD P. BUCK

Bell & Howell Research Center, Pasadena, Calif. (U.S.A.)

(Received July 25th, 1962)

The dependence of half-wave potentials on the concentration of species involved in pre-electrochemical solution reactions can be a sensitive criterion in the analysis of electrode processes. While it is commonly believed that half-wave potentials of processes involving rapid electron transfers reflect mainly thermodynamic behavior of the system[1], both half-wave potentials and limiting currents depend upon kinetic factors as well. For systems composed of a multiplicity of soluble species, *i.e.* complex ion reductions and the reduction of unsaturated dibasic acids, not only can thermodynamic quantities be calculated, but also some information on the actual reducible species and rate of pre-electrochemical solution reactions can be obtained. Thus, the behavior of the half-wave potential as a function of ligand concentration in complex ion reductions and as a function of pH in dibasic acid reductions can be an important link in the chain of events leading to a consistent mechanism for the reduction. In this paper it will be shown that thermodynamic half-wave potentials can be calculated from kinetic models and that the resulting expressions are valid over the entire ligand concentration range. Expressions for the half-wave potentials are derived for systems involving pre-electrochemical solution reactions for all possible values of rate constants. Real systems, however, seem usually to have large rate constants in the prior solution reactions, but cannot exceed the limiting, diffusion controlled, activation-free rate constant[2,3] whose magnitude is approximately 10^{10}–10^{12} l mole^{-1} sec^{-1}. For simplicity, linear diffusion to a plane electrode will be considered, and it is reasonable to assume that the results can be transferred to the polarographic case by inserting numerical factors into the equations. Complex ions will be used in the model, although the reduction of unsaturated dibasic acids is the same upon redefining dissociation constants.

Expressions for the half-wave potentials in terms of ligand concentration require a prior derivation of the i–E characteristic of the model system at the dropping mercury electrode or at a plane electrode under unstirred conditions, at an essentially discontinuous application of potential[4]. The derived currents in these cases are functions of time and the i–E characteristics depend upon the time of measurement of i after application of E. Time-dependent behavior is commonly observed and has been derived for other electrode processes. Among those for which the i–E characteristics have been stated mathematically are one-step reversible oxidations and reductions, and irreversible oxidations and reductions resulting from slow electron transfer. Expres-

sions appropriate to polarography are summarized by KOLTHOFF AND LINGANE[5]. Until recently[6-16] the large class of electrode processes, including kinetic and catalytic-controlled oxidations and reductions and processes where adsorption of the reactant limits the current had not been treated completely, and no exact general equations for i *vs.* E were available, although approximate equations have been summarized by KOLTHOFF AND LINGANE[17]. DELAHAY, in his description of kinetic and catalytic currents[18], restricted the analysis to the dependence of the limiting currents on the pre- or post-electrochemical solution reaction rate constants. Similarly, KOUTECKY's work[19-34] on various pre-electrochemical and post-electrochemical reaction schemes, was specifically addressed to the expression of limiting currents as a function of concentrations, rate constants, diffusion coefficients and time for cases where the electron transfer step was rapid compared with other steps.

Since the appearance of the theory of kinetic processes by MATSUDA AND AYABE[6] an equation relating i and E for both reversible and irreversible electron transfers with prior kinetic complication has been stated. Their results are unfortunately limited to cases in which only one species in an equilibrium mixture is electro-active and is further limited to large values of the prior solution reaction rate constants. They also found it necessary to introduce the DEFORD–HUME expression[35] for the half-wave potential into their theory, rather than deriving this expression from the treatment. The MATSUDA AND AYABE theory was the first treatment to show that prior solution reactions do not affect the shape of a polarographic wave, but only diminish the limiting current. Thus, a plot of log $(i_l-i)/i$ is diagnostic for slow or rapid electron transfers whether or not the reacting species is produced by a slow pre-electrochemical solution reaction. It can be shown that this conclusion, and the resulting kinetic term in the expression for half-wave potential, is exact when the pre-electrochemical reaction rate constant is large and is still a good approximation when used for small values. The dependence of half-wave potentials on kinetic parameters has been further explored by KORYTA *et al.*[7-16].

Expressions for half-wave potentials for complex ion reductions were originally derived on thermodynamic grounds by VON STACKELBERG AND VON FREYHOLD[36], and by LINGANE[37]. Their expressions, summarized by KOLTHOFF AND LINGANE[1], were applicable for the reduction of complex ions to the metallic state (amalgam), or to other soluble oxidation states. Calculated half-wave potentials for the reversible reduction of complex ions $(E_{\frac{1}{4}})_c$ do not converge to the half-wave potential for a simple ion $(E_{\frac{1}{4}})_s$ when ligand concentration approaches zero or the complex dissociation constants approach infinity. Thus, these expressions are limited in applicability to systems involving essentially one very stable complex, and they can give accurate values only in a limited range of ligand concentration, such that only one complex exists. Exact expressions which converge to the proper value at infinite dilution of ligand, will be derived kinetically in the following section.

KINETIC BEHAVIOR WHEN A COMPLEX ION, SIMPLE ION, AND REDUCTION PRODUCTS HAVE EQUAL DIFFUSION COEFFICIENTS

Consider the reaction sequence

$$Y \underset{k_b}{\overset{k_f}{\rightleftharpoons}} O + pX \xrightarrow{ne^-} R \qquad (1)$$

where Y is the complex ion $MX_p^{(n-pb)+}$; O is the simple, hydrated metal ion M^{n+}; X^{b-} is the complexing agent, and R is the reduced metal, which in the case of a mercury cathode is in the form of the dilute amalgam. Assuming that the rate constants for formation and decomposition of the complex ion are finite, the formation rate is p order in C_X, and the decomposition rate is first order in C_Y, the diffusion equations for the reacting species at a plane electrode are:

$$\frac{\partial C_Y}{\partial t} = D\frac{\partial^2 C_Y}{\partial x^2} - k_f C_Y + k_b C_O C_X{}^p = D\frac{\partial^2 C_Y}{\partial x^2} - k_b C_X{}^p\left[\frac{KC_Y}{C_X{}^p} - C_O\right] \tag{2a}$$

$$\frac{\partial C_O}{\partial t} = D\frac{\partial^2 C_O}{\partial x^2} + k_f C_Y - k_b C_O C_X{}^p = D\frac{\partial^2 C_O}{\partial x^2} + k_b C_X{}^p\left[\frac{KC_Y}{C_X{}^p} - C_O\right] \tag{2b}$$

$$\frac{\partial C_R}{\partial t} = D\frac{\partial^2 C_R}{\partial x^2} \tag{2c}$$

No equation for C_X is written since it is assumed that this species is present in excess and remains essentially constant with passage of current. Here

$$K = \frac{C_O C_X{}^p}{C_Y} = \frac{k_f}{k_b} = \frac{k_f' f_Y}{k_b' f_O f_X{}^p} \tag{3}$$

where K is the overall dissociation constant of the complex. For mathematical simplicity, the diffusion coefficients of all species are assumed equal to D and activity coefficients, f_Y, f_O and f_X, are omitted from the diffusion equations; otherwise, separation of variables becomes cumbersome. Thus, k_f and k_b are formal rate constants for the forward and backward reactions.

Case I. Reducible simple ion

The well-tested absolute reaction rate theory applied to electrochemical reactions leads to the general equation

$$\frac{i}{nFA} = k_{f_Y}^0 C_Y(0,t)e^{-\frac{\alpha_Y nFE}{RT}} + k_{f_O}^0 C_O(0,t)e^{-\frac{\alpha_O nFE}{RT}} - k_{b_Y}^0 C_R(0,t)(C_X)^p e^{\frac{(1-\alpha_Y)nFE}{RT}} - k_{b_O}^0 C_R(0,t)e^{\frac{(1-\alpha_O)nFE}{RT}} \tag{4}$$

for this system. It is possible, in principle, that the rate constants for the reduction of the complex ion and the reverse process may be essentially zero. If the simple ion is the only reducible species and electron transfer rate is rapid compared with all other steps, the electrode is Nernstian with respect to the simple metal ion and the reduced form, and the equation[4]

$$\theta = \frac{C_O(0,t)}{C_R(0,t)} = \frac{f_R}{f_O}\exp\left[\frac{nF}{RT}(E - E^0)\right] \tag{5}$$

obtains where $C_O(0,t)$ and $C_R(0,t)$ are surface concentrations corresponding to $x = 0$. Initially let

$$C_O{}^0 + C_Y{}^0 = \alpha$$

or

$$C_O{}^0 = \frac{KC_X{}^{-p}\alpha}{1 + KC_X{}^{-p}} \tag{6}$$

and

$$C_Y{}^0 = \frac{\alpha}{1 + KC_X{}^{-p}}$$

The boundary conditions are listed below.

$$t = 0 \quad x \geqslant 0 \quad C_O(x,0) = C_O^0 \tag{7a}$$
$$t = 0 \quad x \geqslant 0 \quad C_Y(x,0) = C_Y^0 \tag{7b}$$
$$t = 0 \quad x \geqslant 0 \quad C_R(x,0) = C_R^0 \tag{7c}$$
$$t > 0 \quad x = 0 \quad C_O(0,t) = \theta C_R(0,t) \tag{7d}$$
$$t > 0 \quad x = 0 \quad \partial C_Y/\partial x = 0 \tag{7e}$$
$$t > 0 \quad x = 0 \quad \partial C_O/\partial x = -\partial C_R/\partial x \tag{7f}$$

In order to separate variables, linear combinations of $C_O(x,t)$ and $C_Y(x,t)$ are used[19]. Let

$$\psi(x,t) = C_Y(x,t) + C_O(x,t) \tag{8a}$$
$$\varphi(x,t) = C_Y(x,t) - KC_X{}^p C_Y(x,t) \tag{8b}$$

then it follows that

$$\frac{\partial \psi}{\partial t} = D\frac{\partial^2 \psi}{\partial x^2} \tag{9a}$$
$$\frac{\partial \varphi}{\partial t} = D\frac{\partial^2 \varphi}{\partial x^2} - l\varphi \tag{9b}$$
$$\frac{\partial C_R}{\partial t} = D\frac{\partial^2 C_R}{\partial x^2} \tag{9c}$$

where

$$l = k_b C_X{}^p(1 + KC_X{}^{-p}) = k_b C_X{}^p + k_f \tag{10}$$

and

$$C_O(x,t) = \frac{\varphi + KC_X{}^{-p}\psi}{1 + KC_X{}^{-p}}; \quad C_Y(x,t) = \frac{\psi - \varphi}{1 + KC_X{}^{-p}} \tag{11}$$

Passing to the Laplace transforms of the partial differential equations, after solving algebraically and applying the transformed boundary conditions, the transformed variables become

$$\bar{\psi}(x,s) = \left\{\frac{[1 + K/C_X{}^p]\theta C_R{}^0 - [K/C_X{}^p]\alpha}{K/C_X{}^p + [1 + K/C_X{}^p]\theta + \sqrt{s/s + l}}\right\} \frac{e^{-\sqrt{\frac{s}{D}}x}}{s} + \frac{\alpha}{s} \tag{12a}$$

$$\bar{\varphi}(x,s) = \left\{\frac{[1 + K/C_X{}^p]\theta C_R{}^0 - [K/C_X{}^p]\alpha}{K/C_X{}^p + [1 + K/C_X{}^p]\theta + \sqrt{s/s+l}}\right\} \frac{e^{-\sqrt{\frac{s+l}{D}}x}}{\sqrt{s}\sqrt{s + l}} \tag{12b}$$

$$\bar{C}_R(x,s) = \left\{\frac{[K/C_X{}^p]\alpha - [1 + K/C_X{}^p]\theta C_R{}^0}{K/C_X{}^p + [1 + K/C_X{}^p]\theta + \sqrt{s/s + l}}\right\} \frac{e^{-\sqrt{\frac{s}{D}}x}}{s} + \frac{C_R{}^0}{s} \tag{12c}$$

where s is the transform variable. When $l \to \infty$ the case corresponding to rapid, reversible reduction of the complex ion via the simple or hydrated ion is obtained.

Case IA. Rapid prior solution reactions. For rapid interconversion when $l \to \infty$, the transform inversion yields:

$$\psi(x,t) = \left\{\frac{[1 + K/C_X{}^p]\theta C_R{}^0 - [K/C_X{}^p]\alpha}{K/C_X{}^p + [1 + K/C_X{}^p]\theta}\right\} \operatorname{erfc}\frac{x}{2\sqrt{Dt}} + \alpha \tag{13a}$$
$$\varphi(x,t) = 0 \tag{13b}$$

$$C_R(x,t) = \left\{\frac{[K/C_X{}^p]\alpha - [1 + K/C_X{}^p]\theta C_R{}^0}{K/C_X{}^p + [1 + K/C_X{}^p]\theta}\right\} \operatorname{erfc}\frac{x}{2\sqrt{Dt}} + C_R{}^0 \tag{13c}$$

The current for this system is given by

$$i = -nFAD\left(\frac{\partial C_R}{\partial x}\right)_{x=0} = nFAD\left[\left(\frac{\partial C_O}{\partial x}\right)_{x=0} + \left(\frac{\partial C_Y}{\partial x}\right)_{x=0}\right] \tag{14}$$

which by differentiation of C_R and/or ψ yields

$$i = \frac{nFAD^{\frac{1}{2}}}{\sqrt{\pi t}}\left\{\frac{[K/C_X{}^p]\alpha - [1 + K/C_X{}^p]\theta C_R{}^0}{K/C_X{}^p + [1 + K/C_X{}^p]\theta}\right\} \tag{15}$$

The diffusion limited currents for the reduction and oxidation processes are

$$(i_d)_c = i_{\lim\,\theta\to 0} = \frac{nFAD^{\frac{1}{2}}\alpha}{\sqrt{\pi t}} \tag{16a}$$

$$(i_d)_a = i_{\lim\,\theta\to\infty} = \frac{-nFAD^{\frac{1}{2}}C_R{}^0}{\sqrt{\pi t}} \tag{16b}$$

The current for any θ is given by

$$i = \frac{[K/C_X{}^p](i_d)_c + [1 + K/C_X{}^p]\theta(i_d)_a}{K/C_X{}^p + [1 + K/C_X{}^p]\theta} \tag{17}$$

Rearranging to give θ in terms of i,

$$\theta = \frac{K/C_X{}^p}{1 + K/C_X{}^p}\left[\frac{(i_d)_c - i}{i - (i_d)_a}\right] \tag{18}$$

$$E = E^0 + \frac{RT}{nF}\ln\frac{f_O}{f_R} + \frac{RT}{nF}\ln\frac{K/C_X{}^p}{1 + K/C_X{}^p} + \frac{RT}{nF}\ln\left[\frac{(i_d)_c - i}{i - (i_d)_a}\right] \tag{19}$$

Restricting the equation to the common voltammetric case *e.g.* $C_R{}^0 = 0$, introducing the remaining activity coefficients by the substitution

$$K/C_X{}^p \rightarrow \frac{Kf_p}{f_m C_X{}^p f_X{}^p} \tag{20}$$

and defining

$$\varepsilon = E^0 - \frac{RT}{nF}\ln a_{Hg}$$

the expression for the electrode potential of a massive mercury electrode results.

$$E = \varepsilon + \frac{RT}{nF}\ln\frac{Kf_p}{f_{M(Hg)}} - p\frac{RT}{nF}\ln C_X f_X - \frac{RT}{nF}\ln\left(1 + \frac{Kf_p}{C_X{}^p f_X{}^p f_M}\right) + \frac{RT}{nF}\ln\frac{(i_d)_c - i}{i} \tag{21}$$

The activity coefficients f_M, $f_{M(Hg)}$, f_p, and f_X refer to the simple ion, the dilute amalgam, the complex ion, and the ligand ion, respectively. The half-wave potential for the rapid reversible complex ion reduction, $(E_{\frac{1}{2}})_c$ is given by

$$(E_{\frac{1}{2}})_c = \varepsilon + \frac{RT}{nF}\ln\frac{Kf_p}{f_{M(Hg)}} - p\frac{RT}{nF}\ln C_X f_X - \frac{RT}{nF}\ln\left(1 + \frac{Kf_p}{C_X{}^p f_X{}^p f_M}\right) \tag{22}$$

In the case of a massive electrode of the metal M, ε becomes E^0 and $f_{M(Hg)}$ becomes unity. For the dropping mercury electrode, the equations above must be modified so that when $D^{\frac{1}{2}}$ appears, this term is multiplied by the Ilkovic factor, $\sqrt{7/3}$.

It should be noted that the limiting cathodic current is independent of ligand con-

centration. The result appears to imply that both the complex ion and the simple ion are reducible at the electrode surface. This apparent contradiction follows from the final assumption that the pre-electrochemical rate constants are infinite.

In terms of the original model which assumes finite pre-electrochemical rate constants, the gradient of the concentration of the complex ion can be zero at the electrode surface. Zero gradient condition for the complex species is equivalent to the assumption that the simple ion is the only reducible species. However, as the rate constants approach infinity, this condition can no longer hold and the concentration gradient for each species near the electrode approaches a constant, non-zero, proportionality with the gradient of the simple metal ion concentration.

The equation for current *vs.* time is obtained either by calculating the gradient of the concentration of the reduced species, or the *sum* of the concentration gradients of the oxidized species at the electrode surface.

Case I B. No prior solution reactions. When the rate of the prior solution reactions is zero, the value of l in eqns. (12a), (12b), and (12c) is set up equal to zero. The transform inversion yields

$$\psi(x,t) = \left\{\frac{[1 + K/C_X{}^p]\theta C_R{}^0 - [K/C_X{}^p]\alpha}{[1 + K/C_X{}^p][1 + \theta]}\right\} \operatorname{erfc} \frac{x}{2\sqrt{Dt}} + \alpha \tag{23a}$$

$$\varphi(x,t) = \psi(x,t) - \alpha \tag{23b}$$

$$C_R(x,t) = \left\{\frac{[K/C_X{}^p]\alpha - [1 + K/C_X{}^p]\alpha C_p{}^0}{[1 + K/C_X{}^p][1 + \theta]}\right\} \operatorname{erfc} \frac{x}{2\sqrt{Dt}} + C_R{}^0 \tag{23c}$$

Since eqn. (14) is obeyed, the current is given by

$$i = \frac{nFAD^{\frac{1}{2}}}{\sqrt{\pi t}} \left\{\frac{[K/C_X{}^p]\alpha - [1 + K/C_X{}^p]\theta C_R{}^0}{[1 + K/C_X{}^p][1 + \theta]}\right\} \tag{24}$$

However, in this case, the limiting cathodic current is dependent on ligand concentration

$$(i_l)_c = i_{\lim\, \theta\to 0} = \frac{nFAD^{\frac{1}{2}}\alpha}{\sqrt{\pi t}} \left\{\frac{K/C_X{}^p}{1 + K/C_X{}^p}\right\} \tag{25a}$$

$$(i_d)_a = i_{\lim\, \theta\to \infty} = \frac{-nFAD^{\frac{1}{2}}C_R{}^0}{\sqrt{\pi t}} \tag{25b}$$

The current for any θ is given by

$$i = \frac{(i_l)_c + (i_d)_a\theta}{1 + \theta} \tag{26}$$

and by rearrangement

$$\theta = \frac{(i_l)_c - i}{i - (i_d)_a} \tag{27}$$

or

$$E = E^0 + \frac{RT}{nF} \ln \frac{f_O}{f_R} + \frac{RT}{nF} \ln \left[\frac{(i_l)_c - i}{i - (i_d)_a}\right] \tag{28}$$

In the common polarographic case $C_R{}^0 = 0$ and

$$E_{Hg} = \varepsilon + \frac{RT}{nF} \ln \frac{f_M}{f_{M(Hg)}} + \frac{RT}{nF} \ln \left[\frac{(i_l)_c - i}{i}\right] \tag{29}$$

the half-wave potential for the kinetically slow reversible reduction, $(E_{\frac{1}{2}})_c$ is given by

$$(E_{\frac{1}{2}})_c = \varepsilon + \frac{RT}{nF} \ln \frac{f_M}{f_{M(Hg)}} \tag{30}$$

This expression is, in fact, the half-wave potential of the simple metal ion and is independent of ligand concentration. Only the cathodic current depends upon ligand concentration and may very well be nearly zero for a system in which the ligand concentration is high and the complex is very stable.

Case I C. Finite prior solution reaction rate constants. An exact solution for finite values of l in eqns. (12a), (12b), and (12c) can be given. However, the expression for i is desired and can be obtained from the transforms of

$$\partial\psi/\partial x \text{ or } \partial C_R/\partial x$$

Writing ψ in shorthand notation

$$\bar{\psi}(x,s) = \left\{\frac{-Q\sqrt{s+l}}{M\sqrt{s+l}+N\sqrt{s}}\right\} \frac{e^{-\sqrt{\frac{s}{D}}x}}{s} + \frac{\alpha}{s} \tag{31}$$

then

$$\frac{\partial\bar{\psi}(x,s)}{\partial x} = \left\{\frac{Q\sqrt{D}\sqrt{s+l}}{M\sqrt{s+l}+N\sqrt{s}}\right\} \frac{e^{-\sqrt{\frac{s}{D}}x}}{\sqrt{s}} \tag{32}$$

and

$$\frac{i}{s} = \frac{nFAQ\sqrt{D}}{\sqrt{s}} \left\{\frac{\sqrt{s+l}}{M\sqrt{s+l}+N\sqrt{s}}\right\} \tag{33}$$

where

$$Q = [K/C_X{}^p]\alpha - [1 + K/C_X{}^p]\theta C_R{}^0 \tag{34a}$$

$$M = K/C_X{}^p + [1 + K/C_X{}^p]\theta \tag{34b}$$

$$N = 1 \tag{34c}$$

thus

$$i = \frac{nFA\sqrt{D}Q}{\sqrt{\pi t}}\left\{\frac{Ne^{-lt} - M}{N^2 - M^2} - \frac{N^2\sqrt{\pi lt}}{(N^2 - M^2)^{3/2}} e^{\frac{M^2 lt}{N^2 - M^2}}\left[\operatorname{erfc}\sqrt{\frac{N^2 lt}{N^2 - M^2}} - \operatorname{erfc}\sqrt{\frac{M^2 lt}{N^2 - M^2}}\right]\right\} \tag{35}$$

By applying the well-known asymptotic expansion of erf x for large x, then as $l \to \infty$ the current approaches

$$i = \frac{nFAD^{\frac{1}{2}}Q}{M\sqrt{\pi t}} \tag{36}$$

which is precisely eqn. (15). On the other hand, when $l \to 0$ the current

$$i = \frac{nFAD^{\frac{1}{2}}Q}{(M+N)\sqrt{\pi t}} \tag{37}$$

which is precisely eqn. (24).

In view of eqn. (16a), eqn. (37) can be rewritten as

$$i = \left[\frac{[K/C_X{}^p]i_\infty + [1 + K/C_X{}^p]\theta(i_d)_a}{K/C_X{}^p + [1 + K/C_X{}^p]\theta}\right]\left\{\frac{M(Ne^{-lt} - M)}{N^2 - M^2} - \frac{N^2 M}{(N^2 - M^2)^{3/2}}\sqrt{\pi lt}\, e^{\frac{M^2 lt}{N^2 - M^2}}\right.$$
$$\left.\left[\operatorname{erfc}\sqrt{\frac{N^2 lt}{N^2 - M^2}} - \operatorname{erfc}\sqrt{\frac{M^2 lt}{N^2 - M^2}}\right]\right\} \tag{38}$$

where i_∞ becomes $(i_d)_c$ as l approaches ∞.
Then

$$i = \left\{\frac{[\sigma i_\infty + [1 + \sigma]\theta(i_d)_a}{\sigma + [1 + \sigma]\theta}\right\} F(l,\theta,\sigma,t) \tag{39}$$

where $\sigma = K/C_X{}^p$ and $F(l,\theta,\sigma,t)$ is the complicated function within the braces of eqn. (38). The limiting cathodic current i_l is given by

$$(i_l)_c = i_{\lim\ \theta\to 0} = i_\infty F(l,0,\sigma,t) \tag{40a}$$

$$(i_l)_a = i_{\lim\ \theta\to\infty} = (i_d)_a F(l,\infty,\sigma,t) \tag{40b}$$

In the limit $l \to \infty$, $F(l,\theta,\sigma,t) \to 1$ for all θ, σ and t; and, similarly, for

$$l \to 0,\ F(l,\theta,\sigma,t) \to \frac{\sigma + (1 + \sigma)\theta}{(1 + \sigma)(1 + \theta)}$$

for all θ, σ and t.

A general expression for i in terms of θ, which can be solved for θ is impossible in this general case. However, approximations can be introduced for $lt >> 1$, $\sigma < 1$ and $lt << 1$, $\sigma < 1$.

Beginning with the exact expression

$$\frac{i_l - i}{i} = \frac{i_l}{i_\infty}\left[\frac{\sigma + (1 + \sigma)\theta}{\sigma F(l,0,\sigma,t)}\right] - 1 \tag{41}$$

we note from the asymptotic expansion of F for large l

$$F(l,\theta,\sigma,t) = 1 + \frac{M}{2Nlt}\left[e^{-lt} - \frac{N^3}{M^3}\right] - \frac{3}{4}\frac{M(N^2 - M^2)}{N^3(lt)^2}\left[e^{-lt} - \frac{N^5}{M^5}\right] \tag{42a}$$

$$\approx 1 - \frac{1}{2[\sigma + (1 + \sigma)\theta]^2 lt} \tag{42b}$$

Then

$$\frac{i_l - i}{i} \approx \frac{i_l}{i_\infty}\left(\frac{1 + \sigma}{\sigma}\right)\theta \tag{43}$$

In the case that $lt << 1$, then

$$F(l,\theta,\sigma,t) \approx \frac{\sigma + (1 + \theta)\sigma}{(1 + \sigma)(1 + \theta)} \tag{44}$$

and

$$\frac{i_l - i}{i} \approx \frac{i_l}{i_\infty}\left(\frac{1 + \sigma}{\sigma}\right)(1 + \theta) \tag{45}$$

Expanding eqn. (43) gives

$$E = E^0 + \frac{RT}{nF}\ln\frac{f_O}{f_R} + \frac{RT}{nF}\ln\frac{K/C_X{}^p}{1 + K/C_X{}^p} - \frac{RT}{nF}\ln\frac{i_l}{i_\infty} + \frac{RT}{nF}\ln\frac{i_l - i}{i} \tag{46}$$

The half-wave potential is given by

$$(E_{\frac{1}{2}})_c = E^0 + \frac{RT}{nF}\ln\frac{f_O}{f_R} + \frac{RT}{nF}\ln\frac{K/C_X{}^p}{1 + K/C_X{}^p} - \frac{RT}{nF}\ln\frac{i_l}{i_\infty} \tag{47}$$

As $l \to \infty$, $i_l \to i_\infty$ and $E_{\frac{1}{2}}$ is identical with eqn. (22). As $l \to 0$ $\frac{i_l}{i_\infty} \to \frac{\sigma}{1+\sigma}$ and $E_{\frac{1}{2}}$ is identical with eqn. (30). The approximation made in eqn. (43) will be generally valid at the foot of the wave where $\theta >> 1$, even for cases where σ is not less than 1. Thus, plots of $\log (i_l - i)/i$ will yield linear plots as is customary with rapid electron transfers even though the pre-electrochemical step has a finite rate which limits the current. The behavior of the plot for $1 > \theta > 0$ will deviate from linearily unless $\sigma < 1$.

The half-wave potential can be used to calculate the rate constants of the limiting pre-electrochemical steps. For the linear diffusion case, eqn. (47) can be written

$$E_{\frac{1}{2}} = E^0 + \frac{RT}{nF}\ln\frac{f_O}{f_R} + \frac{RT}{nF}\ln\frac{K/C_X{}^p}{1 + K/C_X{}^p} - \frac{RT}{nF}\ln \mathrm{F}(l,0,\sigma,t) \tag{48}$$

and for the usual polarographic case, $(i_d)_a = 0$, $\mathrm{Q} = \sigma\alpha$, $\mathrm{M} = \sigma$ and $\mathrm{N} = 1$.

$$\mathrm{F}(l,0,\sigma,t) = \frac{\sigma}{1-\sigma^2}(e^{-lt} - \sigma) - \frac{\sigma\sqrt{\pi lt}}{(1-\sigma^2)^{3/2}} e^{\frac{\sigma^2 lt}{1-\sigma^2}}\left[\mathrm{erfc}\frac{\sqrt{lt}}{\sqrt{1-\sigma^2}} - \mathrm{erfc}\frac{\sigma\sqrt{lt}}{\sqrt{1-\sigma^2}}\right] \tag{49}$$

If, in addition, $lt >> 1$ and $\sigma < 1$, the first term may be neglected and the second error function term is determining. Then $\mathrm{F}(l,0,\sigma,t) = \mathrm{F}(y) = \sqrt{\pi}/(1-\sigma^2)\, y e^{y^2} \operatorname{erfc} y$ the Koutecky function with $y = \sigma\sqrt{lt}/(\sqrt{1-\sigma^2})$. If mean diffusion currents are observed rather than instantaneous currents, $\mathrm{F}(y)$ is replaced by $\mathrm{f}(y)$ which has been tabulated by KOUTECKY AND BRDICKA[19]. Thus, for linear diffusion with stepwise application of constant potential, it is possible to calculate pre-electrochemical rate constants from plots of $E_{\frac{1}{2}}$ *vs.* $\log C_X$ at several values of C_X from the equation

$$(E_{\frac{1}{2}})_{c(\mathrm{obs.})} = E_{\frac{1}{2}(l=\infty)} - \frac{RT}{nF}\ln f(y) \tag{50}$$

Even when $E_{\frac{1}{2}(l=\infty)}$ is not experimentally observable, it may be calculated from eqn. (19) or (22).

For the polarographic case

$$(E_{\frac{1}{2}})_C = \varepsilon + \frac{RT}{nF}\ln\frac{f_M}{f_{M(\mathrm{Hg})}} + \frac{RT}{nF}\ln\frac{Kf_p/f_M C_X{}^p f_X{}^p}{1 + Kf_p/f_M C_X{}^p f_X{}^p} - \frac{RT}{nF}\ln\frac{i_l}{i_\infty} \tag{51}$$

The last term can be written $-RT/nF \ln \mathrm{F}(\chi)$ where $\mathrm{F}(\chi)$ is the polarographic Koutecky function[23,28].

For Case I

$$\chi = \sqrt{\frac{12}{7}}\frac{\sigma\sqrt{lt}}{\sqrt{1-\sigma^2}} \tag{52}$$

and the restrictions $lt >> 1$, and $\sigma < 1$ still apply. When $\chi << 1$ and $lt > 1$

$$\mathrm{F}(\chi) \approx \frac{\sqrt{\pi}}{2}\chi \tag{53}$$

and when $\chi << 1$ and $lt < 1$ we use

$$F(\chi) \approx \frac{\sqrt{\pi}}{2}\chi + \frac{\sigma}{1-\sigma^2}(e^{-lt} - \sigma) \tag{54}$$

From the usual plot of $E_{\frac{1}{2}(obs.)}$ *vs.* log C_X, rate constants can be calculated from the equation,

$$(E_{\frac{1}{2}})_{C(obs.)} = E_{\frac{1}{2}(l=\infty)} - \frac{RT}{nF} \ln F(\chi) \tag{55}$$

using the tables of $F(\chi)$ for various values of χ given by KOUTECKY and reprinted by DELAHAY[18]. As before, t is time after application of the constant potential and in polarography, where currents are measured at the maximum, t is the drop time. If average currents are measured, the $F(\chi)$ must be replaced by $\bar{F}(\chi)$, which KOUTECKY has shown[23] to be approximated to $\pm 1\%$ by

$$\bar{F}(\chi) = \frac{\chi}{1.5 + \chi} = \frac{\sigma\sqrt{lt}}{0.87\sqrt{1-\sigma^2}} \Big/ \left(1 + \frac{0.87\ \sigma\sqrt{lt}}{\sqrt{1-\sigma^2}}\right) \tag{56}$$

Case II. Reducible complex ion

Referring to eqn. (4), let it be assumed that k_{fo}^0 and k_{bo}^0 are essentially zero and that the complex ion reduces directly on the electrode surface. If the direct electron transfer rates are rapid compared with all other processes, the electrode is Nernstian with respect to the complex and the reduced form. Then

$$\theta = \frac{C_Y(o,t)}{C_R(o,t)} = (f_X C_X)^p \frac{f_R}{f_Y} \exp\left[\frac{nF}{RT}(E - E_0')\right] \tag{57}$$

where $E^{0\prime}$ is the standard potential for the reaction

$$Y \xrightarrow{ne^-} R + pX \tag{58}$$

It follows that

$$\theta' = \theta \frac{C_X{}^p}{K} \tag{59}$$

where K was defined in eqn. (5) and

$$E_0' = E^0 + \frac{RT}{nF} \ln K + \frac{RT}{nF} \ln \frac{f_o f_X{}^p}{f_Y} \tag{60}$$

Equations (6) – (10) remain unchanged with the exceptions (7d), (7e), and (7f). They are modified

$$t > o \quad x = o \quad C_Y(o,t) = \theta' C_R(o,t) \tag{7d}$$

$$t > o \quad x = o \quad \partial C_O/\partial x = o \tag{7e}$$

$$t > o \quad x = o \quad \frac{\partial C_R}{\partial x} = -\frac{\partial C_Y}{\partial x} \tag{7f}$$

The transformed variables are:

$$\bar{\psi}(x,s) = \left\{\frac{(1 + K/C_X{}^p)\theta' C_R{}^0 - \alpha}{1 + (1 + K/C_X{}^p)\theta' + K/C_X{}^p\sqrt{\frac{s}{s+l}}}\right\}\frac{e^{-\sqrt{\frac{s}{D}}x}}{s} + \frac{\alpha}{s} \tag{61a}$$

$$\bar{\varphi}(x,s) = \left\{\frac{(K/C_X{}^p)\alpha - K/C_X{}^p(1 + K/C_X{}^p)\theta' C_R{}^0}{1 + (1 + K/C_X{}^p)\theta' + K/C_X{}^p\sqrt{\frac{s}{s+l}}}\right\}\frac{e^{-\sqrt{\frac{s+l}{D}}x}}{\sqrt{s}\sqrt{s+l}} \tag{61b}$$

$$\bar{C}_R(x,s) = \left\{\frac{\alpha - (1 + K/C_X{}^p)\theta' C_R{}^0}{1 + (1 + K/C_X{}^p)\theta' + K/C_X{}^p\sqrt{\frac{s}{s+l}}}\right\}\frac{e^{-\sqrt{\frac{s}{D}}x}}{s} + \frac{C_R{}^0}{s} \tag{61c}$$

Case II A. Rapid prior solution reaction. For rapid interconversion, $l \to \infty$, the transform inversion yields

$$\psi(x,t) = \left\{\frac{(1 + K/C_X{}^p)\theta' C_R{}^0 - \alpha}{1 + (1 + K/C_X{}^p)\theta'}\right\}\operatorname{erfc}\frac{x}{2\sqrt{Dt}} + \alpha \tag{62a}$$

$$\varphi(\chi \cdot t) = 0 \tag{62b}$$

$$C_R(x \cdot t) = \left\{\frac{\alpha - (1 + K/C_X{}^p)\theta' C_R{}^0}{1 + (1 + K/C_X{}^p)\theta'}\right\}\operatorname{erfc}\frac{x}{2\sqrt{Dt}} + C_R{}^0 \tag{62c}$$

By substituting for θ' its equivalent from eqn. (59), eqns. (62a), (62b) and (62c) are identical to eqns. (12a), (12b), and (12c). Since eqn. (14) is generally valid, it follows the results of Case II A and are identical with those of Case I A.

Case II B. No prior solution reactions. Setting $l = 0$ eqns. (61a), (61b), and (61c) and applying the inverse transform yields

$$\psi(x,t) = \left\{\frac{[1 + K/C_X{}^p]\theta' C_R{}^0 - \alpha}{[1 + K/C_X{}^p][1 + \theta']}\right\}\operatorname{erfc}\frac{x}{2\sqrt{Dt}} + \alpha \tag{63a}$$

$$\varphi(x,t) = K/C_X{}^p[\psi(x,t) - \alpha] \tag{63b}$$

$$C_R(x,t) = \left\{\frac{\alpha - [1 + K/C_X{}^p]\theta' C_R{}^0}{[1 + K/C_X{}^p][1 + \theta']}\right\}\operatorname{erfc}\frac{x}{2\sqrt{Dt}} + C_R{}^0 \tag{63c}$$

By eqn. (14), the current is given by

$$i = \frac{nFAD^{\frac{1}{2}}}{\sqrt{\pi t}}\left\{\frac{\alpha - [1 + K/C_X{}^p]\theta C_R{}^0}{[1 + K/C_X{}^p][1 + \theta']}\right\} \tag{64}$$

The limiting cathodic current is dependent on ligand concentration according to

$$(i_l)_c = i_{\lim\theta\to 0} = \frac{nFAD^{\frac{1}{2}}\alpha}{\sqrt{\pi t}[1 + K/C_X{}^p]} \tag{65}$$

and

$$(i_d)_a = i_{\lim\theta\to\infty} = \frac{-nFAD^{\frac{1}{2}}C_R{}^0}{\sqrt{\pi t}} \tag{66}$$

The current for any θ' is given by

$$= \frac{(i_l)_c + (i_d)_a\theta'}{1 + \theta'} \tag{67}$$

and the $i-E$ characteristic is

$$E = E^{0\prime} - \frac{RT}{nF}\ln C_X{}^p + \frac{RT}{nF}\ln\frac{f_Y}{f_R f_X{}^p} + \frac{RT}{nF}\ln\left[\frac{(i_l)_c - i}{i - (i_d)_a}\right] \tag{68a}$$

and by substituting eqn. (60) into (68a)

$$E = E^0 + \frac{RT}{nF}\ln K - \frac{RT}{nF}\ln C_X{}^p + \frac{RT}{nF}\ln\frac{f_O}{f_R} + \frac{RT}{nF}\ln\left[\frac{(i_l)_c - i}{i - (i_d)_a}\right] \tag{68b}$$

For a massive mercury electrode,

$$E = \varepsilon + \frac{RT}{nF}\ln K - \frac{RT}{nF}\ln C_X{}^p + \frac{RT}{nF}\ln\frac{f_M}{f_{M(\mathrm{Hg})}} + \frac{RT}{nF}\ln\left[\frac{(i_l)_c - i}{i - (i_d)_a}\right] \tag{69}$$

and in the usual polarographic case, $C_R{}^0 = 0$

$$E_{\frac{1}{2}} = \varepsilon + \frac{RT}{nF}\ln K + \frac{RT}{nF}\ln\frac{f_M}{f_{M(\mathrm{Hg})}} - \frac{RT}{nF}\ln C_X{}^p \tag{70}$$

Thus, when the pre-electrochemical step does not occur, as in case I B, the limiting cathodic current is dependent on ligand concentration. However, the half-wave is also dependent upon ligand concentration.

Case II C. Finite prior solution reaction rate constants. An exact solution can be given for this case by the same procedure used in I C. Equations (31), (32), and (33) are still valid. However, the coefficients Q, M and N must be redefined

$$Q = \alpha - (1 + K/C_X{}^p)\theta' C_R{}^0 \tag{71a}$$

$$M = 1 + (1 + K/C_X{}^p)\theta' \tag{71b}$$

$$N = K/C_X{}^p \tag{71c}$$

The general expression for current is

$$i_c = \left[\frac{i_\infty + [1 + K_{Gz}\,r]\,\theta'\,(i_d)\,a}{i + [1 + K_{Hz}\,r]\,\theta'}\right]\left\{\frac{M}{N^2 - M^2}\left(N\,e^{-lt} - M\right) - \frac{N^2\,M}{(N^2 - M^2)^{3/2}}\sqrt{\pi lt}\;e^{\frac{M^2\,lt}{N^2 - M^2}}\left[\mathrm{erfc}\sqrt{\frac{N^2\,lt}{N^2 - M^2}} - \mathrm{erfc}\sqrt{\frac{M^2\,lt}{N^2 - M^2}}\right]\right\} \tag{72}$$

and

$$\frac{i_l - i}{i} = \frac{i_l}{i_\infty}\left[\frac{1 + (1 + \sigma)\theta'}{\mathrm{F}(l,\theta',\sigma,t)}\right] - 1 \approx \frac{i_l}{i_\infty}(1 + \sigma)\theta' \tag{73}$$

which, when rearranged gives

$$E = E_0' + \frac{RT}{nF}\ln\frac{f_Y}{f_R f_X{}^p} + \frac{RT}{nF}\ln\frac{1}{(1 + \sigma)C_X{}^p} + \frac{RT}{nF}\ln\frac{i_l - i}{i} - \frac{RT}{nF}\ln\frac{i_l}{i_\infty} \tag{74}$$

In view of eqn. (60), eqn. (74) is identical to eqn. (47). For rapid pre-electrochemical reactions $i_l = i_\infty$ and eqn. (74) becomes eqn. (22). When $l \to 0$, $i_l/i_\infty \to 1/1 + \sigma$ and eqn. (74) becomes eqn. (68) or (69). The half-wave potential is then given by

$$(E_{\frac{1}{2}})_c = E^0 + \frac{RT}{nF}\ln\frac{f_O}{f_R} + \frac{RT}{nF}\ln\frac{K/C_X{}^p}{1 + K/C_X{}^p} - \frac{RT}{nF}\ln \mathrm{F}(l,0,\sigma,t) \tag{75}$$

But

$$F(l,o,\sigma,t) \approx F(Y)$$

where

$$y = \frac{\sqrt{lt}}{\sqrt{\sigma^2 - 1}} \tag{77}$$

For the polarographic case $F(l,o,\sigma,t) = F(\chi)$ where

$$\chi = \sqrt{\frac{12}{7}} \frac{\sqrt{lt}}{\sqrt{\sigma^2 - 1}} \tag{78}$$

When $lt >> 1$, $\chi << 1$ and $\sigma > 1$, $F(\chi)$ can be simplified in the same manner as eqn. (53). In the case $\chi << 1$ $lt < 1$, use

$$F(\chi) \approx \frac{\sqrt{\pi}}{2}\chi + \frac{\sigma e^{-lt} - 1}{\sigma^2 - 1} \tag{79}$$

Case III. Both simple and complex ions are reducible

When the heterogeneous electron transfer rate constants in eqn. (4) are large for both the simple and complex ions, it follows that both species will approach Nernstian behavior such that eqn. (5) and (57) are simultaneously obeyed. If this behavior can be proved, then it is not difficult to show that the pre-electrochemical rate constants must be large so that φ is always zero.

DISCUSSION AND CONCLUSIONS

The current–voltage characteristic and the half-wave potential have been derived from a kinetic model for systems containing a simple metal ion, M^+, complex ion $MX_p^{(n-pb)+}$, ligand X^{-b} and reduced phase M or M(Hg). For simplicity, linear diffusion was assumed, but the results were adapted to the polarographic case.

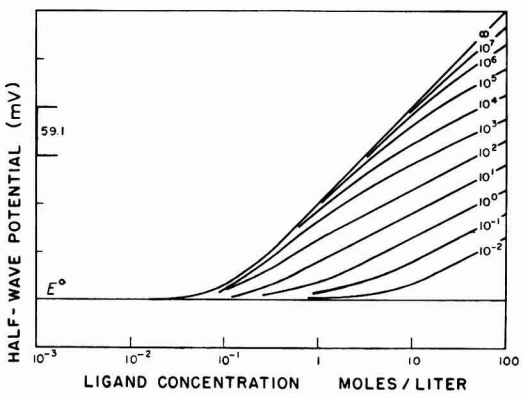

Fig. 1. Calculated half-wave potentials for complex ion reduction:

$$MX_2^- \underset{k_b}{\overset{k_f}{\rightleftharpoons}} M^+ + 2\,X^- \xrightarrow{1e^-} M(\mathrm{Hg})$$

It is assumed that $K = 10^{-2}$ and that only the simple ion is reducible. Numbers on each curve refer to the rate constant function $l = l(k_f, k_b, C_X)$ [see eqn. (10)].

Expressions for half-wave potentials valid over the whole range of ligand concentration have been given for finite, zero and infinite pseudo first order pre-electrochemical solution reaction rate constants. In the derivation, the reducible species was restricted to the simple metal ion only in Case I, the complex ion only in Case II, and both in Case III. The expressions for $(E_{\frac{1}{2}})_c$ can be evaluated in terms of the functions tabulated by KOUTECKY[23,28].

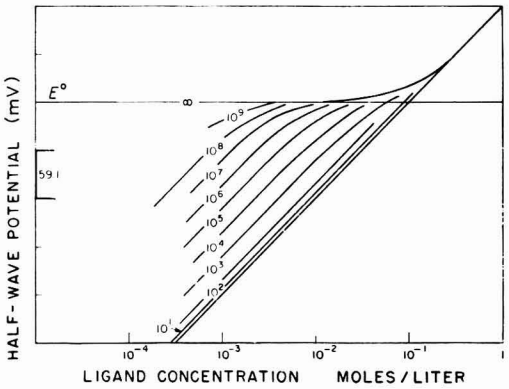

Fig. 2. Calculated half-wave potentials for complex ion reduction

$$MX_2^- \underset{k_b}{\overset{k_f}{\rightleftharpoons}} M^+ + 2\,X^- \xrightarrow{1e^-} M(\mathrm{Hg})$$

It is assumed that $K = 10^{-2}$ and that only the complex ion is reducible. Numbers on each curve refer to the rate constant function $l = l(k_f, k_b, C_X)$ [see eqn. (10)].

The results can be illustrated by considering a typical system: a complex ion MX_2^- with $K = 10^{-2}$, in which M is an unipositive element. A plot of $E_{\frac{1}{2}}$ *vs.* log C_X for case I, the reversible curve ($l = \infty$) was calculated from eqn. (22), assuming all activity coefficients are unity. The curve for $l = 0$ is represented by eqn. (30). Equation (51) was used to calculate $E_{\frac{1}{2}}$ for intermediate values of l. The function $\mathrm{F}(\chi)$ was calculated from eqns. (52), (53), or (54), depending upon the magnitudes of lt and σ. A value of $t = 3$ sec was assumed as a typical drop time.

Rather than complicating Fig. 1 unnecessarily, calculations based on the model in case II are shown in Fig. 2. The reversible curve is the same as in Fig. 1 and the curve for $l = 0$ was obtained from eqn. (70). Curves for intermediate values of l were obtained from eqn. (75) and $\mathrm{F}(\chi)$ was calculated from Tables and eqns. (53) or (79), depending upon the magnitudes of lt and σ.

It is apparent from these curves that plots of $E_{\frac{1}{2}}$ *vs.* log C_X could yield erroneous values for complex equilibrium constants and altogether fictitious values of p if it has not been proven that no kinetic complications exist. As was shown earlier, plots of log $(i_l - i)/i$ *vs.* E yield straight lines for reversible electron transfers whether a current-limiting, pre-electrochemical kinetic complication exists or not. Thus, it is not sufficient to show linearity of log $(i_l - i)/i$ *vs.* E as a criterion for validity of the $E_{\frac{1}{2}}$ *vs.* log C_X plot as a means of determining stoichiometric quantities. Some other method, such as the dependence of the limiting current on the square root of the mercury column height must be shown as well.

The mathematical results show that for l very large (extremely labile complexes), it is not possible to distinguish from limiting current measurements or half-wave potentials whether the simple ion, complex ion or both are reducible. Models based upon the assumption that only one of the species is reducible lead to the same expression for half-wave potentials *vs.* $\log C_X$ in the limiting case of $l \to \infty$. However, when a slow prior solution reaction produces a reducible species from non-reducible materials, it is possible to make a reasonably certain assignment of the reducible species from either dependence of limiting current on $\log C_X$ or dependence of $E_{\frac{1}{2}\,(\text{obs.})}$ on $\log C_X$.

Two major omissions of principle in this treatment were made for mathematical simplicity: one is the variation in the ligand concentration near the electrode surface as current flows. Throughout the treatment, the ligand concentration is presumed constant throughout the solution — a requirement which cannot be realized physically at very dilute ligand levels. Incorporation of outward diffusion of ligand from the electrode surface makes the problem considerably more difficult. Approximate account of this effect can be taken by the method of LINGANE[38] where the ligand concentration at the electrode surface, $(C_X)_0$, is expressed in terms of current, thus, for a plane electrode,

$$(C_X)_0 \simeq C_X + \frac{\bar{p}i}{D_X^{\frac{1}{2}}}$$

or, for a dropping mercury electrode,

$$(C_X)_0 \simeq C_X + \frac{\bar{p}i}{\sqrt{7/3}\, D_X^{\frac{1}{2}}}$$

The experimental result of the higher-than-bulk concentration of ligand at the electrode surface is that the measured value of $(E_{\frac{1}{2}})_c$ will be more negative than the value calculated from eqns. (22) or (70). The exact solution to this problem has been given by CIZEK, KORYTA AND KOUTECKY[33], who have shown that the proper expression for i_l/i_d at low ligand concentrations is their $G(\beta)$, rather than $F(\chi)$ used above.

The second major omission is that of double layer structure and its significant effect on measured pre-electrochemical rate constants. Experimental evaluation of the effect has been given by DELAHAY and co-workers[39,40] and by GIERST[41]. The exact theory developed by GIERST AND HURWITZ[42], HURWITZ[43], and by MATSUDA[44] suggests that a suitable correction can be made by inserting the Matsuda G function into χ in eqns. (51), (52), (54), (55), (75) and (79). For mathematical convenience, a constant diffusion coefficient for complex ion, simple ion and reduced form was assumed. A discussion of this assumption is given in the Appendix, and two types of approximation are considered in accounting for different diffusion coefficients.

Applicability of the half-wave potential equations to systems in mobile equilibrium is well known through the numerous studies using the DeFord-Hume equation. No examples of reversible complex ion reductions with completely immobile equilibrium between complex and simple ions are known to the author. Experimentally, kinetic complexity in complex ion reductions has been often observed. Early literature is summarized by PARRY AND LYONS[45] and other examples are given by DELAHAY[46,47] and by KORYTA *et al.*[7-16]. Testing the behavior of $(E_{\frac{1}{2}})_c$ *vs.* log ligand concentration in these systems is often complicated by other factors which become im-

portant during the dilution of ligand concentration relative to metal concentration. Among these are: (1) multiple complexes which would require a more elaborate theory, (2) irreversible reduction of either complex, simple ion or intermediate complexes, and (3) rate constants too fast so that extreme ligand dilution is required to observe deviations in $E_{\frac{1}{2}}$ from the reversible curve.

SUMMARY

A kinetic model for electrode processes with prior solution reactions has been explored for the case of reversible electron transfers. A general expression for the current–voltage characteristic has been derived which is valid for all values of the pre-electrochemical solution reaction rate constants. The equations have been applied to the case of polarographic complex ion reductions where either the simple ion, complex ion, or both are electrochemically active. The following results were derived:

(1) For very large rate constants, the current–voltage characteristic and half-wave potential are independent of the reaction mechanism.

(2) For intermediate and small values of the rate constants, $E_{\frac{1}{2}}$ *vs.* log ligand concentration depends upon the mechanism and is diagnostic for the electroactive species.

(3) For complex ion reductions with slow prior solution reactions, the slope of a plot of $E_{\frac{1}{2}}$ *vs.* log ligand concentration yields spurious values of the ligand-to-metal ratio in the complex.

(4) A modification of the Lingane–Freyhold–von Stackelberg equation for $E_{\frac{1}{2}}$ of reversible complex ion reductions is derived which is valid for all concentrations of the ligand.

REFERENCES

1 I. M. KOLTHOFF AND J. J. LINGANE, *Polarography*, Interscience Publishers, Inc., New York, 1952, pp. 199–202; 211–234.
2 P. DELAHAY AND T. J. ADAMS, *J. Am. Chem. Soc.*, 74 (1952) 1437.
3 L. ONSAGER, *J. Chem. Phys.*, 2 (1934) 599.
4 P. DELAHAY, *New Instrumental Methods in Electrochemistry*, Interscience Publishers, Inc., New York, 1954, chapters 3 and 4.
5 I. M. KOLTHOFF AND J. J. LINGANE, *Polarography*, Interscience Publishers, Inc., New York, 1952, chapters 11 and 12.
6 H. MATSUDA AND Y. AYABE, *Bull. Chem. Soc. Japan*, 29 (1956) 134.
7 J. KORYTA, *Collection Czech. Chem. Commun.*, 23 (1958) 1408.
8 J. KORYTA, *Collection Czech. Chem. Commun.*, 24 (1959) 2903.
9 J. KORYTA, *Collection Czech. Chem. Commun.*, 24 (1959) 3057.
10 Z. ZABRANSKY, *Collection Czech. Chem. Commun.*, 24 (1959) 3075.
11 M. PRYSZCHZEWSKA, R. RALEA AND J. KORYTA, *Collection Czech. Chem. Commun.*, 24 (1959) 3796.
12 J. BIERNAT AND J. KORYTA, *Collection Czech. Chem. Commun.*, 25 (1960) 38.
13 J. KORYTA AND Z. ZABRANSKY, *Collection Czech. Chem. Commun.*, 25 (1960).
14 J. KORYTA, *Zeit Physik. Chem. (Leipzig)*, Sonderheft (1958) 157.
15 J. KORYTA, *Electrochim. Acta*, 1 (1959) 26.
16 J. KORYTA, *Zeit Electrochem.*, 64 (1960) 23.
17 I. M. KOLTHOFF AND J. J. LINGANE, *Polarography*, Interscience Publishers, Inc., New York, 1952, chapter 15.
18 P. DELAHAY, *New Instrumental Methods in Electrochemistry*, Interscience Publishers, Inc., chapter 5, p. 88.
19 J. KOUTECKY AND R. BRDICKA, *Collection Czech. Chem. Commun.*, 12 (1947) 138.
20 J. KOUTECKY, *Collection Czech. Chem. Commun.*, 18 (1953) 11.
21 J. KOUTECKY, *Collection Czech. Chem. Commun.*, 18 (1953) 183.
22 J. KOUTECKY, *Collection Czech. Chem. Commun.*, 18 (1953) 311.
23 J. KOUTECKY, *Collection Czech. Chem. Commun.*, 18 (1953) 597.
24 J. KOUTECKY, *Collection Czech. Chem. Commun.*, 19 (1954) 1045.

[25] J. KOUTECKY, *Collection Czech. Chem. Commun.*, 19 (1954) 857.
[26] J. KOUTECKY, *Collection Czech. Chem. Commun.*, 19 (1954) 1093.
[27] J. KOUTECKY, *Collection Czech. Chem. Commun.*, 20 (1955) 116.
[28] J. WEBER AND J. KOUTECKY, *Collection Czech. Chem. Commun.*, 20 (1955) 980.
[29] J. KOUTECKY, *Collection Czech. Chem. Commun.*, 21 (1956) 433
[30] J. KOUTECKY, *Collection Czech. Chem. Commun.*, 21 (1956) 652.
[31] J. KOUTECKY, *Collection Czech. Chem. Commun.*, 21 (1956) 1056.
[32] J. KOUTECKY, *Collection Czech. Chem. Commun.*, 22 (1957) 160.
[33] J. CIZEK, J: KORYTA AND J. KOUTECKY, *Collection Czech. Chem. Commun.*, 24 (1959) 663.
[34] J. CIZEK, J. KORYTA AND J. KOUTECKY, *Collection Czech. Chem. Commun.*, 24 (1959) 3844.
[35] D. D. DEFORD AND D. N. HUME, *J. Am. Chem. Soc.*, 73 (1951) 5321.
[36] M. VON STACKELBERG AND H. VON FREYHOLD, *Zeit. Elektrochem.*, 46 (1940) 120.
[37] J. J. LINGANE, *Chem. Revs.*, 29 (1941) 1.
[38] I. M. KOLTHOFF AND J. J. LINGANE, Polarography, Interscience Publishers, Inc., New York, 1952, pp. 232–233.
[39] M. BREITER, M. KLEINERMAN AND P. DELAHAY, *J. Am. Chem. Soc.*, 80 (1958) 5111.
[40] P. DELAHAY AND M. KLEINERMAN, *J. Am. Chem. Soc.*, 82 (1960) 4509.
[41] GIERST, *Transactions of the Symposium on Electrode Processes, Philadelphia, May, 1959*, G. Wiley and Sons, Inc., New-York, 1961, p. 109.
[42] L. GIERST AND H. HURWITZ, *Z. Elektrochem.*, 64 (1960) 36.
[43] H. HURWITZ, *Z. Elektrochem.*, 65 (1961) 178.
[44] H. MATSUDA, *J. Phys. Chem.*, 64 (1960) 332.
[45] R. W. PARRY AND E. H. LYONS, *The Chemistry of the Coordination Compounds*, edited by J. C. BAILAR, Reinhold Publishing Co., New York, 1956, pp. 625–71.
[46] P. DELAHAY, *Discs. Farad. Soc.*, 17 (1954) 205.
[47] P. DELAHAY, *Ann. Rev. Phys. Chem.* 8 (1957) 229.
[48] I. M. KOLTHOFF AND J. J. LINGANE, *Polarography*, Interscience Publishers, Inc., New York, 1952, p. 213, equation (14).
[49] I. M. KOLTHOFF AND J. J. LINGANE, *Polarography*, Interscience Publishers, Inc., New York, 1952, p. 213, equations (8)–(11).

APPENDIX

KINETIC BEHAVIOR WHEN THE COMPLEX ION, AND REDUCTION PRODUCT HAVE DIFFERENT DIFFUSION COEFFICIENTS

When account is taken of differences in the diffusion coefficients of the species $MX^{(n-pb)+}$, M^{+n} and $M(Hg)$, eqn (2) must be modified by inserting the appropriate diffusion coefficients D_Y, D_O, and D_R in the first terms on the right. Boundary conditions in eqns (7a)–(7e) are unchanged, while (7f) becomes for

$$t > 0, x = 0$$

$$D_R \frac{\partial C_R}{\partial x} = -D_O \frac{\partial C_O}{\partial x} \tag{80}$$

It is not difficult to show that defining $\psi(x,t)$ and $\varphi(x,t)$ by eqns. (8a) and (8b) fails to give separation of variables; consequently, exact solution of the problem cannot be made on this basis.

KOUTECKY[25] has given a useful approximation in analyses of currents limited by the combination of two electro-inactive materials to yield an electro-active species. For the present problem, we define by analogy

$$\psi(x,t) = \frac{D_Y C_Y(x,t) + D_O C_O(x,t)}{D_\psi} \tag{81}$$

where

$$D_\psi = \frac{D_Y C_{MX^p} + D_O C_M}{C_{MX^p} + C_M} = \frac{D_Y + D_O K/C_X{}^p}{1 + K/C_X{}^p} \tag{82}$$

D_ψ represents a mean diffusion coefficient. Similarly, if we define

$$\varphi(x,t) = \frac{D_O C_O(x,t) - K/C_X{}^p D_Y C_Y(x,t)}{D_\varphi} \tag{83}$$

where

$$D_\varphi = \frac{D_Y + D_O K/C_X{}^p}{1 + K/C_X{}^p} \tag{84}$$

we have *approximately*,

$$\frac{\partial \psi}{\partial t} \simeq D_\psi \frac{\partial^2 \psi}{\partial x^2} \tag{85a}$$

$$\frac{\partial \varphi}{\partial t} \simeq D_\varphi \frac{\partial^2 \varphi}{\partial x^2} - l\varphi \tag{85b}$$

$$\frac{\partial C_R}{\partial t} \simeq D_R \frac{\partial^2 C_R}{\partial x^2} \tag{85c}$$

which become exact at the extreme conditions that $C_X >> 0$ or $C_X \approx 0$ where

$$D_\psi = D_\varphi = D_Y \quad \text{or} \quad D_\psi = D_\varphi = D_O. \tag{86}$$

respectively. Carrying through the same steps indicated in eqns. (11)–(13) and remembering that as $l \to \infty$

$$i = -nFAD_R\left(\frac{\partial C_R}{\partial x}\right)_{x=0} = nFA\left[D_O\left(\frac{\partial C_O}{\partial x}\right)_{x=0} + D_Y\left(\frac{\partial C_Y}{\partial x}\right)_{x=0}\right] \simeq nFAD_\psi\left(\frac{\partial \psi}{\partial x}\right)_{x=0} \tag{87}$$

and that

$$(i_d)_c = \frac{nFAD_\psi{}^{\frac{1}{2}}\alpha}{\sqrt{\pi t}} \tag{88}$$

$$(i_d)_a = \frac{nFAD_R{}^{\frac{1}{2}}C_R{}^0}{\sqrt{\pi t}} \tag{89}$$

one obtains

$$i = \frac{K/C_X{}^p(i_d)_c D_R{}^{\frac{1}{2}} - [1 + K/C_X{}^p]\theta(i_d)_a D_\psi{}^{\frac{1}{2}}}{K/C_X{}^p D_R{}^{\frac{1}{2}} - [1 + K/C_X{}^p]\theta D_\psi{}^{\frac{1}{2}}} \tag{90}$$

and

$$\theta = \frac{K/C_X{}^p D_R{}^{\frac{1}{2}}}{[1 + K/C_X{}^p]D_\psi{}^{\frac{1}{2}}}\left(\frac{(i_d)_c - i}{i - (i_d)_a}\right)$$

or

$$E = E^0 + \frac{RT}{nF}\ln\frac{f_O}{f_R} + \frac{RT}{nF}\ln\frac{K/C_X{}^p}{1 + K/C_X{}^p} + \frac{RT}{nF}\ln\left(\frac{D_R}{L_\psi}\right)^{\frac{1}{2}} + \frac{RT}{nF}\ln\frac{(i_d)_c - i}{i - (i_d)_a} \tag{92}$$

Equation (92) compares with eqn. (19) when the diffusion coefficient of each species is different; and the approximations defined in eqns. (82) and (84) are used. These approximations are not particularly useful since $D_\psi{}^{\frac{1}{2}}$ cannot be readily expanded, in terms of individual diffusion coefficients.

In polarography, an alternate approximation can be used which yields the i–E characteristic in a more tractable form. Instead of eqn. (82), we define a mean-root diffusion coefficient $D_\psi{}'$

$$(D_\psi{}')^{\frac{1}{2}} = \frac{D_Y{}^{\frac{1}{2}}C_{MXp} + D_O{}^{\frac{1}{2}}C_M}{C_{MXp} + C_M} = \frac{D_Y{}^{\frac{1}{2}} + D_O{}^{\frac{1}{2}}K/C_X{}^p}{1 + K/C_X{}^p} \tag{93}$$

and a corresponding D_ψ. These equations are again exact at the extremes $C_X >> 0$ or $C_X \approx 0$.

The kinetic derivation yields an equation of the form of (92) with $(D_\psi')^{\frac{1}{2}}$ substituted for $(D_\psi)^{\frac{1}{2}}$. For the case of a mercury electrode, the half-wave potential becomes

$$(E_{\frac{1}{2}})_c = \varepsilon + \frac{RT}{nF} \ln \frac{f_M}{f_{M(Hg)}} \cdot K/C_X{}^p \cdot D_{M(Hg)}{}^{\frac{1}{2}} - \frac{RT}{nF} \ln \left[D_p{}^{\frac{1}{2}} + D_M{}^{\frac{1}{2}} \cdot K/C_X{}^p\right] \tag{94}$$

or, in a form similar to the often-quoted equation of LINGANE[18],

$$(E_{\frac{1}{2}})_c = \varepsilon + \frac{RT}{nF} \ln \frac{f_M K_{DM(Hg)}{}'^{\frac{1}{2}}}{f_{M(Hg)} D_p{}^{\frac{1}{2}}} - p\frac{RT}{nF} \ln C_X - \frac{RT}{nF} \ln \left[1 + \frac{K}{C_X{}^p}\left(\frac{D_M}{D_p}\right)^{\frac{1}{2}}\right]$$

where D_p is the diffusion coefficient of the complex.

Although we have not solved the boundary value problem when activity coefficients of the species $MX_p{}^{(n-pb)+}$, M^{n+} and M(Hg) are introduced into the diffusion equations, it is thermodynamically consistent to substitute $Kf_Y/f_O C_X{}^p f_X{}^p$ for $K/C_X{}^p$ and to insert activity coefficients in the expression for D_ψ'. Then

$$(D_\psi')^{\frac{1}{2}} = \frac{D_Y{}^{\frac{1}{2}} + D_O{}^{\frac{1}{2}} \dfrac{Kf_Y}{f_O C_X{}^p f_X{}^p}}{1 + \dfrac{Kf_Y}{f_O C_X{}^p f_X{}^p}} = \frac{D_p{}^{\frac{1}{2}} + D_M{}^{\frac{1}{2}} \dfrac{Kf_p}{f_M C_X{}^p f_X{}^p}}{1 + \dfrac{Kf_p}{f_M C_X{}^p f_X{}^p}} \tag{96}$$

Equation (95) becomes:

$$(E_{\frac{1}{2}})_c = \varepsilon + \frac{RT}{nF} \ln \frac{Kf_p}{f_{M(Hg)}}\left(\frac{D_{M(Hg)}}{D_p}\right)^{\frac{1}{2}} - p\frac{RT}{nF} \ln C_X f_X - \frac{RT}{nF} \ln \left[\left(1 + \frac{Kf_p D_M{}^{\frac{1}{2}}}{f_M C_X{}^p f_X{}^p D_p{}^{\frac{1}{2}}}\right)\right] \tag{97}$$

This equation differs from that of LINGANE[48], by addition of the last term on the right. Equation (97), when written in the form

$$(E_{\frac{1}{2}})_c = \varepsilon + \frac{RT}{nF} \ln \left\{\frac{\dfrac{Kf_p}{f_{M(Hg)} C_X{}^p f_X{}^p}\left(\dfrac{D_{M(Hg)}}{D_p}\right)^{\frac{1}{2}}}{1 + \dfrac{Kf_p}{f_{M(Hg)} C_X{}^p f_X{}^p}\left(\dfrac{D_M}{D_p}\right)^{\frac{1}{2}}}\right\} \tag{98}$$

is readily seen to converge to the value

$$\varepsilon + \frac{RT}{nF} \ln \frac{f_M}{f_{M(Hg)}}\left(\frac{D_{M(Hg)}}{D_M}\right)^{\frac{1}{2}} \tag{99}$$

when $K \to \infty$ or $C_X f_X \to 0$.

Equation (99) is the expression for the half-wave potential for the reduction of a simple metal ion soluble in mercury $(E_{\frac{1}{2}})_s$. The equation for $(E_{\frac{1}{2}})_c$ given by LINGANE diverges when the dissociation constant is very large or $C_X f_X$ is very small. Thus, the LINGANE equation is valid only for strong complexes or high ligand concentrations such that the term $K/C_X{}^p f_X{}^p << 1$. The omission is equivalent to ignoring the non-complexed metal ion concentration.

The correct equation for $(E_{\frac{1}{2}})_c$ could have been obtained by the quasi-thermodynamic method used by LINGANE[49] if an additional term had been added to the expression for i, corresponding to diffusion of the simple metal ion. Thus, starting

with thermodynamic equation for the potential of the dropping mercury electrode

$$E_{\text{d.e.}} = \varepsilon + \frac{RT}{nF} \ln \frac{Kf_p}{f_{M(\text{Hg})} f_X^p} - \frac{RT}{nF} \ln \frac{C^0_{M(\text{Hg})} (C_X{}^0)^p}{C_p{}^0} \tag{100}$$

and expressing $C_M{}^0{}_{(\text{Hg})}$ and $C_p{}^0$ in terms of current, where the superscript o indicates electrode surface concentrations, the approximate equation is

$$i = k_p(C_p - C_p{}^0) + k_M(C_M - C_M{}^0) = k_{M(\text{Hg})} C_{M(\text{Hg})} \tag{101a}$$

In addition

$$(i_d)_c = k_p C_p + k_M C_M \tag{101b}$$

whence

$$C_p{}^0 = \frac{(i_d)_c - i}{k_p \left[1 + \dfrac{k_M f_p K}{k_p f_M C_X{}^p f_X{}^p} \right]} \tag{102}$$

It follows that

$$(E_{\frac{1}{2}})_c = \varepsilon + \frac{RT}{nF} \ln \frac{f_p K}{f_{M(\text{Hg})} f_X{}^p} - p \frac{RT}{nF} \ln C_X - \frac{RT}{nF} \ln \frac{k_p}{k_{M(\text{Hg})}} \left(1 + \frac{k_M f_p K}{k_p f_M C_X{}^p f_X{}^p} \right) \tag{103}$$

This expression is identical with (97) when it is realized that k_p, $k_{M(\text{Hg},)}$ and k_M are proportional to the square roots of the diffusion coefficients of the complex ion, the metal in the amalgam, and the simple, hydrated metal ion. The omission of the last on the right term occurred by introducing a mechanism into a basically thermodynamic equation. The generalized von Stackelberg–Freyhold–Lingane equation (103) is consistent with the totally kinetic derivation represented in eqn. (97).

Short Communication

Étude électrochimique de la précipitation des halogénures d'argent dans les mélanges eau-tétrahydrofuranne

Malgré une constante diélectrique faible ($\varepsilon = 7.35$) le tétrahydrofuranne anhydre peut être rendu conducteur par addition de perchlorate de lithium. Lorsque ce sel atteint une concentration égale à 0.3 M, la conductivité du solvant est suffisante pour permettre des déterminations voltammétriques[1]. En particulier l'étude de l'oxydation anodique de l'argent en présence de chlorure de lithium[2] a permis de déterminer la constante d'équilibre correspondant à la réaction

$$AgClO_4 + LiCl \rightleftharpoons AgCl\downarrow + LiClO_4 \quad (pK = \log \frac{|LiClO_4|}{|AgClO_4|\,|LiCl|} = 16.5$$

Nous avons repris l'étude de cet équilibre dans différents mélanges eau–tétrahydrofuranne et montré que le pK de cette réaction croit avec le pourcentage x de tétrahydrofuranne (x = % en volume): dans l'eau ($x = 0$) p$K = 9.5$; $x = 90\%$ p$K = 13.6$; $x = 95\%$ p$K = 14.7$; $x = 98\%$ p$K = 15.6$. Dans les mélanges riches en tétrahydrofuranne, la précipitation du chlorure d'argent est donc beaucoup plus quantitative que dans l'eau. De ce fait, on peut envisager dans ces solvants, le titrage de solutions diluées de chlorure. Nous avons choisi d'utiliser la coulométrie pour introduire l'argent nécessaire au dosage. Le point équivalent est mis en évidence par une potentiométrie à courant nul (électrode indicatrice d'argent). Dans ces conditions, les solutions de chlorures 10^{-3} M sont dosées à 0.2%, les solutions 10^{-4} M à 1%, 4 10^{-5} M à 2% et 10^{-5} M à 10% près.

Dans ces mêmes solvants, l'existence de complexes solubles bromure ou iodure d'argent est révélée par les courbes de titrage potentiométrique de ces halogénures par le perchlorate d'argent. Dans le cas des bromures, seuls les solvants riches en tétrahydrofuranne ($x \geqslant 90\%$) permettent de mettre en évidence ces complexes. Plus stables dans le cas des iodures, ces complexes apparaissent déjà en présence de 65% de tétrahydrofuranne. Dans ce solvant pur, on peut observer deux sauts potentiométriques distincts lors du titrage de l'iodure de lithium par le perchlorate d'argent: le premier palier se situe vers -1.0 V/Ag↓ – $AgClO_4$ saturé, et correspond à la formation des complexes riches en iodure (formule probable AgI_2Li), le second palier est placé vers -0.8 V et traduit la précipitation de l'iodure d'argent AgI. L'existence de complexes de ce type a été signalée dans des solvants tel que l'acétone[3]. L'étude détaillée de ces réactions fait l'objet d'un autre mémoire[4].

Laboratoire de Chimie Analytique,
Ecole Supérieure de Physique et de Chimie Industrielles,
Paris (France)

A. LEVAVASEUR
J. BADOZ-LAMBLING

[1] J. BADOZ-LAMBLING ET M. SATO, Congrès de Chimie Analytique avril 1961, Budapest. *Acta Chim. Acad. Sci. Hung.*, 32 (1962) 191; M. SATO, *Diplome d'Etudes Supérieures*, Paris, juin 1961.
[2] J. BADOZ-LAMBLING ET M. SATO, *C.R. Acad. Sci.*, 254 (1962) 3354.
[3] B. ALTHIN, E. WAHLIN ET L. G. SILLEN, *Act. Chim. Scand.*, 3 (1949) 321.
[4] A. LEVAVASSEUR, *Diplôme d'Etudes Supérieures*, Paris, juin 1962.

Reçu le 9 novembre, 1962

Book Reviews

Handbook of Mathematical Tables, by S. M. SELBY, R. C. WEAST, R. S. SANKLAND AND C. D. HODGMAN, Chemical Rubber Co., Cleveland, 1962, x + 579 pages, $7.50

This is a slightly enlarged edition of the mathematical tables contained in the well known *Handbook of Chemistry and Physics*. The following tables appear in the present volume in addition to those in the 42nd edition of the handbook (1960–61). Six-place logarithms; square of sine, cosine and their products; random units; Bessel functions (additional text); Legendre Functions; surface zonal harmonics; algebra, basic concepts for sets, integrals, domains, groups, fields and rings; Taylor and Fouriers series; formulae for vector analysis; planetary orbits; values of $\frac{1}{2}p(1-p)$, $p(1-p^2)$, $E_2(p)$ and $F_2(p)$; binomial distribution functions; summed binomial distribution functions; Poisson distributions; summed Poisson distributions; curves and surfaces often appearing in mathematical literature; interest tables; moment of inertia for various bodies; mathematical symbols and abbreviations.

Because of the increased page size the tables are easier to read than those printed in the handbook.

J. Electroanal. Chem., 5 (1963) 316

Angewandte Konduktometrie, by F. OEHME, A. Huthig, Heidelberg, 1962, 211 pages, D.M. 28.

Conductometric methods have been relatively little used for scientific research or analytical purposes in the last decade, partly because of inherent limitations but partly, also, because of an insufficient knowledge of their possibilities. This short monograph is therefore welcome because it gives a very clear treatment of the basic principles of this method, a good description of the necessary equipment for both low and high frequency methods, and details of applications in widely differing fields of research. Amongst the applications discussed are the preparation and purity control of solvents, the possibilities of structural determinations based on the interaction between different ions and between ions and solvents, the determination of equilibrium constants (complexes, hydrogen bonds, acids and bases, etc.), kinetic measurements from direct conductometric analysis (concentration, electrolyte content of water, solubilities, purity control, water contents of different materials, etc.) and conductometric titrations in non-aqueous solvents.

The monograph is completed by a list of the most significant publications concerning recent applications of conductometric and high frequency titrations which have appeared in the last ten years. In future editions a wider treatment of high frequency methods would be desirable.

G. MILAZZO, Istituto Superiore di Sanità, Rome

J. Electroanal. Chem., 5 (1963) 316

Handbuch der mikrochemischen Methoden, edited by F. HECHT AND M. K. ZACHERL, Volume 3, *Anorganische Chromatographie und Elektrophorese*, by M. LEDERER, H. MICHL, K. SCHLÖGL AND A. SIEGEL, *Gaschromatographische Methoden in der anorganischen Analyse*, by GERALD KAINZ, Springer Verlag, Vienna, 1961, 225 pages, D.M. 67.

This volume consists of two independent contributions: one on adsorption, ion exchange, partition chromatography and paper electrophoresis; and the second on the inorganic applications of gas chromatography.

The first section commences with a series of general chapters dealing with mechanisms, techniques and general data, which cannot be used as an introduction to the subject but serves very well as a reference book in a convenient form. The separation of the various elements is treated in chapters according to the elements, and is arranged in groups corresponding in part to the periodic table and in part to well-known analytical groups. For each group the methods are subdivided into adsorption, ion exchange, partition and electrophoresis where, perhaps, subdivision into techniques *e.g.* column separations, paper strip separations, etc. might have been more useful. It is regrettable that the survey appears four years out of date, no references more recent than 1958 being included.

The second part of the book on gas chromatography presents a reasonably good survey of general gas chromatography techniques but is somewhat inadequate as far as inorganic applications are concerned. Again, all of the recent and, in this field, more important work has been omitted.

G. GRASSINI, University of Rome

J. Electroanal. Chem., 5 (1963) 316

CONTENTS

ELSEVIER PUBLISHING COMPANY, AMSTERDAM

Printed in The Netherlands by

NEDERLANDSE BOEKDRUK INRICHTING N.V., 'S-HERTOGENBOSCH